RD&E

CENTER

# Technical Report

No. 13216

SYNTHESIS AND PHYSICAL BEHAVIOR OF

ION-CONTAINING, SEGMENTED AND

RANDOM COPOLYMER ELASTOMERS

CONTRACT NUMBER TACOM DAAE07-82-C-4094

JANUARY 1987



By Dr. James E. McGrath
Department of Chemistry and
Polymer Materials & Interfaces Laboratory
Virginia Tech
Blacksburg, Virginia 24061



U.S. ARMY TANK-AUTOMOTIVE COMMAND
RESEARCH, DEVELOPMENT & ENGINEERING CENTER
Warren, Michigan 48397-5000

## NOTICES

This report is not to be construed as an official Department of the Army position.

Mention of any trade names or manufacturers in this report shall not be construed as an official indorsement or approval of such products or companies by the U.S. Government.

Destroy this report when it is no longer needed. Do not return it to the originator.

SECURITY CLASSIFICATION OF THIS PAGE

# REPORT DOCUMENTATION PAGE

Form Approved
OMB No. 0704-0188
Exp. Date: Jun 30, 1986

| | |
|---|---|
| 1a. REPORT SECURITY CLASSIFICATION<br>Unclassified | 1b. RESTRICTIVE MARKINGS |
| 2a. SECURITY CLASSIFICATION AUTHORITY | 3. DISTRIBUTION/AVAILABILITY OF REPORT<br>Approved for Public Release<br>Distribution is Unlimited |
| 2b. DECLASSIFICATION/DOWNGRADING SCHEDULE | |
| 4. PERFORMING ORGANIZATION REPORT NUMBER(S) | 5. MONITORING ORGANIZATION REPORT NUMBER(S)<br>13216 |
| 6a. NAME OF PERFORMING ORGANIZATION<br>Virginia Polytechnic Institute & State University<br>6b. OFFICE SYMBOL (If applicable) | 7a. NAME OF MONITORING ORGANIZATION<br>U. S. Army Tank-Automotive Command |
| 6c. ADDRESS (City, State, and ZIP Code)<br>Department of Chemistry<br>Polymer Materials and Interfaces Laboratory<br>Virginia Tech; Blacksburg, VA 24061 | 7b. ADDRESS (City, State, and ZIP Code)<br>Warren, MI 48397-5000 |
| 8a. NAME OF FUNDING/SPONSORING ORGANIZATION<br>8b. OFFICE SYMBOL (If applicable) | 9. PROCUREMENT INSTRUMENT IDENTIFICATION NUMBER |
| 8c. ADDRESS (City, State, and ZIP Code) | 10. SOURCE OF FUNDING NUMBERS<br>PROGRAM ELEMENT NO. / PROJECT NO. / TASK NO. / WORK UNIT ACCESSION NO. |

11. TITLE (Include Security Classification)
Synthesis and Physical Behavior of Ion-Containing, Segmented and Random Copolymer Elastomers (unclassified)

12. PERSONAL AUTHOR(S)
James E. McGrath

| 13a. TYPE OF REPORT | 13b. TIME COVERED | 14. DATE OF REPORT (Year, Month, Day) | 15. PAGE COUNT |
|---|---|---|---|
| Final | FROM Sep 82 TO Dec 85 | 87 Jan | 128 |

16. SUPPLEMENTARY NOTATION

| 17. COSATI CODES | | | 18. SUBJECT TERMS (Continue on reverse if necessary and identify by block number) |
|---|---|---|---|
| FIELD | GROUP | SUB-GROUP | |
| | | | |
| | | | |

19. ABSTRACT (Continue on reverse if necessary and identify by block number)

A research program was conducted by the Polymer Synthesis Group of the Chemistry Department and the Polymer Materials and Interfaces Laboratory on the theme of new elastomer synthesis. The body of the report described herein is subdivided into five areas of discussion. The first deals with a laboratory-scale, low-pressure reactor suitable for living polymerizations and polymer modification studies. This section is followed by a discussion of model homopolymer and block polymer elastomers obtained by hydrogenation. Next, an investigation of a hydrocarbon-soluble organolithium difunctional initiator is described. Elastomers based upon ion-containing block and random copolymers are covered as is a study of the morphology and properties of polyurea(urethane) elastomers. An important conclusion is that saturated elastomers such as butyl rubber and various halogenated derivatives as well as the ethylene-propylene copolymer (EPDM) elastomers should be investigated in high performance applications. Lastly, one concludes that significant

| 20. DISTRIBUTION/AVAILABILITY OF ABSTRACT | 21. ABSTRACT SECURITY CLASSIFICATION |
|---|---|
| ☒ UNCLASSIFIED/UNLIMITED ☐ SAME AS RPT. ☐ DTIC USERS | Unclassified |
| 22a. NAME OF RESPONSIBLE INDIVIDUAL<br>Jacob Patt | 22b. TELEPHONE (Include Area Code)<br>(313) 574-8687 |
| | 22c. OFFICE SYMBOL<br>AMSTA-RTT |

DD FORM 1473, 84 MAR 83 APR edition may be used until exhausted.
All other editions are obsolete.

SECURITY CLASSIFICATION OF THIS PAGE
Unclassified

19. Abstract (Continued)

additional effort should be conducted in the area of reactive castable elastomers based upon soft, thermally stable flexible segments linked together through polyurea type hard segments. This approach to castable elastomers has major potential for developing reactive automated fully cured systems of high strength and good abrasion resistance.

## SUMMARY

A research program was conducted by the Polymer Synthesis Group of the Department of Chemistry and the Polymer Materials and Interfaces Laboratory on the theme of new elastomer synthesis. The body of the report described herein is subdivided into five areas of discussion. The first deals with a laboratory-scale, low-pressure reactor suitable for living polymerizations and polymer modification studies. This section is followed by a discussion of model homopolymer and block polymer elastomers obtained by hydrogenation. Next, an investigation of a hydrocarbon-soluble organolithium difunctional initiator is described. Elastomers based upon ion-containing block and random copolymers are covered as is a study of the morphology and properties of polyurea(urethane) elastomers.

In the first portion of our fundamental research, we found it necessary to design and construct a laboratory-scale reactor that could be used for the controlled polymerization of elastomer precursors such as butadiene and isoprene monomers. These monomers are low boiling and thus easily lost in conventional reactors. However, the reactor designed herein was demonstrated to be very appropriate for polymerizations at 50 or 60°C under relatively mild pressures. The availability of this reactor was crucial for the synthesis of a number of the elastomer systems described. Moreover, the reactor was designed in such a way that it should be amenable to scaleup by engineers concerned with producing larger amounts of the materials described within this report. Clearly, the quantities of the materials feasible in a university environment are not sufficient for commercial testing. The reactor was also useful for modification reactions such as hydrogenation and sulfonation. In the second phase of our work, hydrogenation reactions were studied extensively on both homopolymer elastomers as well as tri- and star-block elastomers based on t-butyl styrene. The model studies were very illuminating in the sense that they showed it was possible to quantitatively hydrogenate sensitive polymeric materials such as polyisoprene without significant chain degradation. This was demonstrated by measuring molecular weights before and after hydrogenation as well as by gel permeation chromatography (GPC) measurements. The resulting hydrogenated homopolymer elastomers were characterized by dynamic mechanical measurements as well as thermal analysis. The results indicated that although the glass temperature was not significantly changed, the modulus at room temperature was significantly increased. Indeed, this higher entanglement density remarkedly increases the dynamic elastic modulus at room temperature from about $10^6$ to $10^7$ megapaschals (M-P). An important conclusion is that saturated elastomers such as butyl rubber and various halogenated derivatives as well as the ethylene-propylene copolymer (EPDM) elastomers should be investigated in high performance applications.

The third area of progress dealt with the hydrocarbon soluble difunctional initiators. We have demonstrated with the system described herein that it is possible to grow living chains in both directions and produce telechelic elastomers bearing hydroxyl end-groups. Additionally, the material can be utilized to prepare triblock copolymer elastomers in one reaction step.

This type of information has been badly needed by commercial firms for many years. The resulting polydienes can also be hydrogenated using the techniques developed during this work. In the fourth area of research, further studies on ion-containing block and random copolymers were conducted. A variety of systems were examined including emulsion copolymers of alkyl acrylates and sulfonated styrene. These novel ion-containing elastomers are quite thermally stable due to the saturated alkyl acrylate backbone. However, we observed significant strengthening of the materials due to ion association of the sulfonate groups. Such materials have also been of interest in post-reaction modifications of saturated EPDM. It appears that the sulfonate groups can associate into at least multiplets and, possibly, clusters. The resulting associated ionic phase reinforces the covalent elastomer and provides additional thermomechanical stability at higher temperatures. Lastly, a significant effort was conducted in the area of reactive castable elastomers based upon soft, flexible segments linked together through polyurethane or polyurea type hard segments. This approach to castable elastomers certainly has a major potential for developing reactive, automated, fully-cured systems of high strength and good abrasion resistance. In the work conducted herein, soft polyether segments were modified to produce essentially all urea hard segments. A novel chemical approach utilizing tertiary alcohols as reactive intermediates was discovered and investigated. Essentially, the tertiary alcohol can undergo intermediate carbamate formation which subsequently rearranges at higher temperatures to produce a urea hard segment. These materials were shown to produce very high strengths when prepared properly and an adequate thermo-mechanical stability which would be of interest for the upper temperatures required in high performance elastomers. Aspects of the morphology and physical properties of these novel elastomers were also investigated and are reported herein.

## PREFACE

The author wishes to thank many helpful collaborators for preparation of this report. These include the graduate students, post-doctoral fellows, and faculty colleagues, especially G. L. Wilkes and T. C. Ward. In addition, the principal investigator would like to thank the technical monitor, Mr. Jacob Patt, for many helpful suggestions and discussions throughout the progress of this work.

TABLE OF CONTENTS

TABLE OF CONTENTS (continued)

LIST OF ILLUSTRATIONS

## LIST OF TABLES

## LIST OF SCHEMES

## 1.0. INTRODUCTION

Elastomeric materials currently utilized at this time are often based on styrene butadiene copolymers prepared by emulsion polymerization. Although they have been utilized for many years and are very important materials, there may be some synthesis variations that can produce new and improved properties, especially for high performance applications. Elastomeric or rubbery polymers are defined by the detailed shape and chemical composition of the macromolecules. Polymers which are rubbery possess relatively weak interchain forces and usually do not have sufficient symmetry to crystallize to any great extent. As one adds stronger interchain forces to the molecule the rubbery properties are gradually modified to those, for example, of fiber-forming materials. Copolymerization may be used to reduce polymer interchain forces and favor rubbery characteristics (for example, ethylene/propylene). On the other hand, it may be desirable to introduce polar groups into hydrocarbon polymers to selectively increase the interchain and intrachain forces. For example, the polar groups can alter the solvent resistance of the polymer, as is commonly done commercially with the so-called nitrile rubber, a copolymer of butadiene and acrylonitrile. Carboxylic groups are of interest since their strong polar nature can increase interchain forces and perhaps increase the strength of the polymer. Carboxyl-containing rubbers have been studied in detail and they demonstrated a number of interesting properties. Hydrogenation of polydienes may also be feasible to produce thermo-oxidatively more stable materials analogous to hydrogenated nitriles, ethylene-propylene copolymers or ethylene-propylene-diene tripolymers (EPDM).

A basic requirement for rubbery material is that it must consist of long flexible chain-like molecules that can undergo rapid rotation as a result of thermal agitation. In the practical sense this means an essentially amorphous polymer that is well above its glass-transition temperature (Tg). A further requirement is that the long chain linear molecules must be cross-linked by a few intermolecular bonds during processing to form an insoluble three-dimensional network. Ordinarily this is done by the reaction of a polydiene with sulfur and accelerators. The thermoplastic elastomers do not require chemical crosslinks, rather they depend upon physical network formation derived from glassy or semi-crystalline block structures. It is now becoming apparent that the ion-containing elastomers are somewhat analogous to other thermoplastic elastomers (TPE's), in the sense that the small concentration of ions that are generated actually can aggregate into a physical domain. The nature of the aggregation depends upon the concentration of ionizable groups, their nature (i.e., are they carboxylates or sulfonates), and the nature of the counter-ion, for example, Zn versus Na, etc. In any event, it is apparent that the upper transition temperature of a multiphase thermoplastic elastomers would have to be significantly higher than its use temperature. Currently available systems based on polystyrene hard blocks (Tg ≈ 100°C) or thermoplastic polyurethanes do not display sufficient thermomechanical stability.

In the current study, the following fundamental research areas were investigated:

- Hydrogenation techniques for polydiene homo- and block copolymers which would be applicable to both nonpolar and polar elastomers.
- Utilization of t-butylstyrene as a higher temperature hard block (Tg ≈145°C).
- Development of a difunctional lithium based initiator which could produce high 1,4-polydienes, block copolymer elastomers and functionally terminated polyols.
- Synthesis of model urea-linked segmented copolymers which could extend the thermomechanical utility of highly automated "cast" or RIM elastomers.
- The design and implementation of an automated scalable laboratory polymerization reactor.

## 2.0 OBJECTIVE

The objective of this work was to conduct a fundamental investigation of new polymer syntheses to elastomer materials which would be useful ultimately for the preparation of higher performance elastomer materials.

## 3.0 CONCLUSIONS

A laboratory scale low-pressure reactor was invented and constructed which enables chemists and chemical engineers to prepare very well defined elastomeric materials via living polymerization. It was also shown to be suitable for important modification reactions such as hydrogenation and, indeed, sulfonation. Work described throughout the project demonstrated hydrogenation of unsaturated polydiene elastomers to nearly 100 percent reduction levels. The resulting product is remarkedly more stable than either polyisoprene or polybutadiene. It is well known that the former undergoes chain scission and the latter undergoes chain cross-linking. Thus, the saturated systems are of particular interest for the demanding temperatures required in high performance elastomer systems. The results demonstrated here could be extended to other elastomeric polymers such as the nitrile rubbers if desired. Important hydrocarbon-soluble organolithium difunctional initiators were produced which offer attractive routes for the synthesis of hydrocarbon-based, reactive telechelic elastomers suitable for further endlinking studies. In addition, the difunctional initiators allowed the growth of macromolecular chains in two directions, thus permitting the synthesis of A-B-A thermoplastic block copolymer elastomers in one step. Ion-containing block and random copolymers were investigated which show some potential towards being more

thermally stable than unsaturated materials while at the same time providing higher strength properties.

Thus, alkyl acrylate-sulfonated styrene produced elastomers which were quite thermally stable and yet showed good mechanical strength even in the "green" thermoplastic state. Further vulcanization of these elastomers should be quite fruitful in obtaining attractive new ion-containing elastomeric materials. Additional novel studies were initiated wherein one could produce block-like ion structures through the use of alkyl methacrylate-type polymerizations followed by hydrolysis. These systems could show important new advantages relative to the randomly placed ion-containing elastomeric block copolymers. The potential of polyurea-cast elastomers was further elucidated. It was demonstrated that the polyurea provided excellent reinforcing mechanisms to produce high strength elastomers. Moreover, the thermomechanical stability was significantly enhanced relative to more conventional carbamate or urethane-type hard segments. The novel route to producing these elastomers focused on the use of t-butyl alcohol reactive intermediates. These materials could produce very high-strength foams directly and, given proper reactive thermoplastic processing, could be devolatilized and remolded into tough high-strength elastomers.

## 4.0 RECOMMENDATIONS

It is recommended that further research be conducted in the area of hydrogenated model homopolymer and block copolymer elastomers, possibly focusing on more polar elastomers such as the unsaturated nitrile-containing systems. Block polymers based upon difunctional initiators should be further investigated as routes for thermoplastic elastomers and high-temperature, thermally stable elastomers. Block-like ion-containing copolymers based upon carboxylate or sulfonate endlinked units should be further studied. The general area of polyureas represents an attractive route to a castable material which may have adequate thermal stability for the intended applications.

In addition to the above areas of fundamental research, it is recommended that a portion of the future work be directed toward scaleup of these concepts and direct utilization into high performance elastomers. As a short-term recommendation, one should investigate properly compounded, high-performance, commercially available EPDM elastomers, butyl rubber systems, and their halogenated counterparts. It is felt that adequate thermal stability does exist with both of those saturated elastomers and that further studies on a practical basis should be investigated as soon as possible. Further investigation of development and newly commercialized materials should also be explored. In particular, hydrogenated nitrile rubbers are believed to be available in both Japan and Germany. On the basis of the work conducted in this study, they should definitely be evaluated for the subject applications. Further, second stage studies should also utilize the recently commercialized, sulfonated EPDM type of elastomers as further outgrowth of the basic data generated in this study.

## 5.0 DISCUSSION

### 5.1. Laboratory-Scale, Low-Pressure Reactor for Living Polymerization and Polymer Modification Studies

5.1.1. General. The synthesis of block copolymers by anionic polymerization is a well-documented technique (1-3) and provides precise control over many important polymer parameters such as molecular weight and distribution, stereochemistry, end group functionality, topology, etc. Thus, it is often the technique of choice in the preparation of well-defined or perhaps model polymers for subsequent structure-property studies (6). Detailed studies often require relatively large amounts of sample (20-50g) for a broad range of analysis (rheological, solid-state thermal mechanical, solution, etc.), and are very often facilitated by the ability to sample a living polymerization or polymer modification reaction as a function of time (as in kinetics studies). Classically rigorous vacuum rack methods (1-5) of anionic polymerization as described by Morton and Fetters (1) and many others, do not conveniently allow the preparation of large samples and virtually prohibit reaction sampling. Consequently, our laboratory has chosen to set up, in addition to our high-vacuum system, several reactor systems centered around low-pressure, inert atmosphere, glass-bowl and stainless steel vessels that are commercially available (7). These systems not only provide for monomer and solvent storage, transfer, purification, measurement, polymerization, and sampling, but also provide a safe and convenient means by which to handle various important and perhaps hazardous monomers such as 1,3-butadiene, ethylene oxide, ethylene, alkyl methacrylates, etc. It is the design of these reactor systems and typical results that may be obtained by their use that is the focus of this discussion.

5.1.2. Reactor System Design. In this section we will briefly describe the design and operation of the integrated reactor system and in slightly more detail, the design and some operations of the reactor itself.

The reactor system employed by our laboratory for anionic polymerization is schematically represented in Figure 5.1-1. Nearly identical systems are also in use by us for coordination polymerization and anionic to coordination transformation reactions.

5.1.2.1. Storage. The monomer (isoprene & butadiene) and solvent (cyclohexane) storage tanks are commercially available (8) 20 pound low pressure gas (LPG)-type cylinders each having a valve modified by us to extend an eduction tube to the bottom of the cylinder while providing a 50 pounds per square inch (gauge) (psig) cylinder atmosphere of purified nitrogen.

5.1.2.2. Measurement. The volumetric measurement of monomer and solvent charges is accomplished by the use of appropriately sized [200-1000 milliliter (ml)] holding tanks (8) equipped with capillary sight glasses and calibrated so that the weight of a charge may be easily calculated, given its density. The holding tanks are plumbed so that they may be

vented, charged with monomer or solvent, pressurized with purified nitrogen, drained to waste, or drained to either of two or more reactors. Metering pumps may be alternately employed to slowly charge the contents of a holding tank, or to circulate the contents of a reactor through a flow-cell for ultraviolet (UV)/visible spectroscopy.

5.1.2.3. Purification. As a given holding tank is charged, the monomer or solvent flows from the storage tank and through steel or stainless steel columns packed with activated alumina (for deinhibition) and molecular sieves (for dehydration). These purification columns must be sized appropriately to provide adequate purification without permitting excessive monomer residence times, which may result in premature polymerization and column fouling. Diene monomers prepared in this manner are typically added to living polymerizations with less than 0.5 percent termination. Alternatively, they may be distilled from organometallic reagents for fundamental research efforts requiring even more rigorous purification.

5.1.2.4. Polymerization. The reactor vessel (see Figure 5.1-2) is a commercially available (7) unit consisting of a heavy-walled, flint glass bowl (hydrostatically tested to 1000 psig), a stand, a stainless steel (S.S.) top plate, and magnetically coupled stirring assembly. This basic unit has been equipped by us with a 1/4-inch outer diameter (O.D.) S.S. heat-exchange coil, a drive system and two S.S. high-lift pitch impellers (8) (for effective stirring of extremely viscous solutions), thermocouple and thermister probes (for temperature measurement and control), a 3/8-inch inner diameter (I.D.) septum port, and various other S.S. fittings and tubing to provide a monomer and solvent inlet, and an inlet/vent for purified nitrogen. A scale drawing of the reactor and some of its components and plumbing is provided as Figure 5.1-2.

5.1.2.5. Temperature control. Temperature control of the reactor is provided by a system (schematically shown in Figure 5.1-1) consisting of a single normally closed solenoid valve, and a relay-equipped thermister-type controller (8). The controller opens (or closes) the solenoid valve when the reactor temperature exceeds (or lags) the set point by 0.1°C, and thereby provides (or inhibits) an increased flow of cold water into a regulated steam/water heating mixture. Constant temperature control is thus provided with fluctuations of about ±0.5°C. Subambient temperature control may alternatively be obtained by placing the solenoid valve downstream from the reactor coil and connecting a pressurized liquid nitrogen supply to the coil inlet.

5.1.2.6. Reactor operation. Before each polymerization, the reactor is typically "conditioned" by the following procedure. A solvent charge of 500-600 ml (700 ml capacity) is heated to 60°C while stirring rapidly [circa 750 revolutions per minute (rpm)], and a two-millimole (mmol) charge of 1,1 diphenylethylene is made with a syringe. Secondary-butyllithium is added dropwise with a syringe to the reactor until a pale yellow color is observed indicating the titration of all protonic impurities and the initial formation of diphenylhexyllithium. A two-mmol charge of butyllithium is made at this point and allowed to react with 1,1-Diphenyl ethylene (DPE) for several hours. A deep red color will then be present

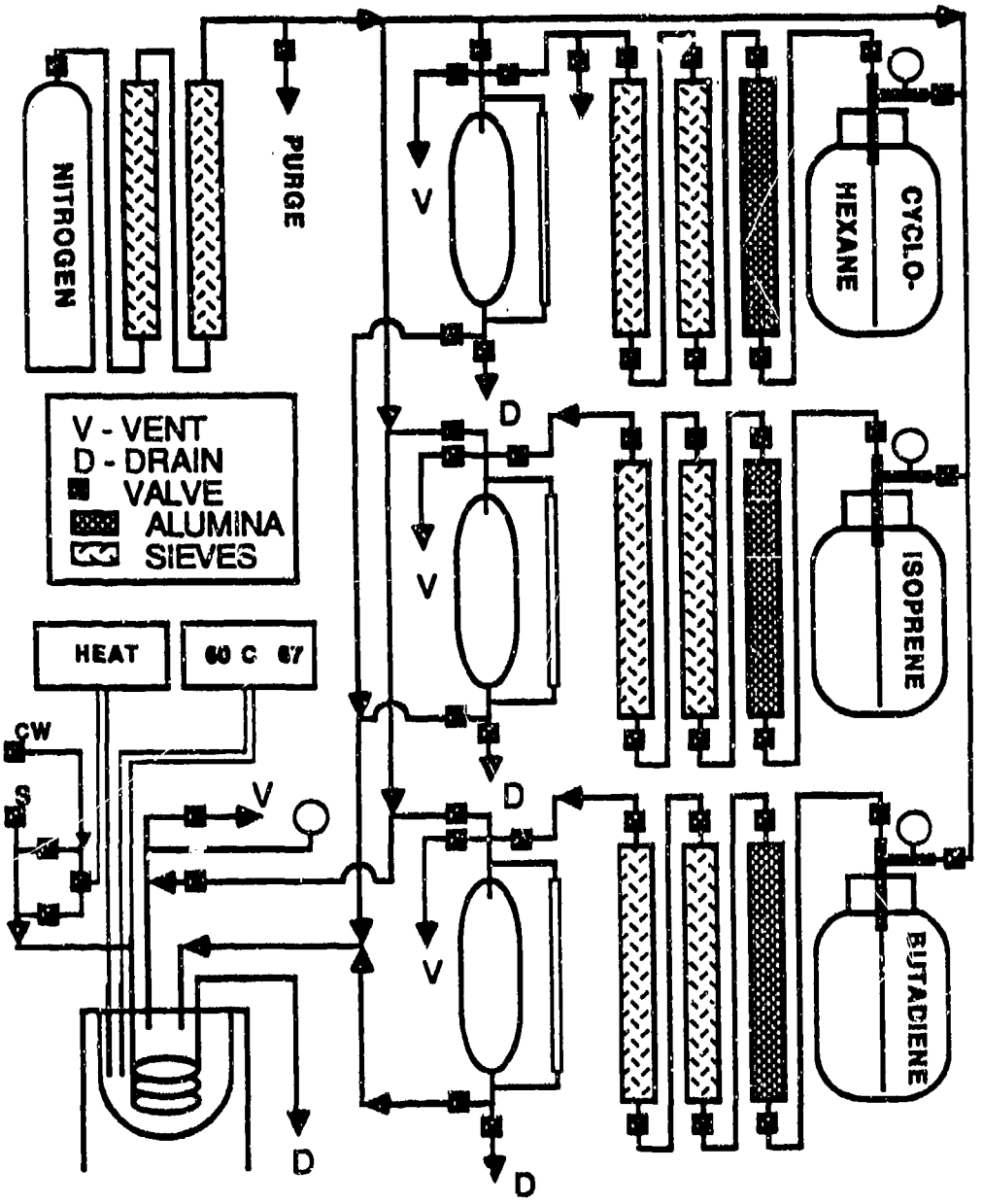


Figure 5.1-1. Anionic Polymerization Reactor Scheme

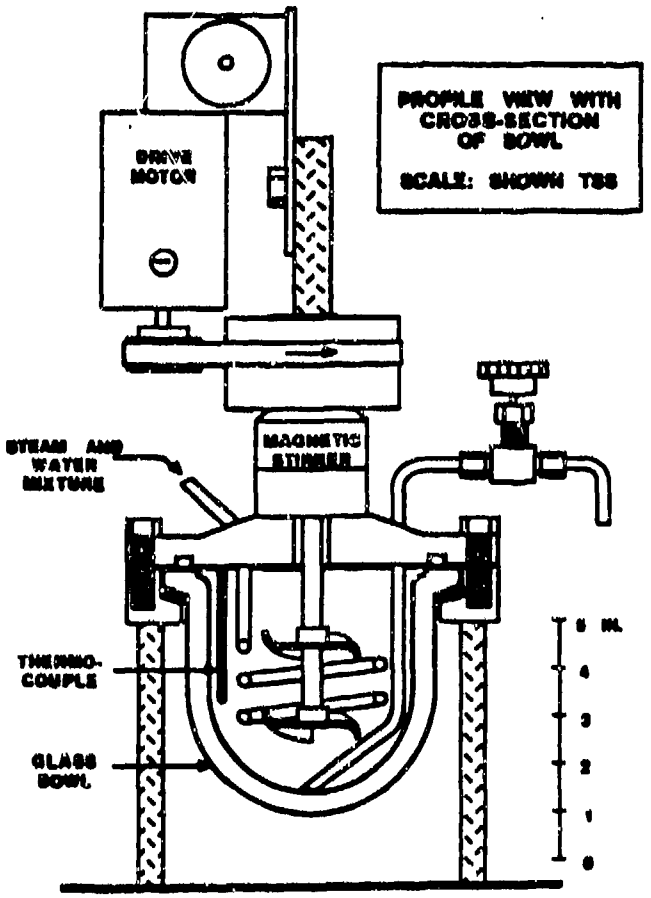


Figure 5.1-2. Anionic Polymerization Reactor

and persist if no additional impurities enter the system. The reactor is rinsed with fresh solvent immediately before charging the polymerization solvent. Polymerizations are typically performed at 50 to 60°C for periods of hours. The polymer solution is then terminated and drained from the reactor or hydrogenated in situ by an appropriate catalyst charge and hydrogen gas supplied through the dip tube. The reactor is then rinsed with solvent prior to reconditioning.

5.1.3. Results and Discussion. Using the reactor system outined above, we have prepared homopolymers, multiblock and star-block copolymers, and hydrogenated polymers of many types. Several examples of GPC chromatographs are included here as Figure 5.1-3. Figure 5.1-3(a,b) illustrates the preservation of a typical, narrow polyisoprene molecular weight distribution (MWD) as the polymer is catalytically hydrogenated in situ, after polymerization and methanol termination. Figure 5.1-3(c,d,e) illustrates the type of polydispersities (Pd) typically obtained in the multiaddition synthesis of star-block copolymers (6). Both of these examples are very useful in assisting to describe the well-defined nature of the block polymers that may be prepared using low-pressure, inert-atmosphere-type reactor technology.

5.1.4. Conclusions. From the figures and discussion provided above, one can begin to appreciate the increased safety, the semi-automated experimental reproducibility, the experimental convenience, and in most cases, the acceptable results that may be achieved through the application of low-pressure, inert-atmosphere reactor technology.

5.1.5. References.


1. M. Morton and L. J. Fetters, Rubber Chem. and Tech., 48, 35 (1975).

2. J. E. McGrath, Anionic Polymerization Kinetics, Mechanisms, and Synthesis, ACS Symposium Series 166, (1981).

3. A. Noshay and J. E. McGrath, Block Copolymers: Overview and Critical Survey, Academic Press, (1977).

4. R. Milkovich, Canadian Patent No. 712245 (Aug. 24, 1965).

5. M. K. Martin, T. C. Ward, and J. E. McGrath, in (2), p.557.

6. J. M. Hoover, T. C. Ward, and J. E. McGrath, Polymer Preprints, 26,1, 253, 1985; Advances in Polyolefins, T. Cheng Edit., inpress (1986).

7. Chemical Equipment Corporation, 7454 East 46th Street, Tulsa, OK 74145, (918) 743-2489.

| | <Mn> | Pd |
|---|---|---|
| a. | 102,000 | 1.05 |
| b. | 87,000 | 1.06 |
| c. | 23,500 | 1.07 |
| d. | 158,000 | 1.01 |
| e. | 1,200,000 | 1.14 |

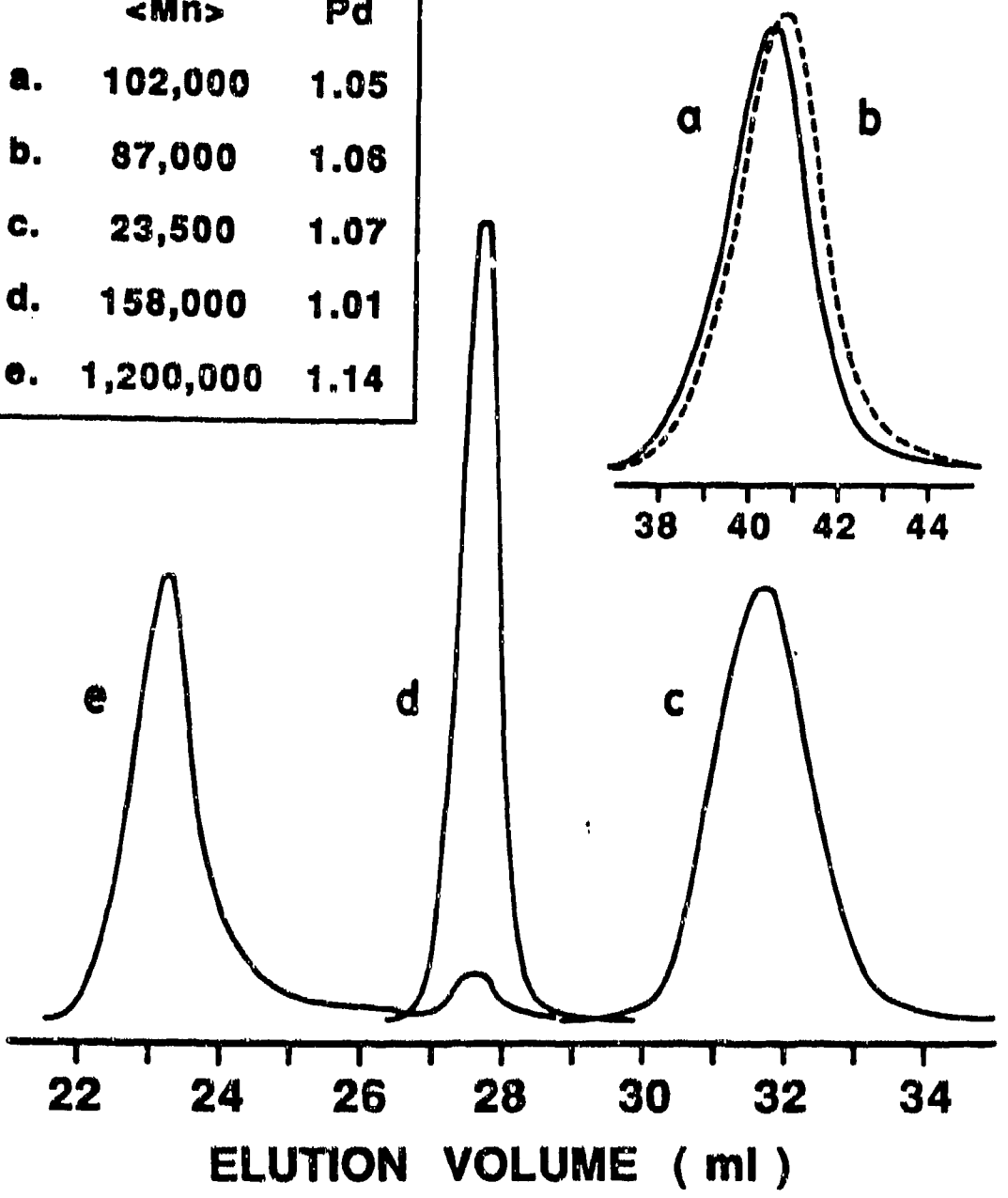


Figure 5.1-3. GPC Chromatograms of a. Hydrogenated Polyisoprene Homopolymer. b. Polyisoprene Homopolymer Precursor. c. Poly(TBS) First Block. d. Poly(TBS-Isoprene) Diblock. e. Poly(TBS-Isoprene) Starblock.

## 5.2. Hydrogenation of Model Homopolymer and Block Polymer Elastomers

5.2.1. Introduction. Anionic polymerization of dienes is well known to offer many advantages to the elastomer chemist who is seeking to prepare well-defined materials of narrow molecular weight distribution, with controlled architecture and end group functionality (1-12). In this section we will discuss some of our work on the synthesis and hydrogenation of model homopolymer and block polymer elastomers. Hydrogenated polyisoprene is an excellent model for ethylene propylene rubber or EPDM.

Unsaturated rubbers based on either polybutadiene (BR) or polyisoprene (NR or IR) have stability problems at temperatures thought to be important in high performance applications. Essentially BR overcrosslinks and IR or NR undergo chain scission. Thus, these two important base elastomers either become hard and inextensible, or very soft and tacky. Others, as well as ourselves, have demonstrated this phenomena via stress-relaxation measurements, and these are illustrated in Figure 5.2-1. Thus, PB is rigid after 100 minutes at 100°C, while PI is completely tacky after about 75 minutes at 100°C. These data illustrate the probably essential requirement of using saturated elastomers in high performance applications. Although commercial EPDM systems may be the most pragmatic approach, our work has generated meaningful, fundamental elastomer information.

Anionically prepared triblock and star-block copolymers of styrene with butadiene and isoprene have been widely synthesized and thoroughly studied by many investigators. These systems have also provided a basis for many commercially important thermoplastic elastomers including KRATON, SOLPRENE, and others. The thermal and mechanical properties of these materials are well established in their microphase-separated morphologies which may be tailored, along with other polymer parameters, to achieve specific physical properties. Anionic polymerization allows the controlled synthesis of block polymers, and thus facilitates the precise engineering of mechanical properties such as tensile strength and modulus by controlling parameters such as block molecular weight, purity and microstructure. A suitable reactor for conducting these experiments was designed and discussed in Section 1 of this report.

Relatively little attention (20,21) has been given to ring substituted styrenic monomers such as paramethylstyrene (PMS) and tertiary-butylstyrene (TBS). These monomers may, in some cases, provide the opportunity to improve the high temperature performance of conventional S-B-S and S-I-S systems. At the same time, other new systems permit one to perform fundamental studies on the role of microphase separation in the structure-property relations of well-defined, thermoplastic, block copolymers. Some investigations of solution behavior have already been reported (19). It has been previously demonstrated (20) that the high miscibility of triblock copolymers of poly(TBS) with polydienes limits the degree of phase separation that can be conventionally achieved in these block copolymers, and thus influences their physical properties. Since polyolefins are believed to exhibit lower solubility parameters then polydienes, we decided to investigate hydrogenation as a method of altering the degree of

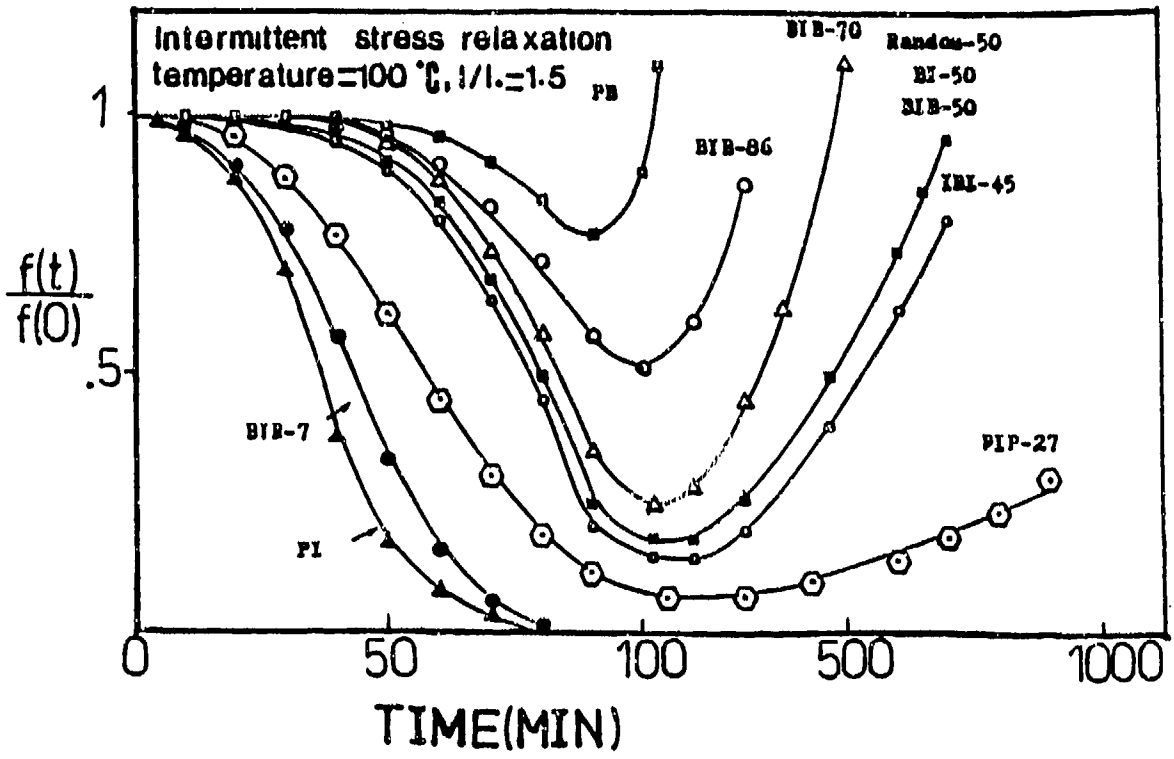


Figure 5.2-1. Effect of Copolymer Structure and Architecture on the Intermittent Stress-Relaxation of Poly(butadiene)-Poly(isoprene) Peroxide-Cured Networks

miscibility. In addition, careful hydrogenation without degradation can be conducted to produce elastomeric polyolefin block polymers having the added benefits of enhanced thermal and oxidative stability and improved mechanical properties. In fact, Fetters and coworkers (20) briefly noted that their hydrogenated sample showed improved mechanical strength.

Catalytic hydrogenation has thus been employed as a tool for enhancing microphase separation in as variety of poly(TBS)-polyisoprene block copolymers and will be briefly discussed. A description of the synthesis and catalytic hydrogenation of homopolyisoprene and poly(TBS)-polyisoprene star block elastomer follows.

5.2.2. Experimental. Homopolymers and radial or star-shaped block copolymers elastomers were synthesized under nitrogen pressure and hydrogenated in the low-pressure glass bowl/stainless steel reactors (described above in Section 1). A procedure used for the synthesis of a star block poly(t-butyl styrene)-polyisoprene elastomer follows. Homopolyisoprene was similarly prepared.

Cyclohexane [$99^+$ mole (mol) percent] was obtained from Phillips Petroleum Company and used as the polymerization solvent. It was stored under a dry nitrogen atmosphere and purified by transfer through steel columns containing molecular sieves. A solvent charge of 436 ml [340 grams (g)] was measured in a calibrated holding tank and transferred to a 700 ml reactor. The solvent was heated to 50°C while stirring under a dry $N_2$ atmosphere of 10 psig.

T-butyl styrene (TBS) (95 percent para isomer) was provided by the Dow Chemical Company. It was purified by exposure to activated alumina, and stored at 5°C under a dry $N_2$ atmosphere. A charge of 18.2 ml (16 g) TBS was measured with a 20 ml syringe and transferred to the reactor.

Secondary butyllithium (1.37 M in hexane) was provided by Lithium Corporation and added dropwise to the reactor via a 1-ml syringe. After the addition (titration) of 0.07 ml, a pale yellow color was observed to persist and an initiator charge of 0.47 ml (0.64 mmol) was added. The orange-colored polymerization was allowed to proceed for 60 minutes before a 30 ml sample of "living" poly(TBS) was removed from the reactor and terminated. GPC characterization using polystyrene standards indicated a peak molecular weight of 22,700 g/mol with a polydispersity of 1.15.

Isoprene was provided by The Goodyear Tire and Rubber Company and purified by transfer through steel columns containing activated alumina and molecular sieves, followed by distillation from dibutylmagnesium. A charge of 66 ml (45 g) was measured and transferred to the reactor via syringe. The resulting colorless polymerization was allowed to proceed for 2 hours at 50°C before a 30 ml sample was removed and terminated. GPC analysis of this diblock copolymer indicated a peak molecular weight of 120,000 g/mol with a polydispersity of 1.10, based on polystyrene standards.

Practical grade divinylbenzene (DVB) was purified by stirring with powdered calcium hydride, followed by exposure to neutral alumina and vacuum distillation from dibutylmagnesium. Purified DVB was diluted with purified hexane to obtain a 0.72 M working solution. Next, 5.4 ml 0.72 M DVB (3.84 mmol) was syringed into the reactor, producing a red color within several minutes. This linking reaction was allowed to proceed for 2 hours at 60°C after which the "living" system was terminated with 0.5 ml high performance liquid chromatography (HPLC) grade, degassed methanol. GPC analysis of this polymer indicated a peak molecular weight greater than $10^6$ g/mol with a polydispersity of 1.2, suggesting that the radial topology molecule contains at least 8 to 10 arms. FTIR and FT $^1$H NMR analysis of this polymer indicated that the polydiene microstructure consisted of 72 percent cis-1,4, 22 percent trans-1,4 and 6 percent 3,4 polyisoprene, which was in agreement with expectations. Membrane osmometry was conducted with a WESCAN Model 231 osmometer in Toluene. GPC analysis utilized a Waters unit in THF fitted with 5 columns and a refractive index detector.

Catalytic hydrogenation of the above star-block copolymer was accomplished in situ (18). The polymer solution was cooled to 50°C and purged well with hydrogen. A preformed catalyst was added via syringe and a 50 psig hydrogen atmosphere was maintained for up to 24 hours. The catalyst was prepared by adding 0.228 g nickel octoate (0.66 mmol or 0.1 mol percent based on polyisoprene) and a magnetic stirring bar to a 50 ml glass serum bottle which was then sealed with a septum and purged well with $N_2$. Then, 15 ml purified cyclohexane was added to dissolve the $Ni(oct)_2$. Triethylaluminum, 1.13 ml (1.65 mmol), was syringed into the bottle dropwise while stirring vigorously. An opaque, black colloidal suspension formed immediately and was allowed to stir for 10 minutes at room temperature. The catalyst was then added to the reactor at 50°C via syringe. Fourier transform infrared spectroscopy (FTIR) (Nicolet MX-1) and Fourier transform (FT) $^1$H nuclear magnetic resonance (NMR) (IBM-270) were used to observe the rate of the hydrogenation reaction. These methods indicated greater than 99.9 percent saturation of the polydiene homopolymer after 24 hours. The copolymers were not quantitatively reduced, but >90 percent was achieved.

Dynamic mechanical thermal analysis (DMTA) (Polymer Laboratories) and differential scanning calorimetry (DSC) (Perkin Elmer Model 2) have been employed to assess the thermal and mechanical behavior of poly(TBS)-polyisoprene star block copolymers, polyisoprene homopolymers, and the hydrogenated derivatives. Thermoplastic elastomers containing 15 to 25 weight percent poly(TBS), and rubber modified thermoplastics containing 60 to 75 weight percent poly(TBS) have been studied.

Stress-strain and stress relaxation experiments were performed with an Instron Model 1130 on four series of elastomeric block copolymers in order to observe their large deformation, property response to progressing and hydrogenation-induced microphase separation characteristics.

5.2.3. Results and Discussion.

5.2.3.1. Synthesis and Characterization. Five series of star-block copolymers were synthesized and hydrogenated to various levels from 0 to >95 percent. Four of these series were of the same composition (25 weight percent poly(TBS), and differed only in the molecular weight of the poly(TBS) blocks which was varied from 10,000 to 25,000 g/mol. These polymers were characterized by DSC, DMTA, and stress-strain experiments. The fifth series was of a non-elastomeric composition (60 weight percent poly(TBS)), and was characterized by DSC and DMTA experiments. Linear polyisoprene homopolymers of approximately 50,000 g/mol or 100,000 were also synthesized and hydrogenated for a series of "control" experiments to examine only the polyisoprene block. These experiments included FT-IR, NMR, DSC, DMTA, GPC, and membrane osmometry analysis.

FT-IR absorbance spectra obtained as a function of percent hydrogenation are shown in Figures 5.2-2 through 5.2-5. When the absorbance peaks for unsaturation are normalized by their reference peaks, they may be ratioed to those in the unhydrogenated spectrum to determine the levels of residual unsaturation. The accuracy of this technique has been confirmed and calibrated by FT $^1$H NMR experiments. Very low levels of unsaturation are possible.

It has not been well appreciated in the past that polyisoprene may be quantitatively catalytically hydrogenated to a "stiffer" and more thermally and oxidatively stable material without the occurrence of degradation. That such well-defined modification may be performed is demonstrated by the information in Figures 5.2-6 and 5.2-7. The molecular weight (mol. wt.) distribution and the number average molecular weight (<Mn>) of polyisoprene hydrogenated ca. 99 percent are virtually unchanged except for a small theoretical increase in <Mn> (ca. 3 percent is expected theoretically from the addition of hydrogen).

In Figure 5.2-8, dynamic mechanical behavior shows that the hydrogenation of polyisoprene to a poly(ethylene-propylene) elastomer, increases the modulus of the elastomer nearly an order of magnitude at room temperature. Most likely this is related to fundamental changes in the entanglement coupling density, or molecular weight between crosslinks.

Figure 5.2-9 is an example of DMTA data for an unhydrogenated star-block elastomer containing 25 weight percent poly(TBS) at 25,000 g/mol. $\text{Log}_{10}$ flexural modulus and tangent delta are plotted as a function of temperature at 1 Hz. The absence of a high-temperature damping peak and the broad low-temperature relaxation are characteristic of a highly phase-mixed block polymer. The polyisoprene and poly(TBS) phases have mixed sufficiently to cause "contamination" of the matrix rubber with the glass, broadening the low temperature relaxation and plasticizating the glass "cross-linking" phase, which essentially eliminates any intermolecular connectivity at temperatures above the lower glass transition. When this same star block polymer is hydrogenated approximately 90 percent, the low-temperature relaxation sharpens greatly (Figure 5.2-9), the room temperature modulus

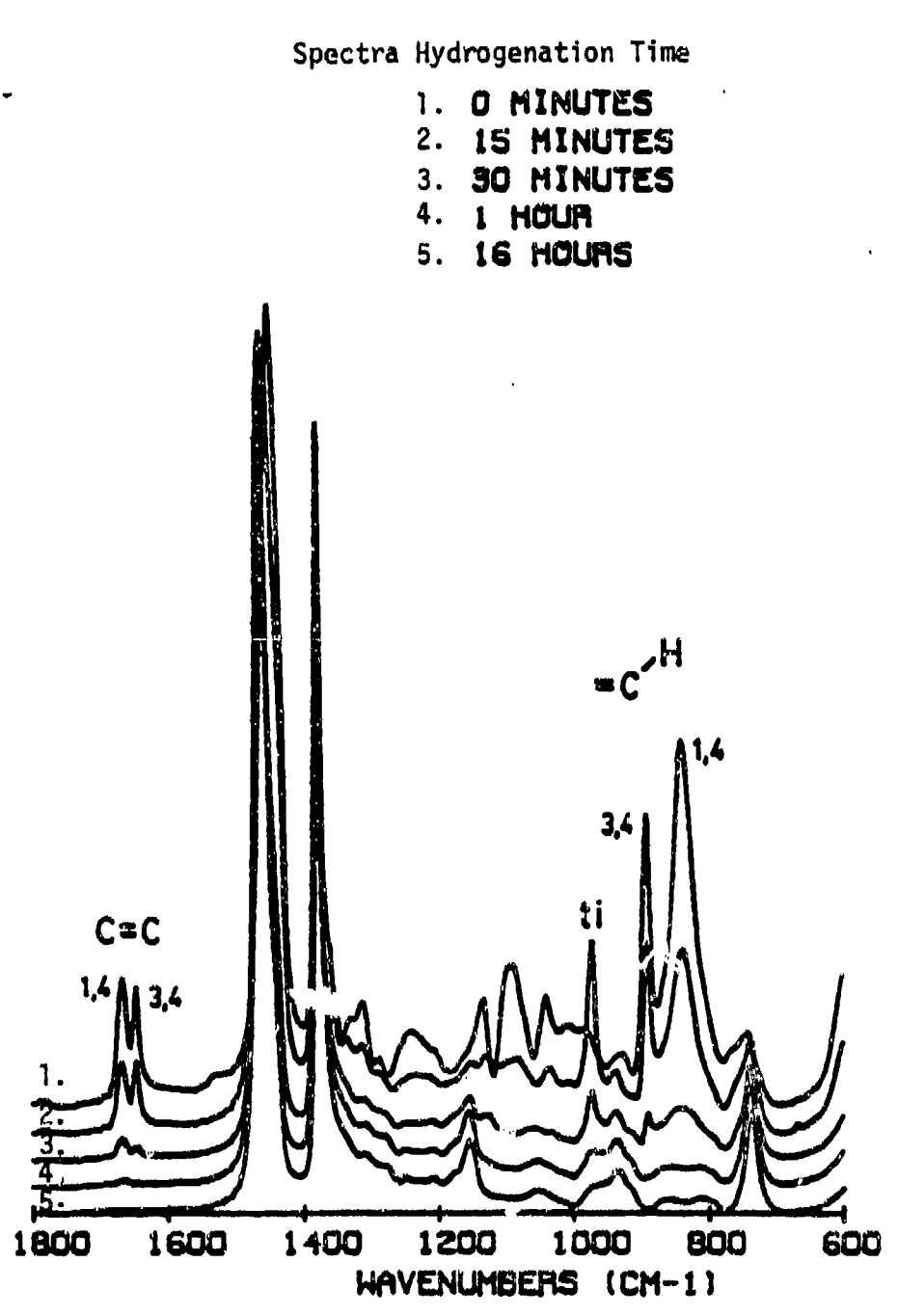


Figure 5.2-2. FT-IR Spectra of Polyisoprene, H0039I Hydrogenated at 50°C, 50 psig Hydrogen 3/1 Triethylaluminum/Nickel Octoate 0.1 mole percent Nickel Octoate

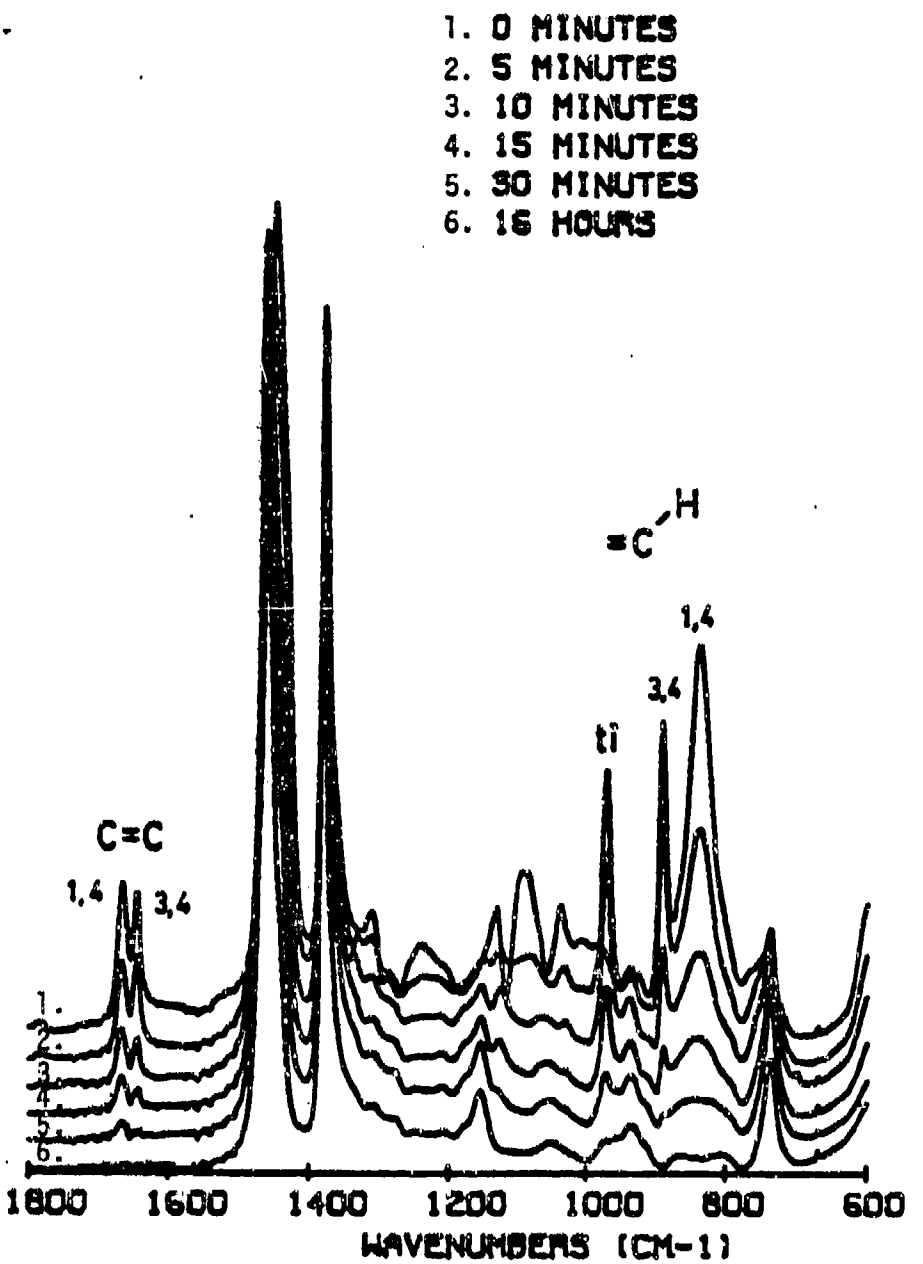


Figure 5.2-3. FT-IR Spectra of Polyisoprene, H0040I Hydrogenated at 80°C, 50 psig Hydrogen 3/1 Triethylaluminum/Nickel Octoate 0.1 mole percent Nickel Octoate

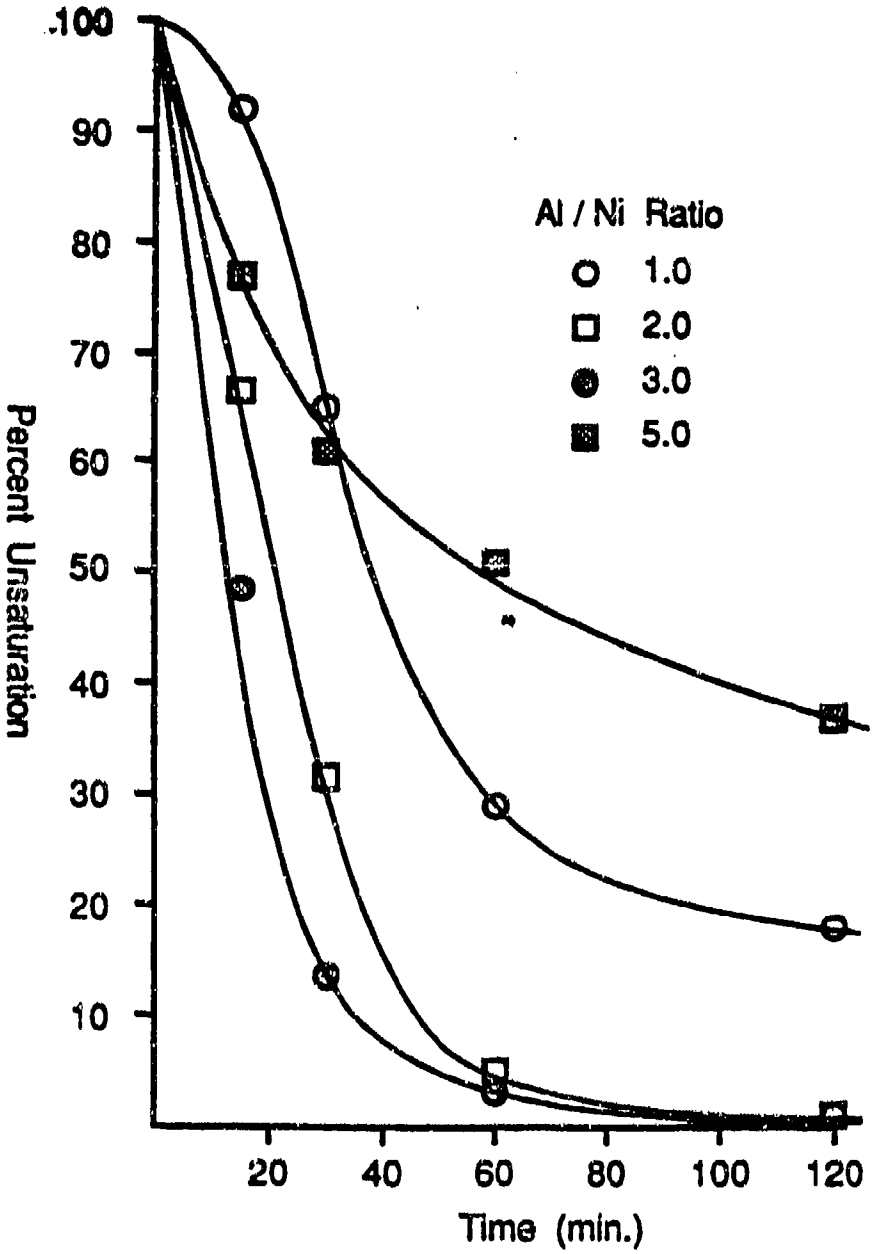


Figure 5.2-4. Percent Unsaturation vs. Time for Hydrogenation at 50°C, 50 psig Hydrogen, 0.1 mole percent Ni FT-IR at 890 $cm^{-1}$

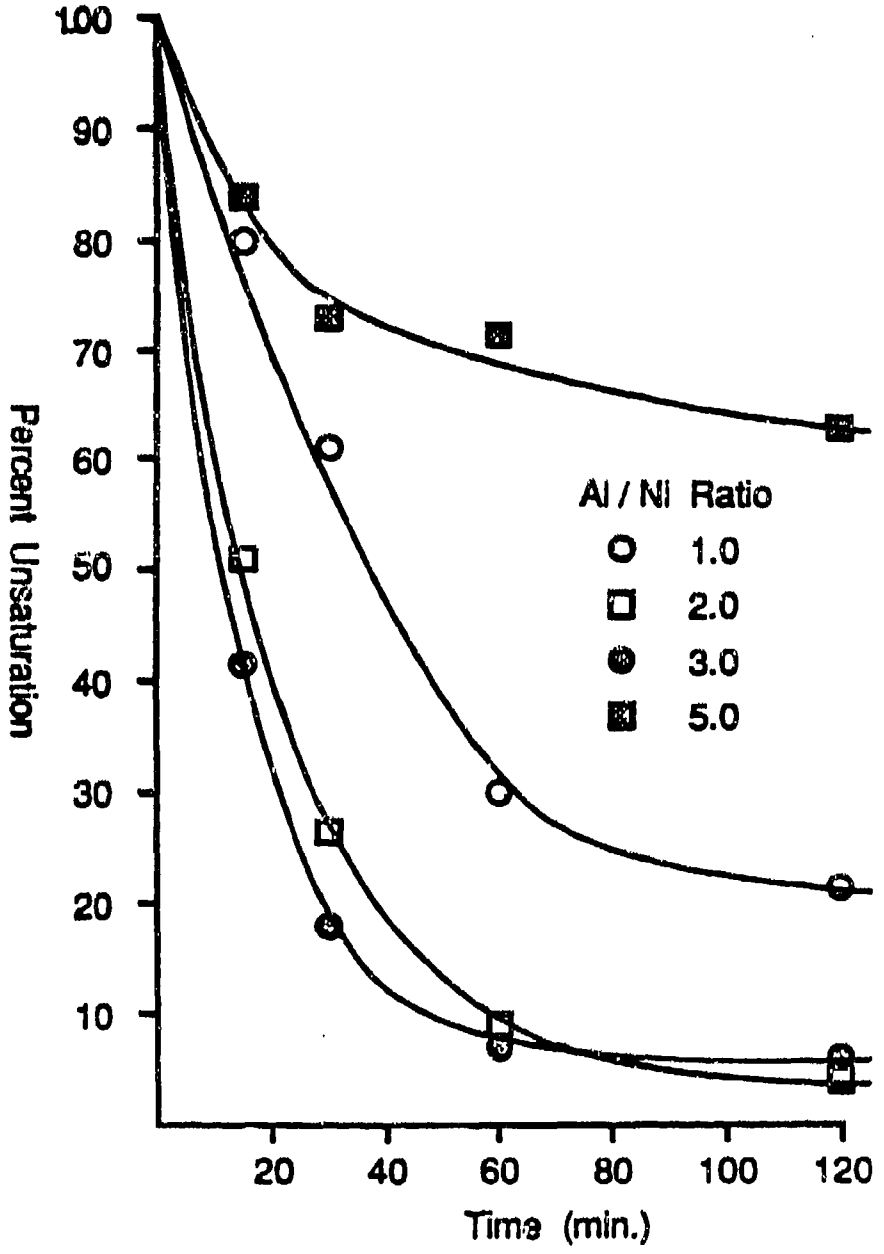


Figure 5.2-5. Percent Unsaturation vs. Time for Hydrogenation at 50°C, 50 psig Hydrogen, 0.1 mole percent Ni FT-IR at 1665 $cm^{-1}$

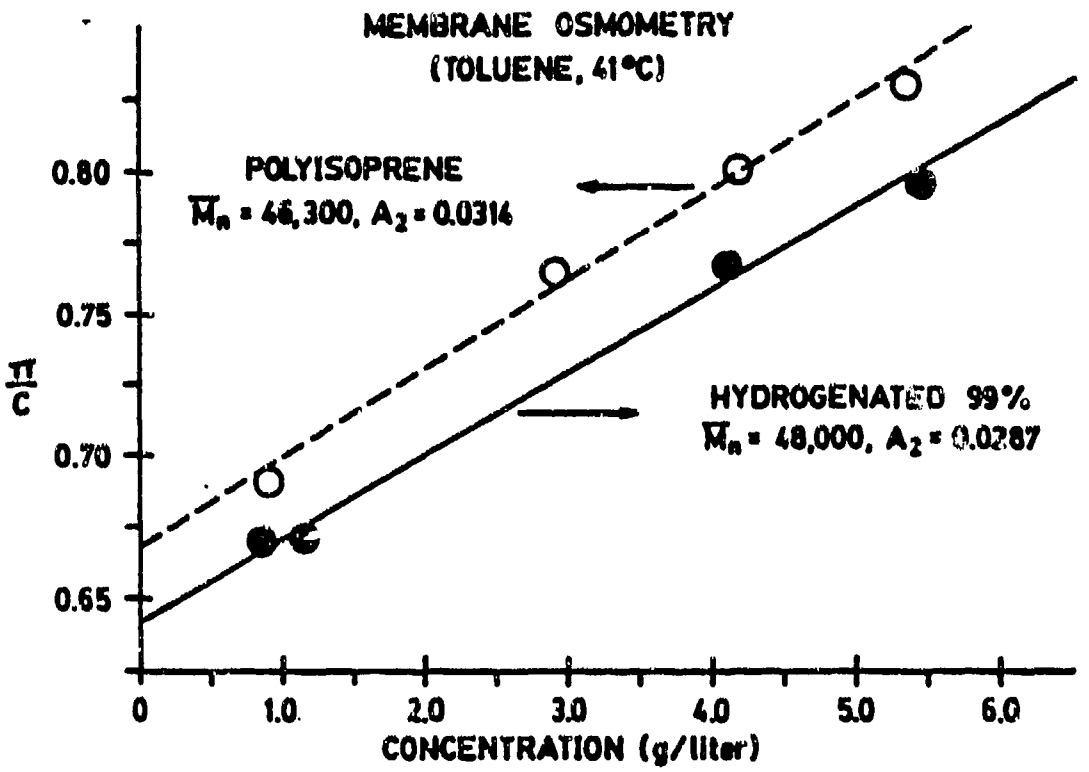


Figure 5.2-6. Membrane Osmometry Measurement of the $\bar{M}n$ of Polyisoprene Before and After Hydrogenation

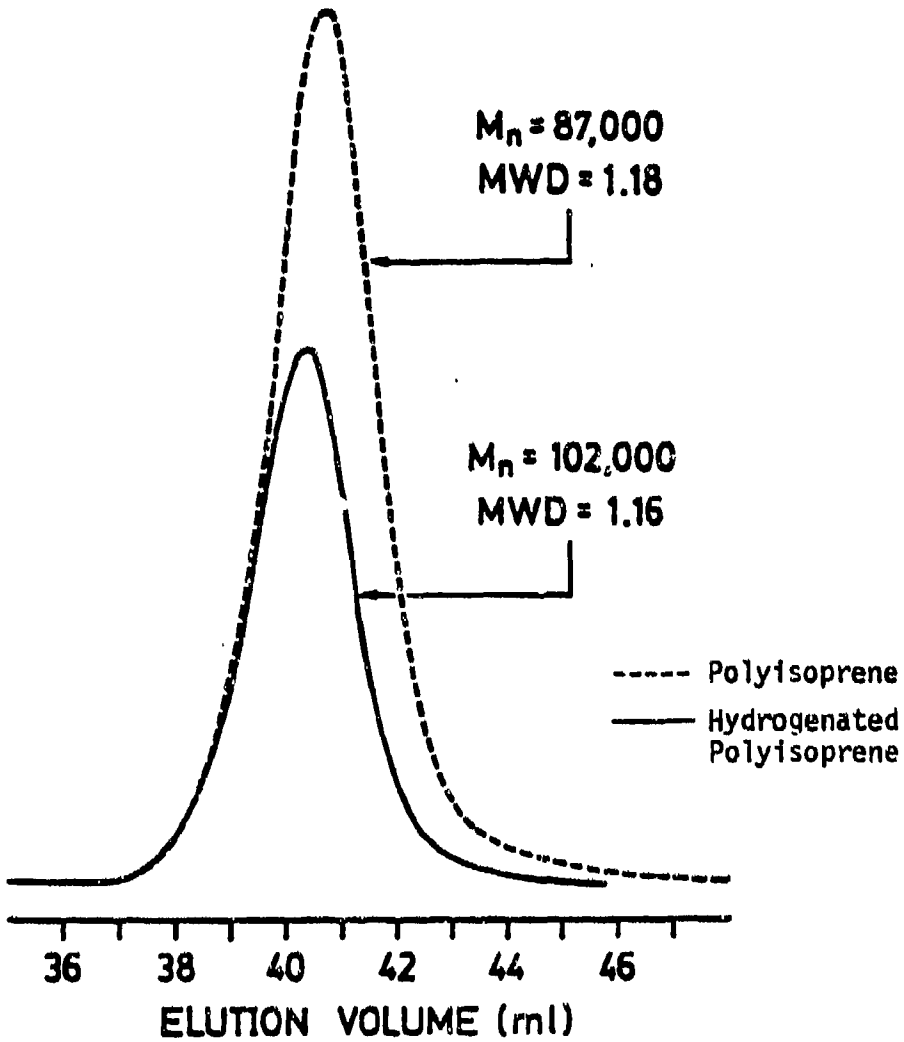


Figure 5.2-7. GPC Analysis of Polyisoprene Hydrogenated 16 Hours, 80°C

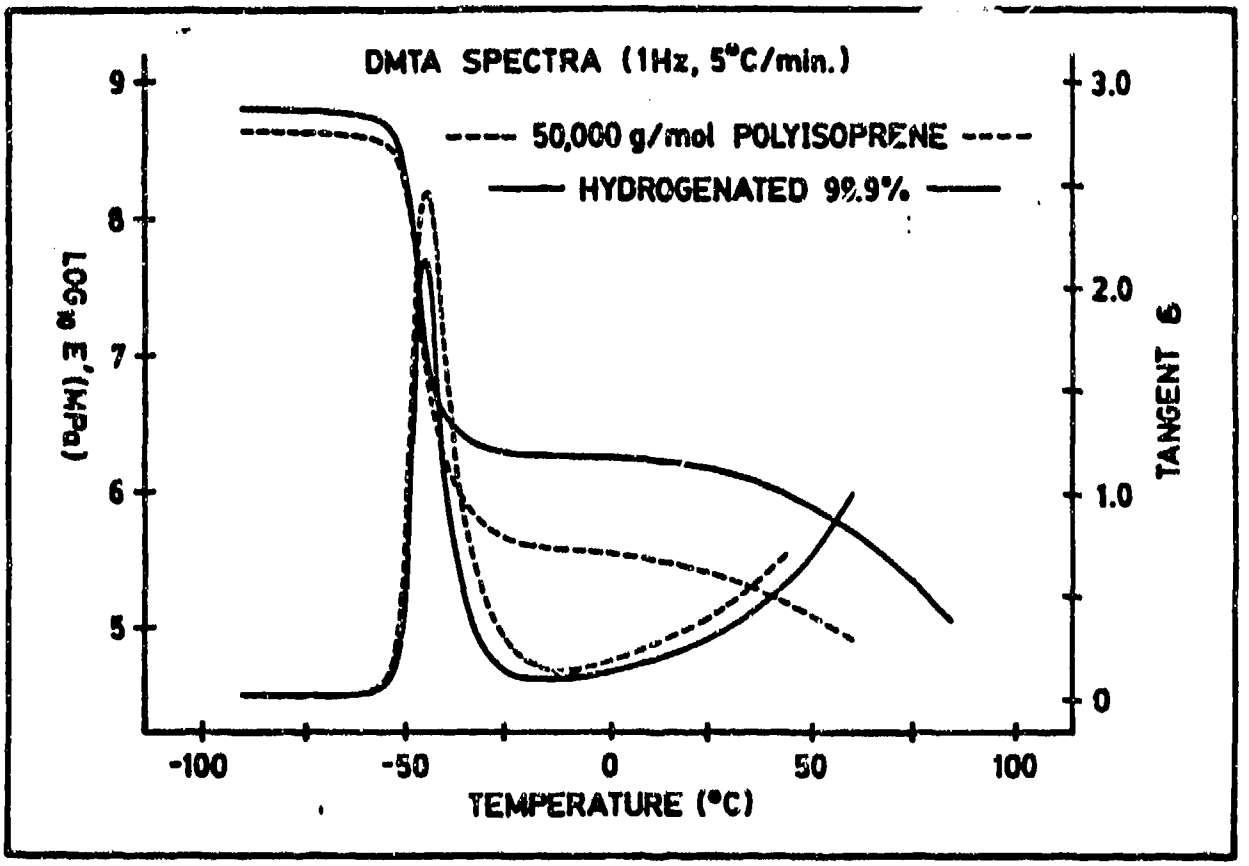


Figure 5.2-8. DMTA Spectra (1Hz, 5°C/min.)

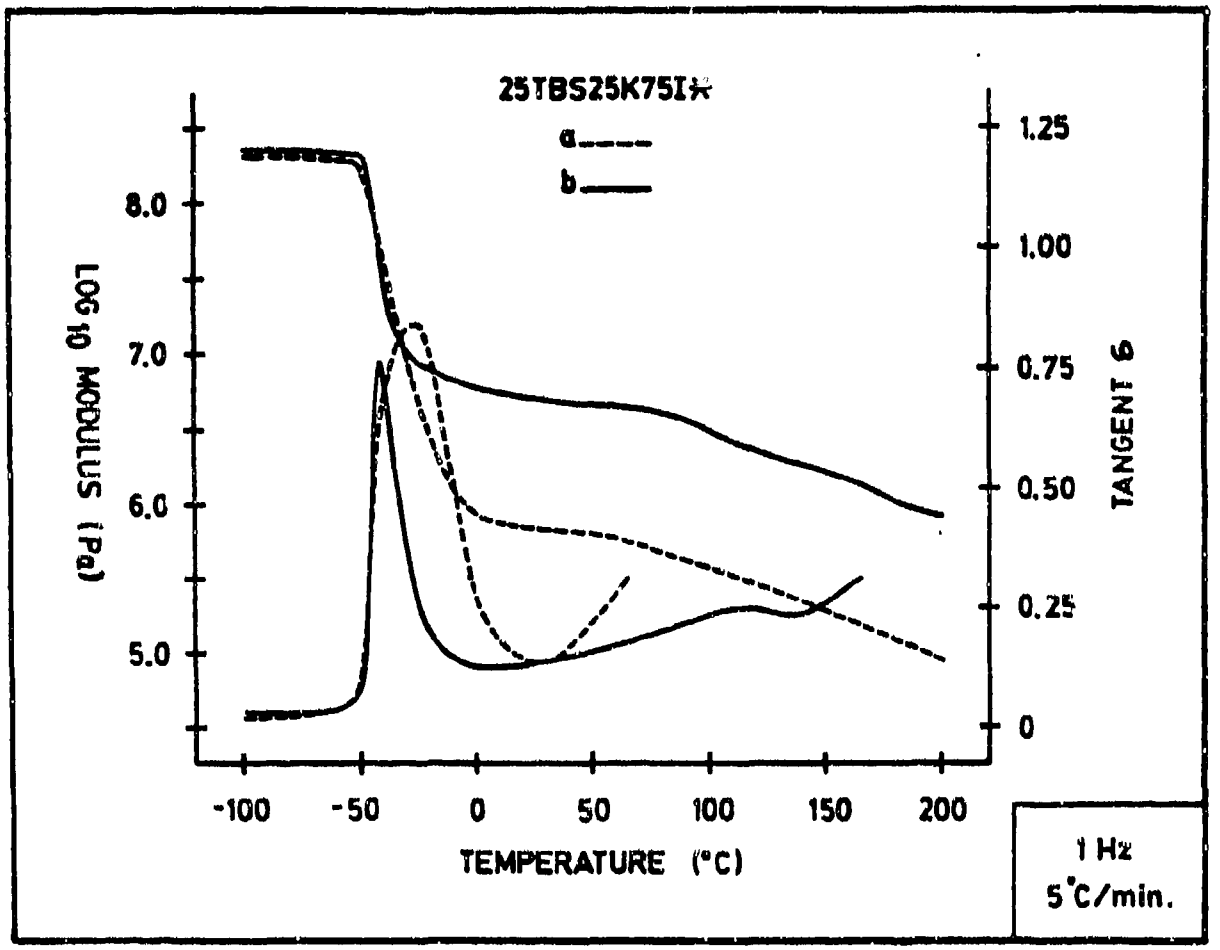


Figure 5.2-9. Influence of Hydrogenation on the Dynamic Mechanical Behavior of Poly(Tert-Butyl Styrene)-Polyisoprene Thermoplastic Elastomers

increases nearly an order of magnitude of 5.0 megapascals (MPa), and a second glass transition is evidenced by the appearance of a high temperature damping maximum at 115°C. These changes suggest that demixing has resulted in more homogeneous or pure phases, with thermal properties more characteristic of the individual block components as shown in Table 5.2-1.

Additional star-block copolymers were prepared in which the poly(TBS)block molecular weight and percent composition were increased to 60,000 g/mol and 60 percent (diblock molecular weight of 100,000 g/mol). The DMTA data provided in Figure 5.2-10 were obtained for a representative sample. In this case, the broad low-temperature damping and the relatively low (64°C) damping peak for the poly(TBS)block are again characteristic of a phase-mixed system. When this block polymer was hydrogenated approximately 80 percent, the curve in Figure 5.2-10 is obtained. One notes again that the low-temperature damping maximum is shifted down 22°C to -48°C and the high-temperature damping maximum is shifted upward 78°C to 142°C. The precursor system also flowed nearly 100°C before its hydrogenated counterpart as judged from compression molding experiments. These trends are further indirect evidence of substantial microphase separation in the hydrogenated copolymers.

5.2.3.2. Mechanical behavior. When the unhydrogenated copolymers were tested in stress-strain experiments at ambient conditions, very low elastic moduli (ca. 0.5 MPa) and very high elongations (ca. 3000 percent) were observed. These polymers were also extremely tacky and proved to be interesting pressure-sensitive adhesives (17). Small to moderate levels of hydrogenation (ca. 50 percent) greatly reduced their tack and ultimate elongation, and increased their modulus and ultimate stress as shown in Figure 5.2-11. The change in solubility parameter that occurs as polyisoprene is hydrogenated to poly(ethylene-propylene), causes the rejection of poly(TBS) from the rubber phase, yielding more discrete domains of poly(TBS). As they develop, these glassy domains act as thermoplastic physical crosslinks which provide the observed improvements in elastomeric properties. As hydrogenation and phase separation proceed, the polymer perfects its phase-separated character and is capable of supporting ultimate stresses in the range of 20 to 30 MPa, similar to previously mentioned, commercial, thermoplastic elastomers, while at the same time, displaying enhanced high-temperature transition behavior. The formation of a higher modulus rubber (as judged by DMTA) also contributes to the development of enhanced mechanical strength prior to faiure. At this time it should be noted that these block copolymers contain only 10 mol percent of the glassy tie-phase, in constrast to conventional triblock systems which typically contain 15 to 20 mol percent or more of the glassy block. It is also pointed out that the 10 minute permanent set (after rupture) of the well-hydrogenated samples is approximately 7 to 8 percent. Thus, hydrogenation is able to produce poly(TBS)-poly(ethylene-propylene) copolymers of not only good strength, but also of reasonable elongation with good recovery after large deformations.

Table 5.2-1. Glass Transitions of Homopolymers at Characteristic Molecular Weight Values (DSC, 10°C/min.)

| | | |
|---|---|---|
| Poly(Tert-Butyl Styrene) | 25,000 g/mol. | 141°C |
| Polyisoprene | 75,000 g/mol. | -62°C |
| (Hydrogenated) Polyisoprene | 75,000 g/mol. | -61°C |

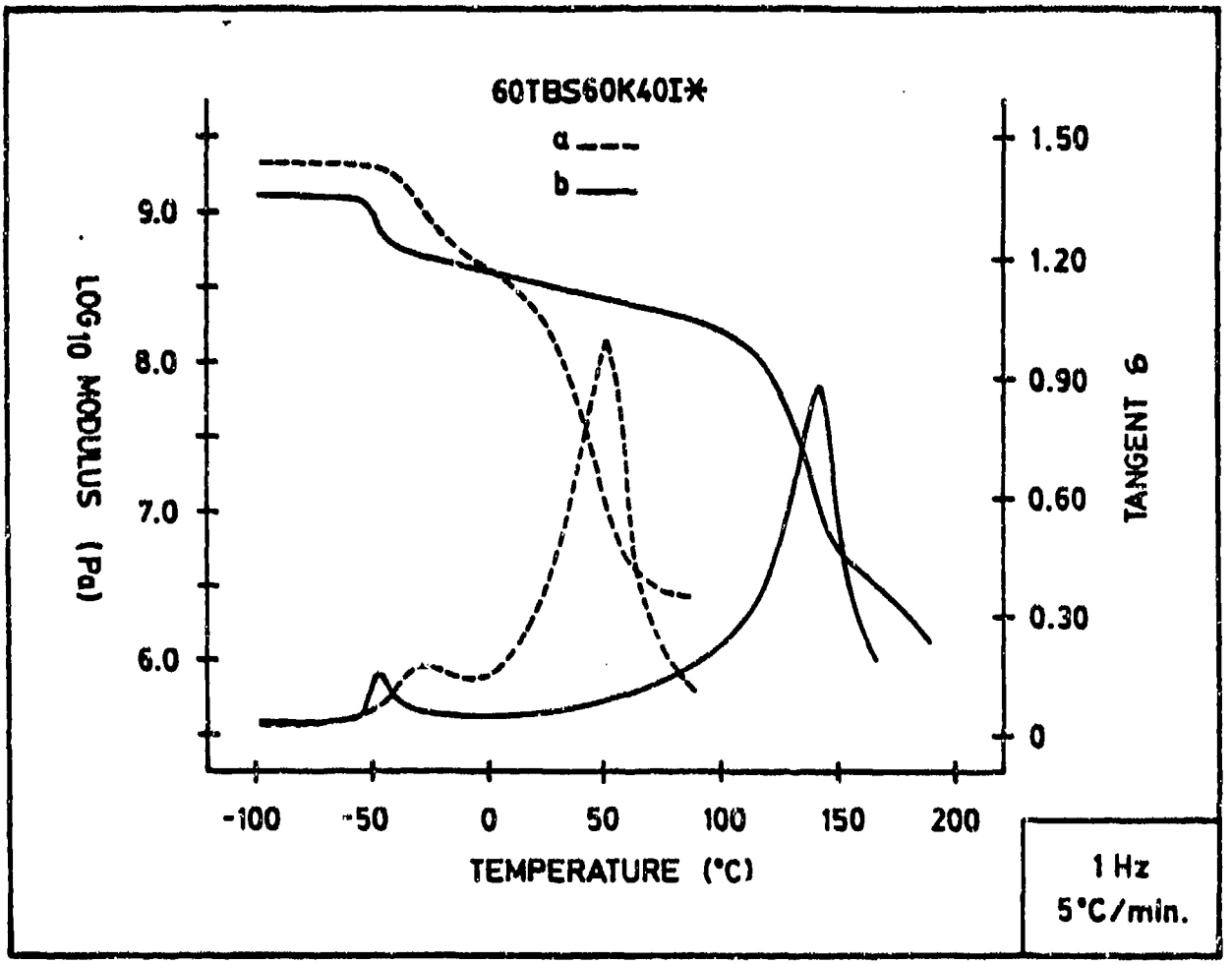


Figure 5.2-10. Influence of Hydrogenation on the Dynamic Mechanical Behavior of a 60 Weight Percent (%) Poly(Tert-Butyl Styrene)-Polyisoprene Block Copolymer

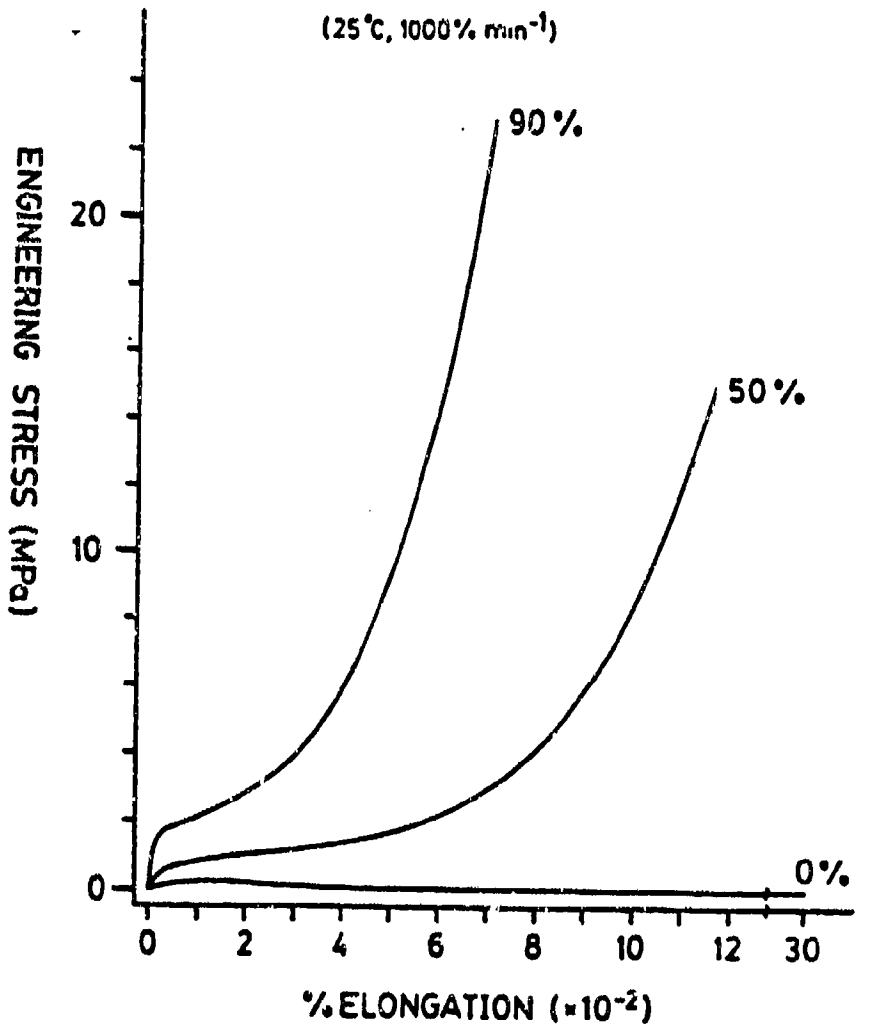


Figure 5.2-11. Stress/Strain Relations for 25TBS20K75I*

Other strength related properties, such as stress at 100 percent and 300 percent elongation, follow the same general trends as elastic modulus and tensile strength. These trends are summarized in Figure 5.2-12 for elastic modulus as a function of poly(TBS) block molecular weight and percent hydrogenation. This property response surface indicates the general trends that were observed for the strength related properties of star-block copolymers in this study. The property improves as a function of microphase separation due to hydrogenation and as block molecular weight increases. Poly(TBS) block mol. weights greater than about 20,000 g/mol appear to result in property decreases due to increases in rubbery (network) chain length and corresponding decreases in physical crosslink density (star branch points). The improvement in properties observed up to 20,000 g/mol may be attributed to enhanced phase separation that occurs as the poly(TBS) block size increases.

Stress relaxation experiments were also performed on these polymers, as a function of poly(TBS) block size and percent hydrogenation, to determine their ability to support a stress over extended periods of time. The series of curves shown in Figure 5.2-13 is typical of the response of these elastomers to strain and time. The shape and slope of these curves strongly suggests their ability to be horizontally shifted to form a time-degree of hydrogenation master curve. This master curve might then be used to predict the stress at extremely long times.

5.2.4. Conclusions. Poly(t-butyl styrene)-polyisoprene star block polymer elastomers were studied and it was demonstrated that hydrogenation appears to induce a much greater degree of microphase separation relative to the diene precursor as evidenced by thermal-mechanical properties and greatly improved stress-strain behavior. It is suggested that this is due to the similarity in solubility parameters between the ring substituted polystyrene and polyisoprene and the subsequentially lower value for the derived elastomeric polyolefin.

The catalytic hydrogenation of polyisoprene containing homopolymer block copolymers may be accomplished in a clean, well-defined manner with no evidence of critical chain degradation, and thus may be used as an additional tool in the synthesis of model elastomers and thermoplastics. Novel stiffening of the hydrogenated polyisoprene was observed which is attributed to changes in chain entanglement coupling density (Me).

In samples where differential scanning calorimetry (DSC) transitions are very difficult to observe, DMTA has been found to be an expecially valuable technique for assessing the relaxation characteristics of multiphase polymers which may posses a broad range of multiple-damping phenomena.

Finally, we may conclude that the poly(TBS)-polydiene block systems provide an excellent model for the investigation of hydrogenation influences on microphase separation phenomena in elastomers and related materials.

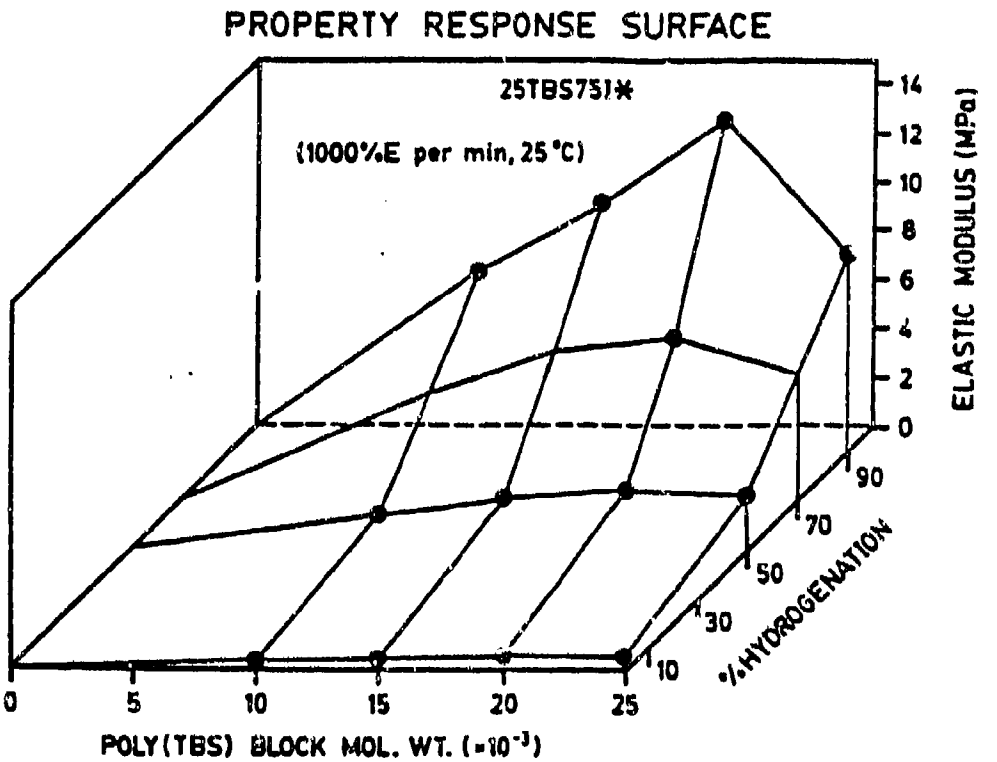


Figure 5.2-12. Three-Dimensional Property Response Surface

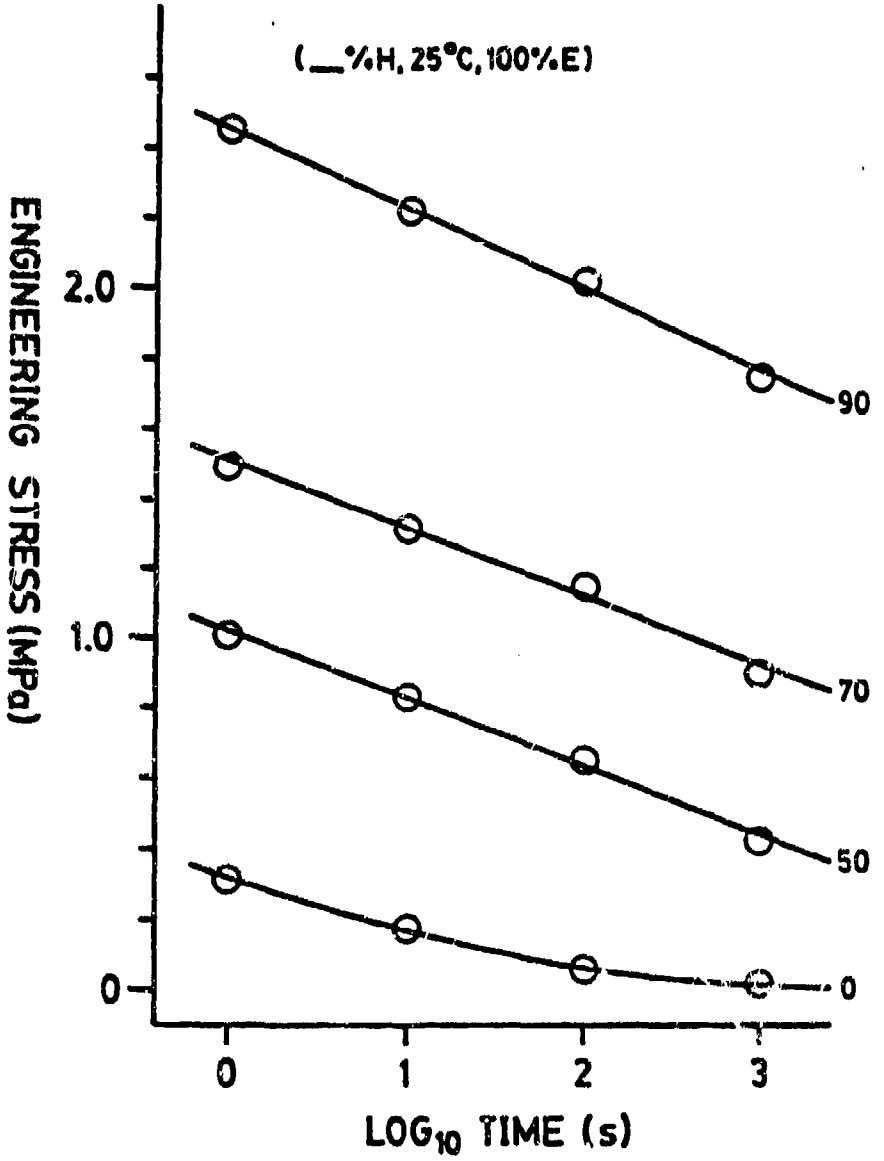


Figure 5.2-13. Stress Relaxation for 25TBS20K75I*

## 5.2.5. References


1. McGrath, J. E., (Editor), "Anionic Polymerization: Kinetics, Mechanisms and Synthesis", ACS Symposium Volume Series, No. 166, 1981.

2. Noshay, A. and McGrath, J. E., "Block Copolymers: Overview and Critical Survey", Academic Press, New York, 1977.

3. Szwarc, M., Adv. Polym. Sci., 49, 1 (1983).

4. Morton, M., "Anionic Polymerization: Principles and Practice", Academic Press, New York, 1983.

5. Young, R. N., Quirk, R. P., and Fetters, L. J., Adv. Polym. Sci., 56, 1 (1984).

6. Rempp, P. F., and Franta, E., Adv. Polym. Sci., 58, 1 1984; see also Y. Yamashita and Y. Tsukahara, J. Macro. Sci.-Chem, A21 (8 & 9), p. 997-1012 (1984).

7. McGrath, J. E. (editor), "Ring Opening Polymerization: Kinetics, Mechanisms, and Synthesis", ACS Symposium Volume Series, No. 286, 1985.

8. Morton, M., and Fetters, L. J. Rubber Rev., 48, 359 (1975).

9. Legge, N. R., Davidson, S., De La Mare, H. E., Holden, G., and Martin, M. K., in "Applied Polymer Science", 2nd ed., R. W. Tess and G. W. Poehlein, editor, ACS Symposium Volume Series, No. 285, 175, 1985.

10. Schulz, D. N., Turner, S. R., and Golub, M. A., Rubber Rev., 55, (1982).

11. Schultz, G. O and Milkovich, R. M., J. Poly Sci., Polymer Chem. Edit., 22 (7), 1633-1652 (1984).

12. J. E. McGrath, Pure and Appl. Chem., 55 1573 (1983).

13. Hoover, J. M., Ward, T. C., and McGrath, J. E., Polymer Preprints, 26(1), 253 (1985).

14. Broske, A. D., and McGrath, J. E., Polymer Preprints, 26(1), 241, 1985; "Advances in Anionic Polymerization" T. E. Hogan-Esch and J. Smid, Editors, Plenum Press, 1987.

15. Allen R. D., Smith, S. D., Long, T. E., and McGrath, J. E., Polymer Preprints, 26(1), 247 (1985).

16. Kornblum, N., and Singaram, S., J. Org. Chem., 44, 4727 (1979).

17. M. M. Sheridan, J. M. Hoover, T. C. Ward and J. E. McGrath, Polymer Preprints, 26(1), 186, 1985; M. M. Sheridan, Ph.D. Thesis, Virginia Polytechnic Institute and State University (1986)

18. R. J. A. Eckert, U S. Patent 4,156,673, (to Shell), May 29, 1979.

19. P. K. Das, J. M. Hoover, T. C. Ward and J. E. McGrath, Polymer Preprints, 25(2), 96 (1984); P. K. Das, Ph.D Thesis, Virginia Polytechnic Institute and State University, December 1984.

20. L. J. Fetters, E. M. Firer and M. Defauti, Macromolecules, 10, 1200 (1977).

21. F. C. Schwab, Polymer Preprints, 25(2), 61 (1984); "Advances in Polymer Synthesis", B. M. Culbertson and J. E. McGrath, Editors, Plenum, Vol. 3, 1985.

## 5.3. Investigation of Hydrocarbon-Soluble Organolithium Initiators

5.3.1. Introduction. A difunctional anionic initiator that will polymerize vinyl and diene monomers has been an academic as well as a commercial goal in elastomer technology since pioneering work in anionic polymerization was reported 30 years ago (1-9). The desire to prepare difunctional reactive oligomers as well as to synthesize triblock or multiblock copolymers has been an incentive to conduct this work. One advantage of using a difunctional anionic initiator is that triblock copolymers can be synthesized in two, or possibly only one monomer addition step. Thus, if the center block is prepared first, followed by the subsequent addition of a second monomer, one may prepare the two end blocks concurrently. A second feature relates to functionalization reactions, such as the reaction of the living chain ends with ethylene oxide. With proper conditions, perfectly difunctional linear (f=2.0) hydrocarbon-based polyols can be produced. These polydiene oligomers can be used as "soft" segments in chain-extended high molecular weight copolymers. In addition, hydrogenation can be conducted which will enhance thermal and oxidative stability. Difunctional initiators also are important where the second monomer is incapable of reinitiating the first monomer (e.g., diene or styrenic-methacrylic systems). Preparation of diene polymers displaying a high 1,4 microstructure has also emphasized the need to avoid, or at least minimize, polar additives, which might otherwise solubilize and enhance reactivity in these systems.

One important method of synthesizing difunctional organolithium reagents has been by addition of a monofunctional organolithium reagent (such as sec-butyllithium) to a compound that contains two double bonds (10-12). The divinyl compound should have reactive double bonds which are not conjugated with each other in order to allow the sites to react essentially independently. Equal reactivity is obviously also desirable. In addition, steric and/or electronic structural features should be designed into the system that would restrict possible oligomerization of the diene which could result in either a gain or loss of perfect difunctionality.

The use of 1,3 divinylbenzene, 1, as a possible precursor was first

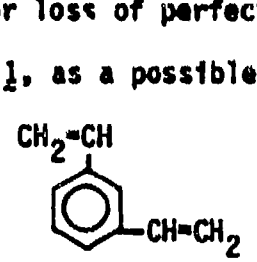


1

patented by Morrison and Kamienski (13) and further studied by Lutz (14) and Popov (15). Unfortunately, this compound can easily oligomerize, which leads to ill-defined functionalities that are greater than two.

Sigwalt and coworkers (16,17) describe the use of the dilithium initiators formed from the reaction of butyllithium with bis (p-isopropenyl-phenyl)

alkanes or diphenyl-alkadienes which were prepared in hydrocarbon solvents without polar additives. Unfortunately, one major drawback with this system is their insolubility in hydrocarbon solvents. They also reported using an excess of butyllithium which would clearly result in diblock and/or homopolymer contamination. Moreover, when a stoichiometric amount of the simple organolithium was employed, the reaction was reported to not go to completion even after 1 week at room temperature. Nevertheless, these initiators were then used to prepare triblock copolymers of styrene-isoprene-styrene and styrene-butadiene-styrene. Mechanical properties of these copolymers were reported to be comparable to those for commercial Kraton standards.

Another precursor, m-diisopropenyl benzene (DIB), 2, has been reacted with alkyllithiums to form a soluble difunctional initiator. Foss and coworkers (18) report that the product of the reaction of DIB with sec-butyllithium in the presence of a small amount of triethylamine, followed by reaction

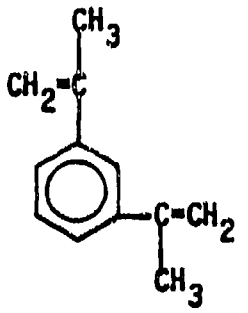

2

with isoprene improves solubility in essentially hydrocarbon solvents. The reaction rate is also increased due to higher solvent polarity. However, the reported polydispersity of the resulting polyisoprene is broader (Mw/Mn = 1.3) than for typical anionic polymerizations. Apparently, the presence of higher concentrations of the amine promotes the formation of trifunctional species in addition to increased vinyl content in polydienes. Cameron, et al. (19), have also investigated the reaction of DIB with butyllithium in benzene or cyclohexane. Even at elevated temperatures, purely difunctional species did not result, but rather a mixture of difunctional and polyfunctional products was observed. Even in the presence of tertiary amines, the products were similar. They concluded that utilization of this system as an efficient difunctional anionic initiator should be considered highly suspect.

In constrast, Lutz, et al. (10), reached a completely different conclusion for this system. They state that in benzene solution, a difunctional initiator was formed even without added polar modifiers. Also, polymerization of styrene and isoprene was achieved. Unfortunately, their own data appear to indicate that a mixture of monofunctional, difunctional, and trifunctional species were observed from GPC results. Also, an excess of sec-butyllithium was added to increase yields of difunctional species,

which must result in residual, unreacted sec-butyllithium and precipitation.

Tung and coworkers (10-12) reported the use of difunctional initiators based on soluble difunctional 1,1-diphenylethylenes where the reactive double bonds are separated by a variety of moieties such as p-phenyl, biphenyl, p,p-biphenylether, and m-phenyl. These divinyl compounds when reacted with sec-butyllithum produce a dilithium initiator which can be used for block copolymer synthesis. Hocker and Lattermann (21-22) studied the use of 1,3- and 1,4 bis(phenylethenyl) benzene in polycombination electron transfer reactions to form multifunctional lithium species. These compounds do not homopolymerize under normal anionic conditions. More recently, they also reported (23-24) that the meta isomer will quantitatively react with sec-butyllithium in toluene to form a hydrocarbon soluble dilithium initiator which is suitable for anionic polymerizations.

We believe these latter meta-linked soluble difunctional systems have high potential as difunctional initiators and have already independently reported our preliminary results at several meetings of the Polymer Division of the American Chemical Society (26-28). This paper represents a more formal contribution. Our work has largely been conducted in cyclohexane, which though kinetically slower, eliminates the possible metalation side reaction of the benzylic methyl group of toluene (6) which becomes significant at elevated temperatures.

5.3.2. Experimental. Kinetic and mechanistic studies of anionic polymerization require the rigorous purification of all materials used. In fact, results and conclusions may be highly dependent on experimental techniques. Any reactive impurities, primarily water and air, must be removed from monomers, solvent, initiators, and glassware by appropriate purification procedures.

In general, organolithium initiators were used at concentrations of between $10^{-3}$ to $10^{-4}$ M, so the level of any impurities which could react with the organolithium initiator or living chain end must be kept below $10^{-5}$ M. An all glass high vacuum system ($10^{-6}$ torr) employing a series of stopcocks similar to the system described by Morton and Fetters (24) and our own studies (7) was used for most of the kinetic studies in order to maintain these reaction conditions. Premature termination of the active species was prevented as judged by the generation of predictable molecular weights and narrow molecular weight distributions.

Cyclohexane is known to contain traces of olefinic impurities which must be removed before use. Cyclohexane (Phillips, 99 percent) was first stirred over concentrated sulfuric acid (about a 10 percent solution) for at least a week at room temperature. This removes the olefinic impurities by converting them to sulfonates which then become soluble in the acid layer. The cyclohexane layer was decanted into a round bottom flask containing crushed calcium hydride. It was then distilled into a round bottom flask containing a sodium dispersion and stirred overnight before being placed on the vacuum line. Following the degassing procedure, the cyclohexane was

distilled into a flask containing low molecular weight polystyryllithium which has a characteristic red color and is used simply as an indicator which insures high purity. Cyclohexane was then vacuum distilled from this flask, as needed, into various reactors.

A variety of polar compounds were investigated as additives to study the spectra of the completely reacted difunctional anionic initiator. In general, the molar ratio of organolithium to polar additive was 0.2 or less. Purification of tetrahydrofuran (THF) involved distillation from calcium hydride into a flask containing the purple colored complex formed from the addition of benzophenone to sodium dispersion and was then distilled as needed.

The reduced volatility and increased reactivity of some of the other polar additives such as triethylamine (TEA) and tetramethylethylene diamine (TMEDA) required utilization of alternate procedures. These amines were first stirred over crushed calcium hydride overnight in a round-bottom flask equipped with a drying tube and then distilled under high vacuum at room temperature. The purified distillate was then split down into ampules. Dipiperidinomethane and 1,2-dipiperidinoethane (Di-PIP) (Aldrich, 98 percent) were purified using an analogous procedure.

The purification of sec-butyl lithium (Lithium Corp., 1.4N in cyclohexane) was necessitated by the fact that the commercially available material contains varying amounts of alkoxide impurities, which may alter the reaction kinetics, microstructure and copolymerization parameters. Purification was achieved by distillation (after removal of solvent) under high vacuum ($<10^{-4}$ torr) at 65°C. The purified sec-butyl lithium was diluted with cyclohexane and also split down into ampules.

The 1,3-bis(phenylethenyl) benzene (DDPE) 4 was provided by Dow Chemical Co. as a yellow liquid which upon standing will slowly crystallize. The resulting yellow crystals are quite oxygen sensitive and were further purified before use. An effective purification method was to distill from n-butyl lithium under high-vacuum conditions. Distillation at about 140°C yields a clear, colorless liquid. Transferring the desired amount to a second flask followed by dilution with a measured amount of cyclohexane under vacuum and splitting down into ampules yields the final solution of approximate concentration. The purity of the white crystallized solid was also verified by differential scanning calorimetry (DSC). A sharp melting point at 39-40°C was observed.

An all-glass reactor was used for studying the kinetics of the reaction between sec-butyllithium and DDPE under high vacuum conditions. The reactor illustrated in Figure 5.3-1 was divided into two sections, one being the main reactor and the other the purge section as described earlier (7,24). The former consisted typically of a 500 ml round bottom flask to which two side arms have been attached. These side arms allow various ampules or dilatometers to be attached. Two break seals were provided which allowed for addition of additional solvent or attachment of more ampules which may contain the various polar additives. Two quartz

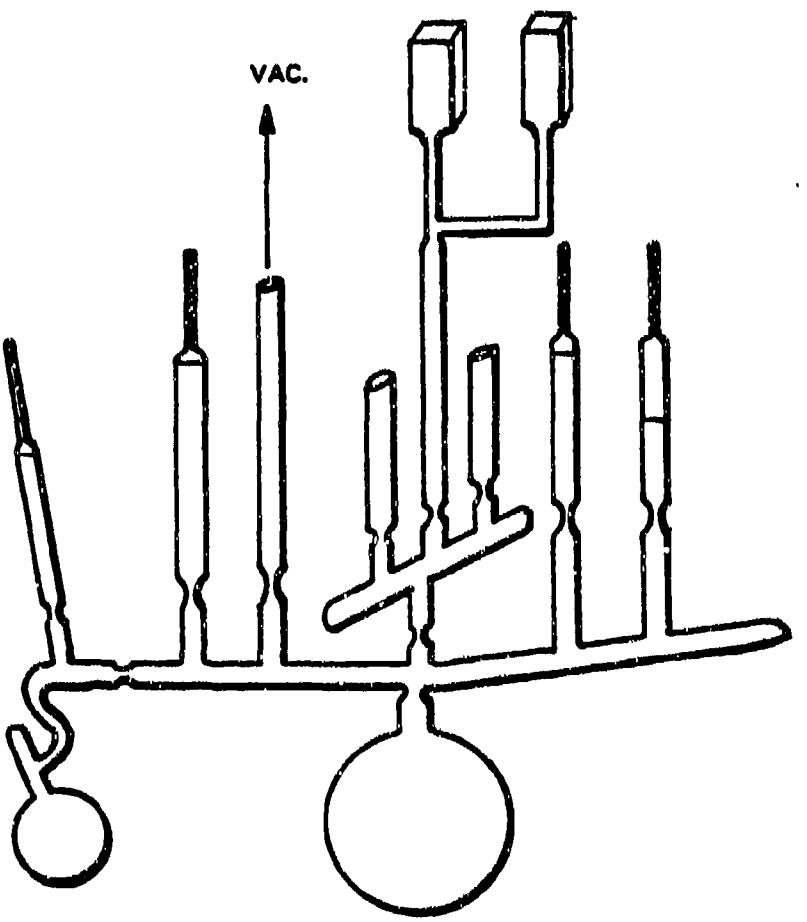


Figure 5.3-1. Anionic Polymerization Reactor for High-Vacuum Studies

UV/Visible cells of 10 mm and 1 mm path lengths were attached at the top of the reactor, which allows a spectrum to be obtained.

The purge system consists typically of a 200 ml round-bottom flask which contained a solution of n-butyllithium in cyclohexane in a side arm. This solution was used to condition the main reactor and to thus remove any reactive impurities from the surface of the flamed glassware. The reactor was assembled by heat sealing on the reagent ampules containing the DDPE, sec-butyllithium, the wash n-butyllithium and if desired, any polar additives. Magnetic stirring bars were used as the break nails. After several rinses with cyclohexane, complete removal of the excess butyllithium from the glassware was achieved. Then, the desired amount of cyclohexane was distilled from the purge system to the main reactor. Subsequently, the solutions were cooled and the purge section was heat sealed from the main reactor.

The main reactor was placed in a circulating water bath which had its temperature controlled to ±0.1°C, until the cyclohexane has reached the desired temperature. When this was achieved, the two ampules containing the two reagents were broken via the break seal and were allowed to mix in the reactor. Thorough mixing of the two reagents was achieved by shaking the reactor and distilling solvent gently into the ampules.

A series of UV/Visible spectra were taken at specified times during the reaction by inverting the reactor and placing the then-filled quartz cells in the spectrophotometer. A Perkin-Elmer (Model 552) microprocessor controlled UV/Visible spectrophotometer equipped with a Model C 550-0555 thermoelectrically controlled cell was used for this analysis. Spectra were obtained by scanning from 650 to 190 nanometer (nm) at 120 nm per minute.

Though quite sensitive, the UV/Visible method does not distinguish between the monoanion and dianion reaction products. Therefore, complementary gas chromatography (GC), FT-IR and $^1$H-NMR methods were utilized employing a high-pressure nitrogen polymerization reactor (25). A schematic diagram of the high pressure nitrogen reactor is shown in Figure 5.3-2. In this case, the desired amounts of DDPE and sec-butyllithium solutions were added to the reactor containing cyclohexane via syringe through the initiator inlet. Samples were removed from the reactor at specific times during the reaction. The samples were terminated with $N_2$ purged methanol and then analyzed via gas chromatography (GLC), FT-IR (Nicolet MX-1) and proton NMR (IBM 270 MHz).

Initially a Gow-Mac series 550 GLC equipped with a thermal conductivity detector was utilized. The detector and injector temperatures were both set at 250°C and the column was maintained at 220°C. Helium was used as the carrier gas with a flow rate of 80 ml per minute through the column. The column was a 4 foot by ¼ inch aluminum column packed with 3 percent OV-101 on 100/120 mesh Anachrom/acrylonitrile-butadiene-styrene (ABS). Subsequently, studies with a more sensitive Varian Model 6000 equipped with a capillary column were conducted.

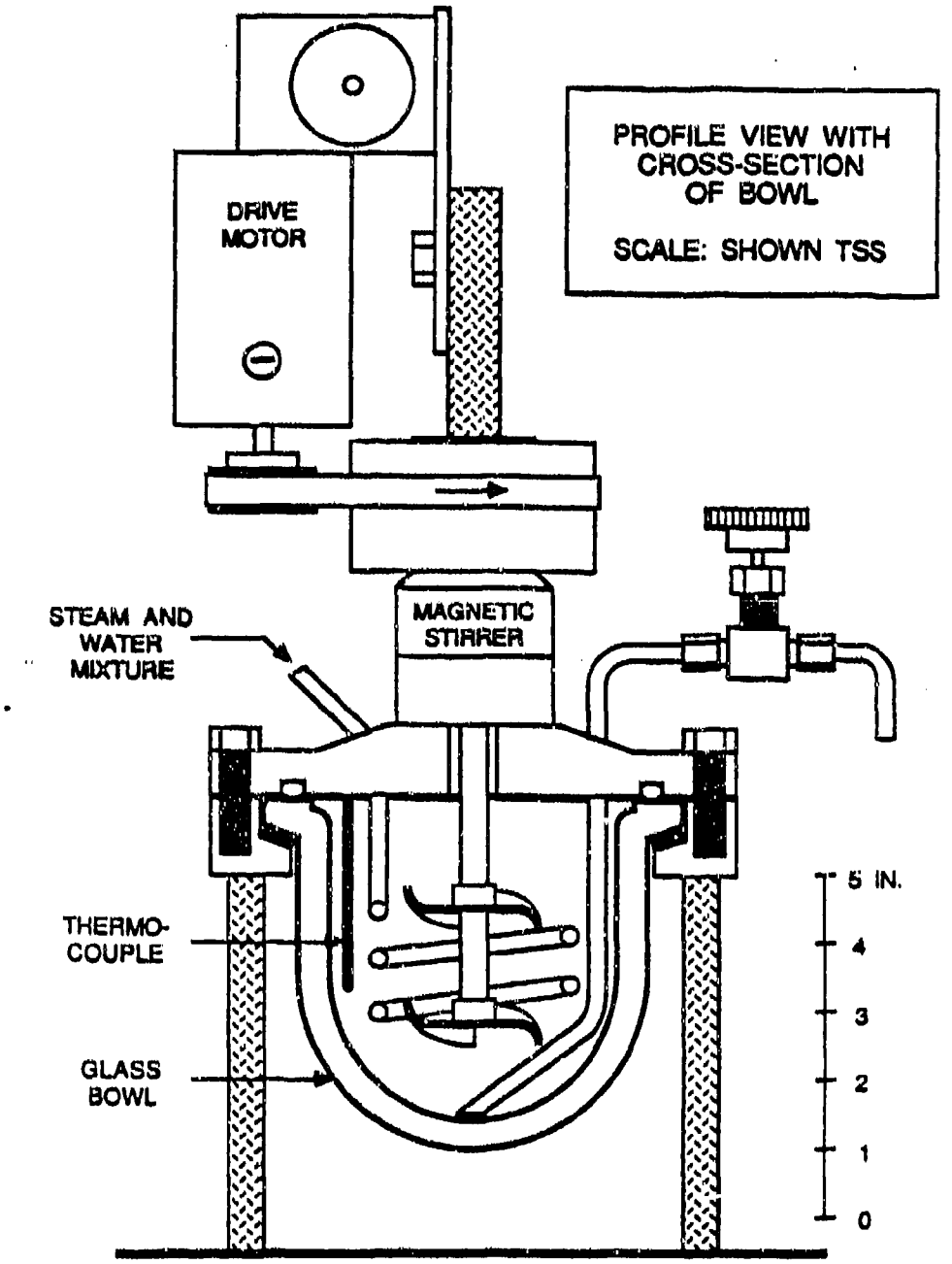


Figure 5.3-2. Glass Bowl Pressurized Reactor

Scheme 5.3-1. Synthesis of a Hydrocarbon Soluble Dilithium Initiator

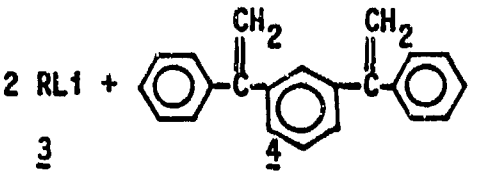


3 4

R = Sec-butyl | Cyclohexane, 18-60°C

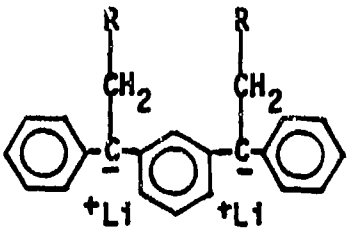


5

5.3.3. Results and Discussion. Several aspects of anionic polymerization were of ' terest in the current investigations. Firstly, the kinetics of the reaction between sec-butyl lithium and DDPE was studied as outlined in Scheme 5.3-1.

Secondly, the effect of polar additives on the nature of the ion pair of the dilithium species was investigated by observing the wavelength shift of the anion as a function of concentration of the additive. Thirdly, this initiator 5 was used to polymerize butadiene and isoprene for purposes of synthesizing hydrocarbon polyols and triblock copolymers based on hydrocarbon monomers, and/or alkyl methacrylates.

Kinetic experiments were first conducted under high-vacuum conditions utilizing the glass apparatus previously described in the experimental section. Spectroscopic analysis of the reaction mixture shows two peaks of interest. One is centered at about 227 nm and assigned to the unreacted nonconjugated DDPE 4 which decreases with time. The other at about 430 nm is assigned to the combined monoanion and dianion 5 species. The latter increases with time and/or reaction temperature. Figure 5.3-3 shows a series of UV/Visible spectra overlayed which were measured with the reaction temperature maintained at 18°C. The reaction is quite slow at this temperature and requires about 80 hours for complete reaction, as evidenced by the time to obtain maximum absorbance at 430 nm. Reactions were also conducted at several temperatures using identical concentrations of reactants. Figure 5.3-4 shows the disappearance of DDPE as a function of reaction time at the indicated reaction temperatures. As expected, the reaction rate increases with increasing temperature and one may note that the reaction is complete in cyclohexane after only two hours at 60°C.

Similar results were obtained by following the appearance of the anionic species at 430 nm. However, due to the insensitivity of this spectroscopic method (i.e., there are apparently not separately distinguishable absorbance peaks for the monoanion and dianion) only an overall kinetic analysis of the reaction is possible via UV-VIS.

If a consecutive reaction mechanism is postulated such as illustrated in equation (1) and (2),

$$\text{DDPE} + \text{sec-butyl Li} \xrightarrow{k_1} \text{Monoadduct} \qquad (1)$$

$$\text{Monoadduct} + \text{sec-butyl Li} \xrightarrow{k_2} \text{Diadduct} \qquad (2)$$

the kinetic expressions for each component of interest could be given in general form as:

$$\frac{-d(\text{DDPE})}{dt} = k_1[\text{DDPE}]^{\alpha}[\text{Li}]^{\beta} \qquad (3)$$

$$\frac{-d[\text{Mono}]}{dt} = k_2[\text{Mono}]^{\gamma}[\text{Li}]^{\delta} - k_1[\text{DDPE}]^{\alpha}[\text{Li}]^{\beta} \qquad (4)$$

$$\frac{d[\text{Di}]}{dt} = k_2[\text{Mono}]^{\alpha}[\text{Li}]^{\delta} \qquad (5)$$

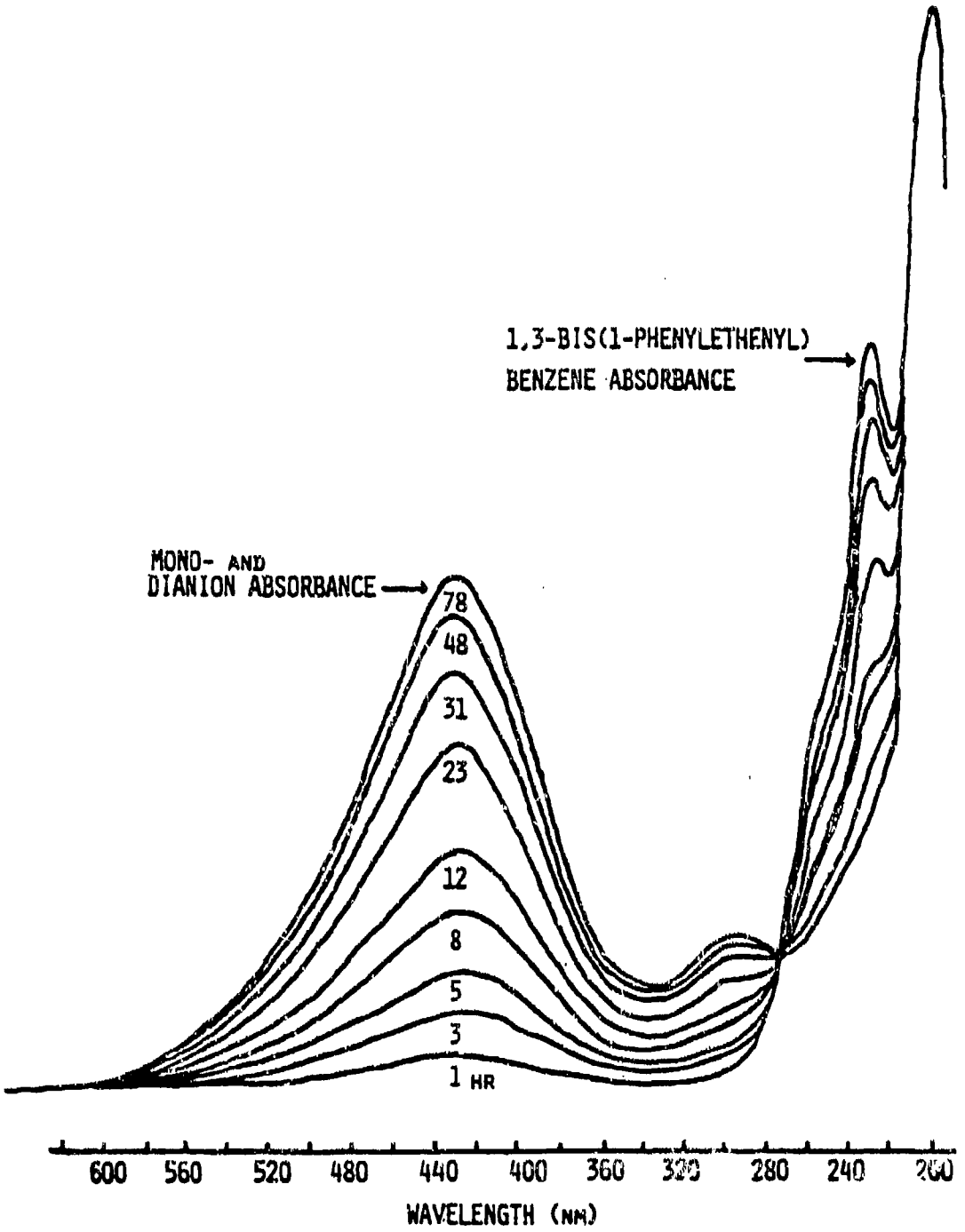


Figure 5.3-3. Spectrophotometric Study of the Reaction of 1,3-Bis(1-Phenylethanyl) Benzene and Sec-Butyl Lithium in Cyclohexane at 18°C

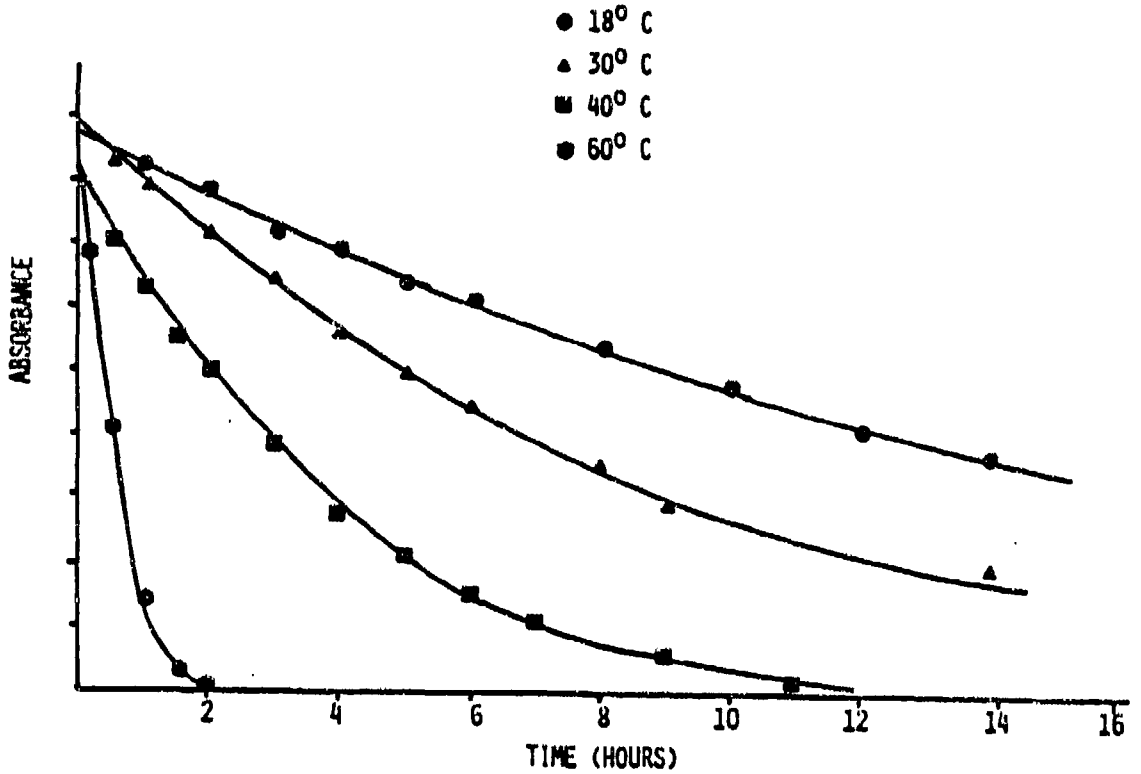


Figure 5.3-4. Absorbance of 1,3 Bis(1-Phenylethenyl) Benzene at 227.5 nm as a Function of Reaction Time at Various Temperatures

where [Mono] and [Di] refer to the concentrations of the monoadduct and diadduct, respectively.

Equations (4) and (5) cannot easily be directly evaluated. However, one notes from Figure 5.3-3 that an absorbance peak attributed to DDPE is well separated from the anions, which allows for kinetic evaluation of at least the first step of the reaction.

Using equations (1)-(3), some assumptions must be made regarding the order of the reaction. Realistic test orders in DDPE concentration as one (19) and one quarter (20) in sec-butyl lithium concentration were assumed. Secondly, since sec-butyllithium cannot be observed spectroscopically, its concentration term was equated with the DDPE concentration as indicated in equation (6),

$$[\text{sec-butyl Li}] = 2[\text{DDPE}] \tag{6}$$

Making these substitutions into equation (1) and simplifying affords:

$$\frac{d[\text{DDPE}]}{dt} = 2\, k_1[\text{DDPE}]^{1.25} \tag{7}$$

which when integrated over the appropriate limits yields

$$\frac{1}{[\text{DDPE}]^{0.25}} = k_1\, t \tag{8}$$

This equation was used to first confirm the validity of the initial assumptions and secondly to evaluate the apparent global rate constant.

Figure 5.3-5 shows the influence of temperature on the disappearance of DDPE obtained using the UV/Visible method. It is consistent with first order reaction kinetics, in terms of DDPE concentration. Straight line behavior is observed at all reaction temperatures. This plot supports one of our first assumptions, that the reaction should be first order in DDPE concentration. Figure 5.3-6 illustrates a plot of equation (8) where the initiator concentration, expressed as $[\text{DDPE}]^{0.25}$, is plotted versus reaction time. Here again, at all temperatures straight line behavior is observed and a correlation coefficient >0.99 was calculated. This demonstrates that our assumption of the one-quarter reaction order in sec-butyl lithium concentration was reasonable. Other orders were tested and did not yield as good a fit. The slope of these straight lines then is a direct measure of the apparent rate constant of this reaction at each temperature.

To further evaluate the kinetic analysis, the rate constants at each temperature were plotted versus reciprocal temperature as shown in Figure 5.3-7. A straight line was again obtained as evidenced by the high correlation coefficient (>0.99). The slope of this line is proportional to

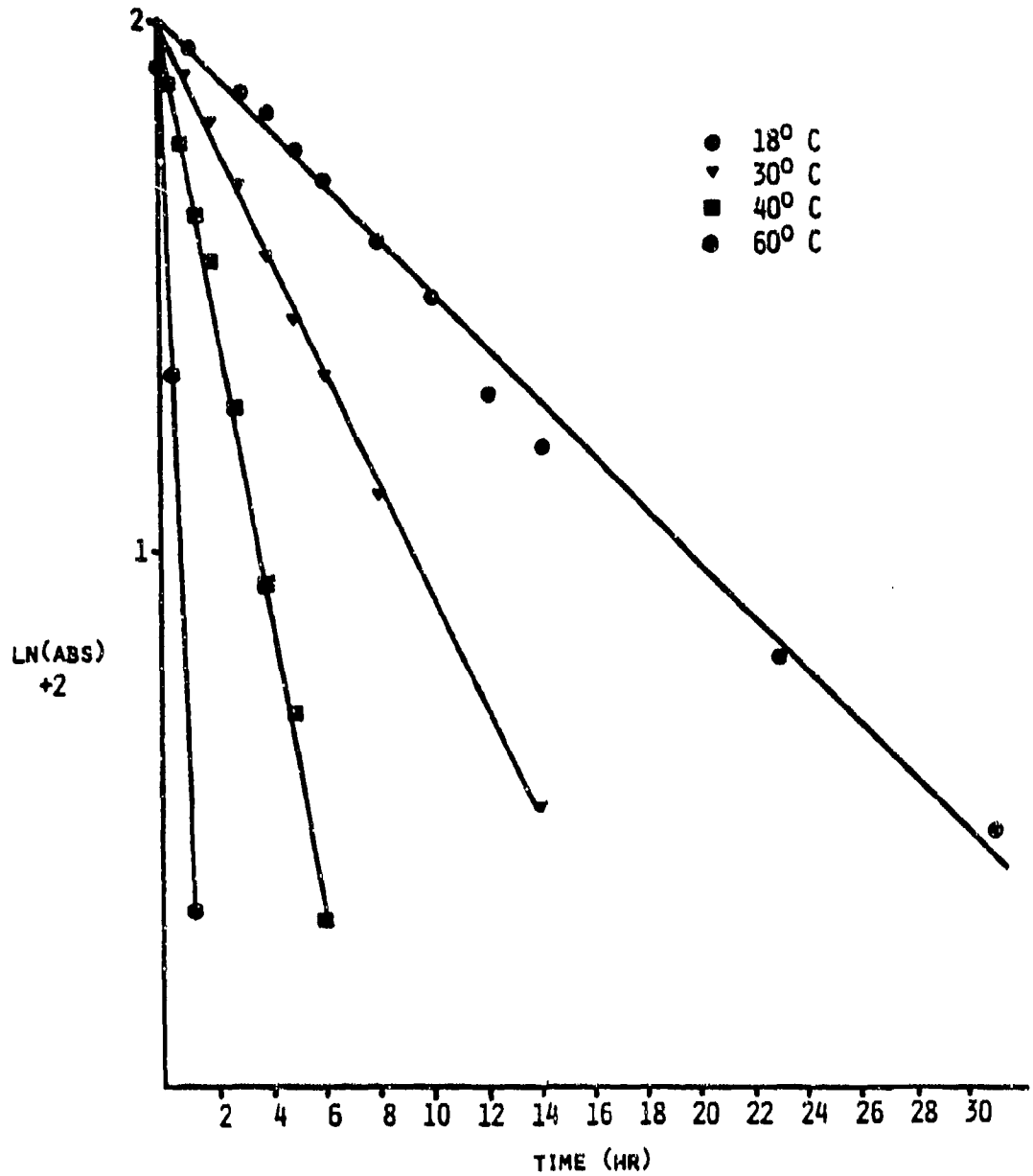


Figure 5.3-5. Influence of Temperature on the Disappearance of 1,3 Bis(1-Phenylethenyl) Benzene

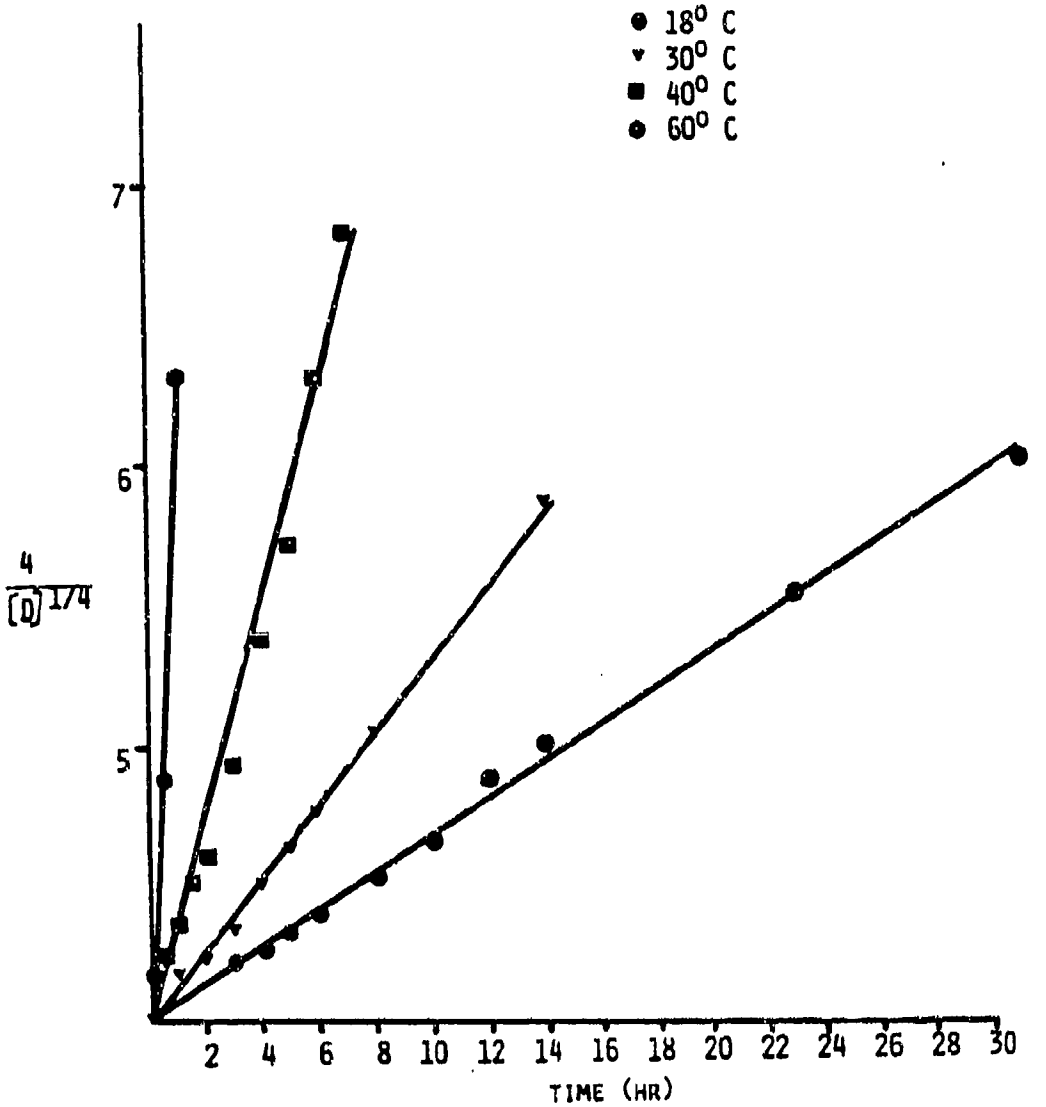


**Figure 5.3-6. Relationship Between Initiator Concentration and Reaction Time**

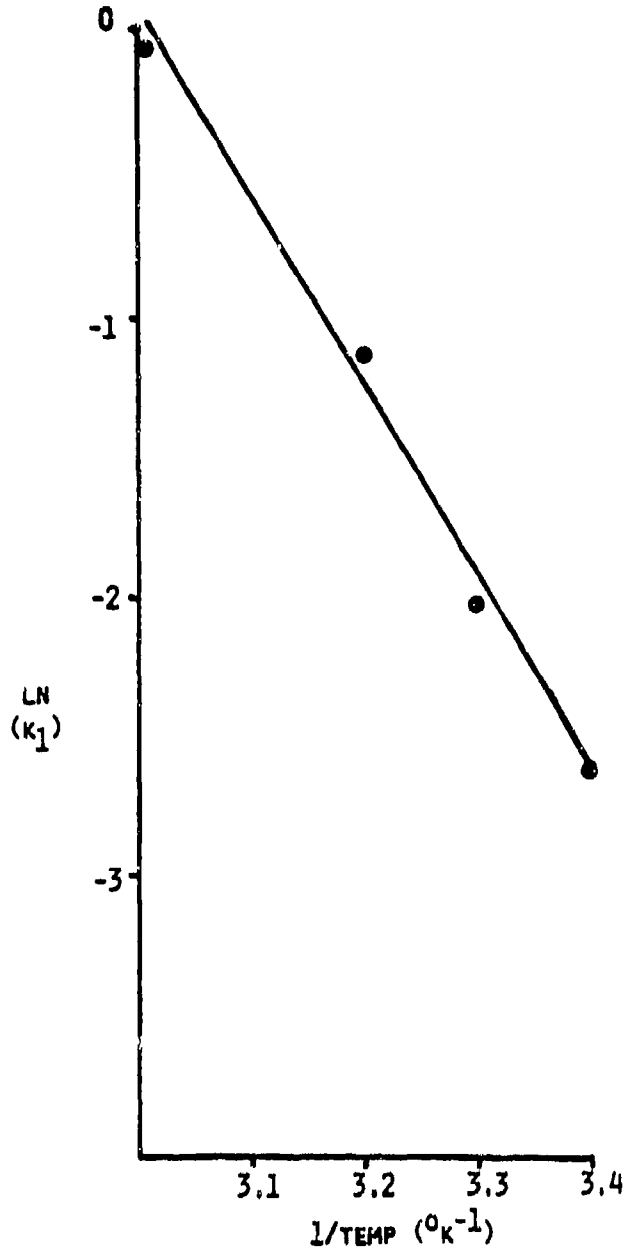


$$LN\ (K_1) = LN\ (A) - \frac{E_A}{RT}$$

$$SLOPE = -\frac{E_A}{RT}$$

$$E_A = 19 \text{ KCAL/MOLE}$$

Figure 5.3-7. Arrhenius Plot for the Sec-Butyl Lithium Reaction with 1,3-Bis(Phenyl Ethenyl) Benzene in Cyclohexane

the energy of activation which was calculated to be about 78.5 (kJ/mole) or 19 kcal/mole in cyclohexane.

Additional kinetic studies utilized reactions conducted in the pressure reactor in conjunction with analytical data obtained by gas liquid chromatography GLC, FT-IR and $^1$H-NMR. Both FT-IR and $^1$H-NMR at first glance appear to be effective methods for studying this reaction by either following the disappearance of carbon-carbon double bond stretching in the IR or the disappearance of vinyl protons in the NMR. However, distinguishing the double bonds of the monoadduct and starting material is impossible.

On the other hand, gas chromatography affords one the ability to separate all components of interest since the boiling points of the three components of interest are different from one another.

Figure 5.3-8 shows three overlayed chromatograms taken at different times during the reaction. The first unattenuated peak decreases with reaction time and is due to unreacted DDPE. The last eluting peak is assigned to the terminated dianion species which increases with reaction time. The intermediate peak is attributed to the terminated monoadduct. The peak assignments were verified by primarily injecting standards of known structure. The unreacted divinyl material was easily identified by injecting a solution of the purified DDPE in cyclohexane.

The diadduct standard was prepared by adding a one molar excess of sec-butyl lithium to DDPE in cyclohexane which maximized the formation of the diadduct. The reaction product was washed with water, dried, dissolved in cyclohexane and injected on the gas chromatograph.

The monoadduct is more difficult to prepare. Statistically, addition of 1 mole sec-butyl lithium to 1 mole of DDPE should produce primarily the monoadduct. However, if the reaction is conducted in cyclohexane, predominantly the diadduct and unreacted DDPE are observed as major products in the reaction. Remarkably, conducting the same reaction in tetrahydrofuran (THF) at -78°C produces the monoadduct in about 90-95 percent purity as evidenced by GC analysis. This solution was then used to identify the monoadduct peak. To confirm the identification of all the components of interest, small amounts of the standards were spiked into samples taken during a kinetic run.

Figure 5.3-9 shows the concentration of all species of interest plotted versus reaction time. This is clear evidence for a consecutive reaction mechanism. It is of interest to note that the concentration of the monoadduct remains relatively low throughout the reaction.

From this initial analysis some interesting observations can be made. Figure 5.3-10 shows a computer-generated plot for a consecutive reaction mechanism where the second rate constant was assumed to be an order of magnitude larger than the first rate. A good correlation with GLC and $^1$H-NMR data was obtained. This indicates that in cyclohexane the two rate constants are clearly not equal. Interpretation as to why the second

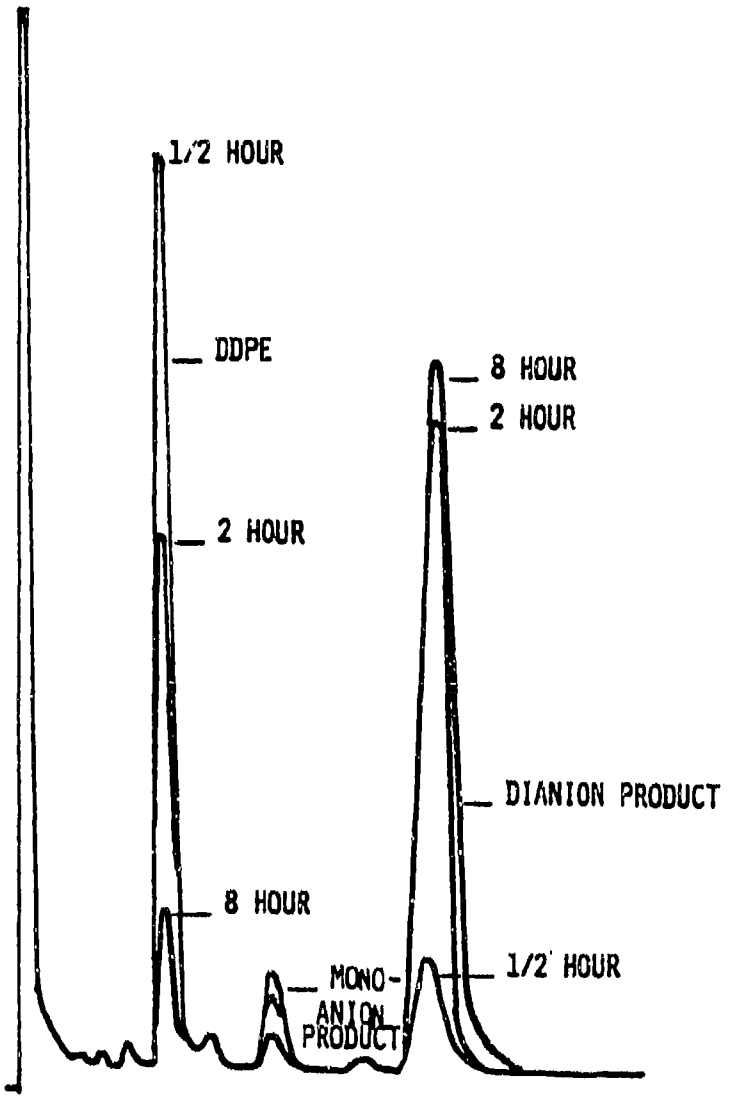


Figure 5.3-8. Gas Chromatographic Study of the Reaction Mixture with Time at 60°C

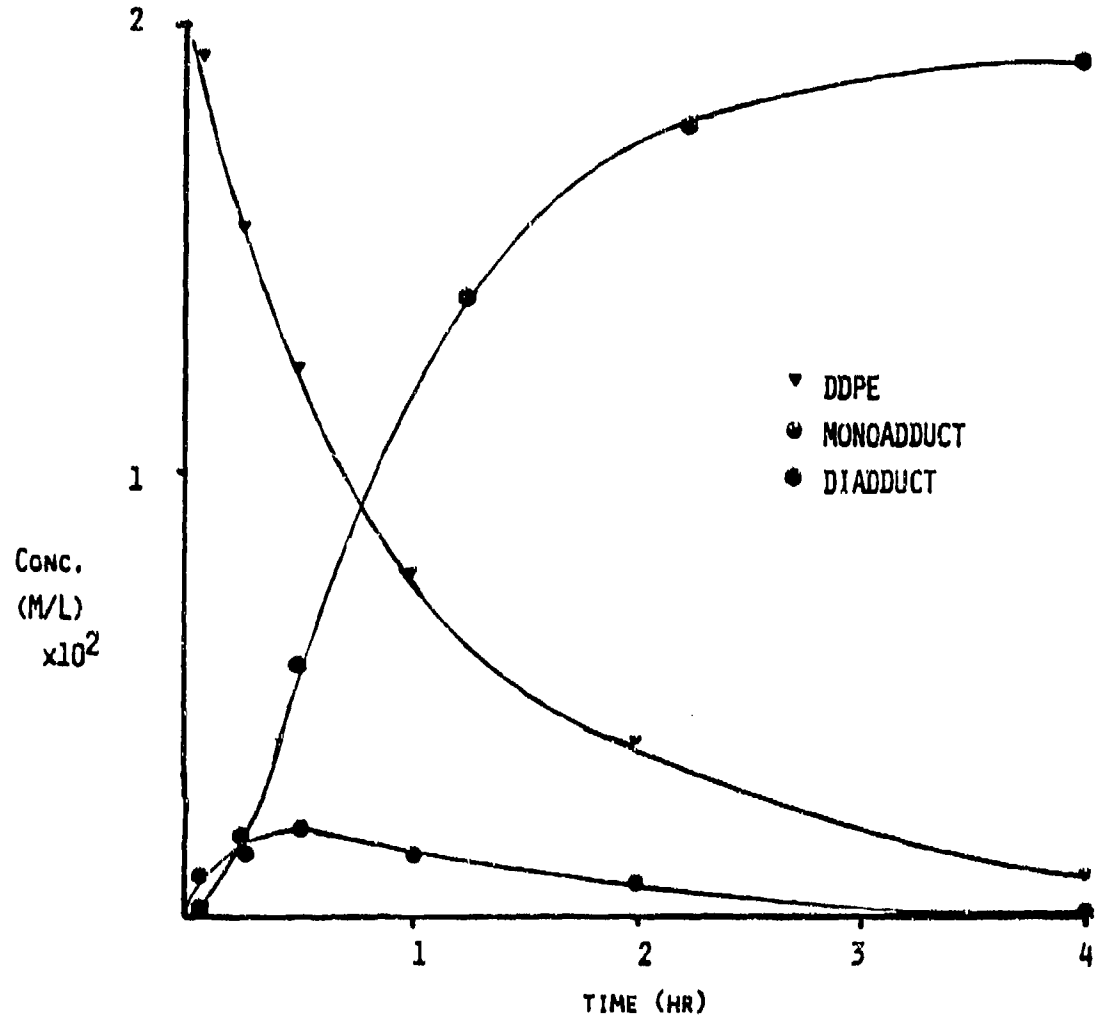


Figure 5.3-9. Concentrations of DDPE, Monoadduct, and Diadduct Versus Time

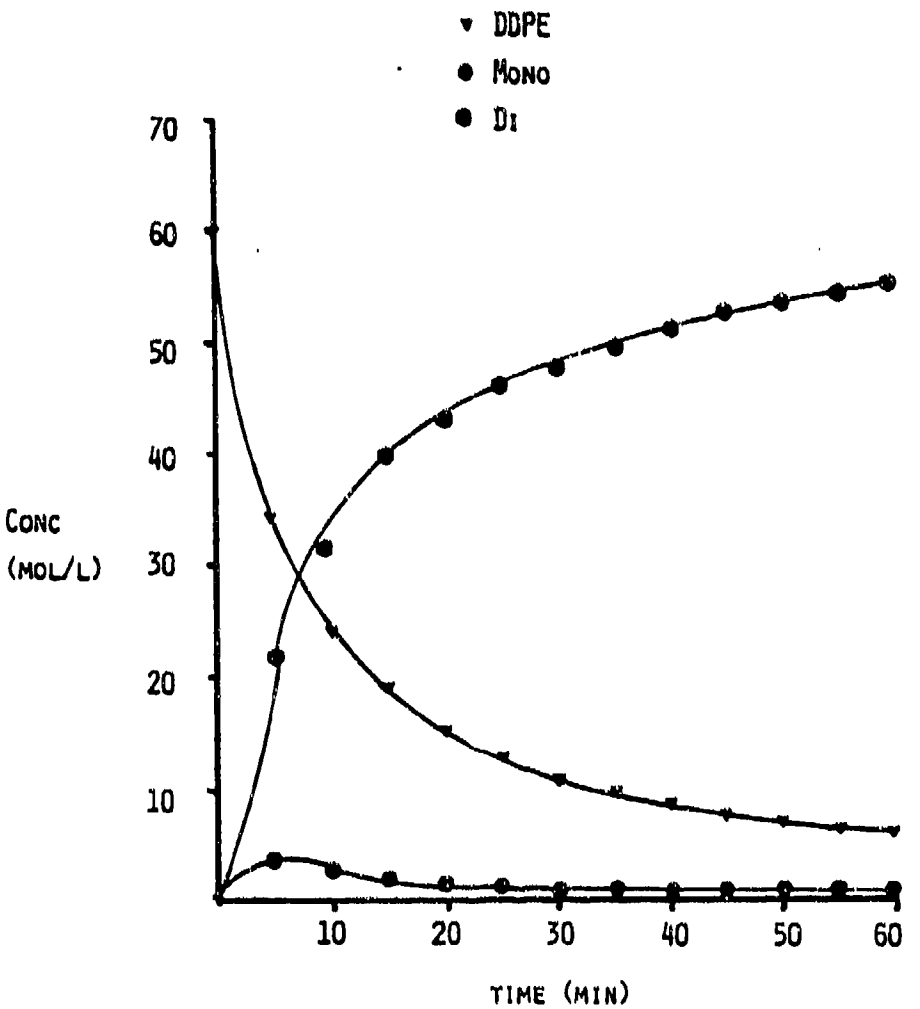


Figure 5.3-10. Calculated Kinetic Data.

adduct is formed at such greatly enhanced rates has not been firmly established. However, we suggest that chain end association (3,6,7) is involved. For example, preliminary reaction measurements in partially polar solvents (29) are quite different.

A second area of interest is in fact to study the effect of polar additives on the UV/Visible spectra of the dianionic species. This was easily accomplished by attaching an ampule which contains the additive to the glass reactor assembly which was then added to a completed reaction from the kinetic study.

A shift to higher wavelengths was observed after addition of each of the additives and the magnitude of this shift was dependent on the relative solvating power (resulting dielectric constant of the solvent system) of the additive. Table 5.3-1 summarizes the results for the variety of additives tested. One may notice that the more powerful solvating liquids (30) show a shift to higher wavelengths. These results are interpretable in terms of the structure of the ion pair which is emplified by the typical Winstein spectrum where a series of equilibria probably exists between tight ion pairs, loose ion pairs, and perhaps free ions. A major factor influencing this series of equilibria is the dielectric constant of the solvent. Thus, the higher dielectric constant solvents raise the concentration of the various ion pairs and free ions and a shift to higher wavelengths is observed. This behavior can be explained in terms of the relationships between frequency and energy. In nonpolar solvents, tight ion pairs are favored. Since these species are relatively energetic species, higher energy radiation is required to observe a transition, hence, the observed transition occurs at a lower wavelength. As conditions are modified to favor the lower energy species, the observed transition shifts to higher wavelengths.

Another major objective of our work was to use this difunctional initiator to polymerize diene and styrene based monomers. Initial experiments were directed towards polymerizing butadiene to high molecular weight in the nitrogen pressure nitrogen reactor. This was most convenient since samples could be removed from the reactor during the reaction as a function of time, etc. Figure 5.3-11 shows two size exclusion chromatograms of samples taken from the reactor during and <u>after</u> the polymerization was complete. The narrow peak at high elution volumes (lower molecular weight) corresponds to a sample taken during the polymerization. Notice the narrow molecular weight distribution which is typical for anionic polymerizations. However, after the polymerization reaches quantitative conversions the molecular weight distribution apparently broadens considerably as evidenced by the second peak at low elution volumes. It is suggested that at 60°C, the dianion chain end is <u>less</u> stable <u>after</u> all of the monomer is consumed. Partial elimination of lithium hydride could generate a diene-like species capable of reacting with residual living-ends, to generate the broader, possibly branched structure. Additional results in this area will be reported later (29). Table 5.3-2 summarizes the size exclusion chromatography (SEC) results on several polybutadiene samples taken as a function of reaction time. Again, narrow molecular weight distributions

Table 5.3-1. Effect of Polar Additives on the UV-Visible Spectra of the Dilithio Anion[1]

| Component | $\lambda_{Max}$(NM) | $\lambda_{Max}$(NM) |
|---|---|---|
| Dianion | 430 | --- |
| Dianion + TEA | 462 | 32 |
| Dianion + THF | 465 | 35 |
| Dianion + Dipip(ethane) | 458 | 38 |
| Dianion + Dipip(methane)[2] | --- | -- |
| Dianion + TMEDA[2] | --- | -- |

(1) Molar ratio of additive to chain end was ≤0.2.

(2) Premature termination was observed.

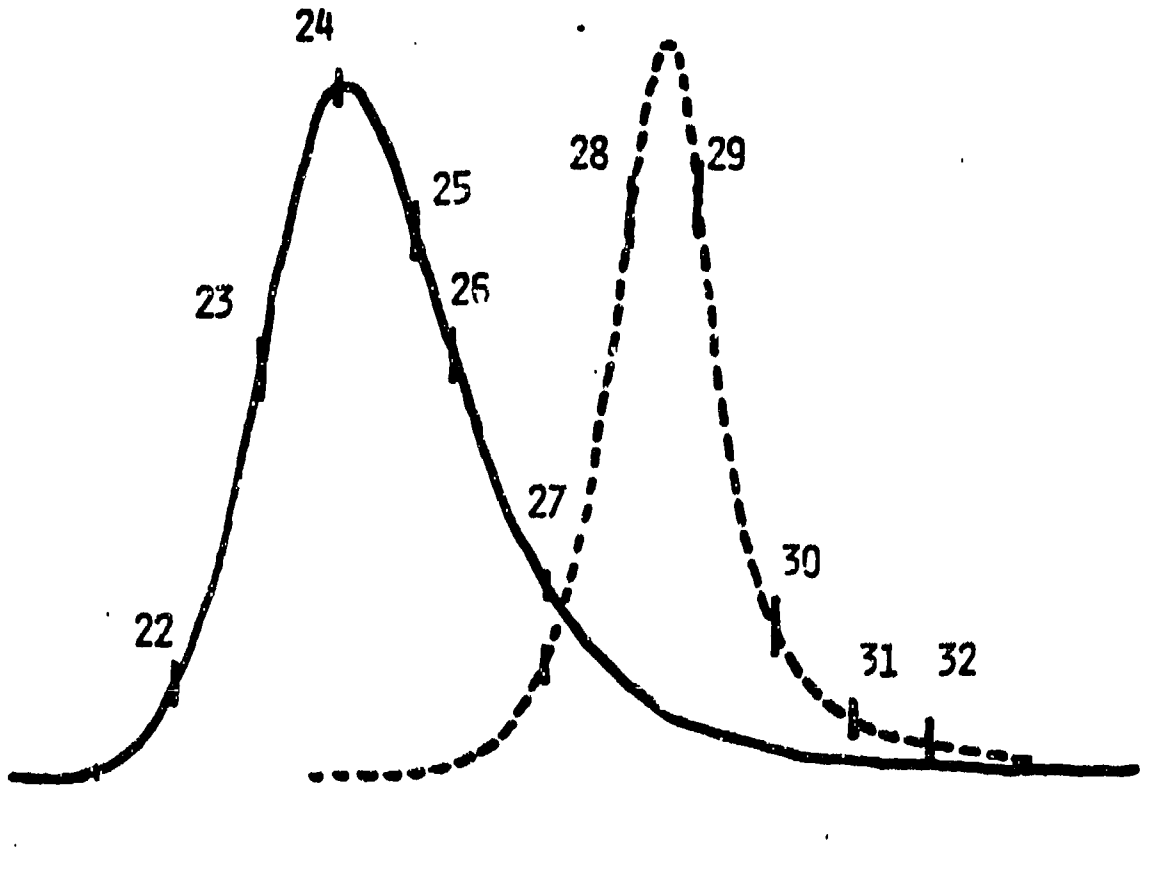


Figure 5.3-11. Size Exclusion Chromatograms of Narrow Distribution Polybutadiene and Broadened Species Obtained after Aging at 60°C

Table 5.3-2. Influence of Reaction Time, Conversion and Polybutadiene Dianion Aging Time at 60°C on $\bar{M}n$ and Polydispersity

| Reaction Time | $\bar{M}n$ | Poly-Dispersity |
|---|---|---|
| 10 Min | 26,700 | 1.16 |
| 20 Min | 54,200 | 1.09 |
| 30 Min | 70,300 | 1.12 |
| 60 Min | 86,400 | 1.28 |
| 90 Min | 86,700 | 1.64 |
| 180 Min | 115,600 | 1.58 |

* 10% solids (weight to weight)

are maintained initially, while later, broadening of the distribution occurs. As judged by the predicted $\bar{M}n$, the branching probably occurs when little or no monomer is present.

Triblock copolymers of styrene and isoprene (S-I-S) or butadiene (SBS) were synthesized using this difunctional initiator. A one-step synthesis was utilized wherein both monomers were charged at the same time. This method takes advantage of reactivity ratio differences between dienes and styrene (2-7). In cyclohexane, the center block of diene is substantially polymerized first followed by the two styrene end blocks. Because both monomers are added simultaneously, a tapered triblock copolymer structure is expected (8,10).

Size exclusion chromatography of this copolymer showed a single monomodal peak and a narrow molecular weight distribution, clearly indicating the absence of homopolymer and diblock contamination. Dynamic mechanical thermal analysis (DMTA) of a typical SIS copolymer (Figure 5.3-12) shows behavior typical of thermoplastic elastomers; namely separate glass transitions (Tg's) for both the isoprene and styrene phase and the presence of an extended rubbery plateau which indicated a phase-separated system. Further work on the synthesis, structure and property behavior of these elastomers is continuing. In particular, hydrogenation of the polydiene blocks is of interest.

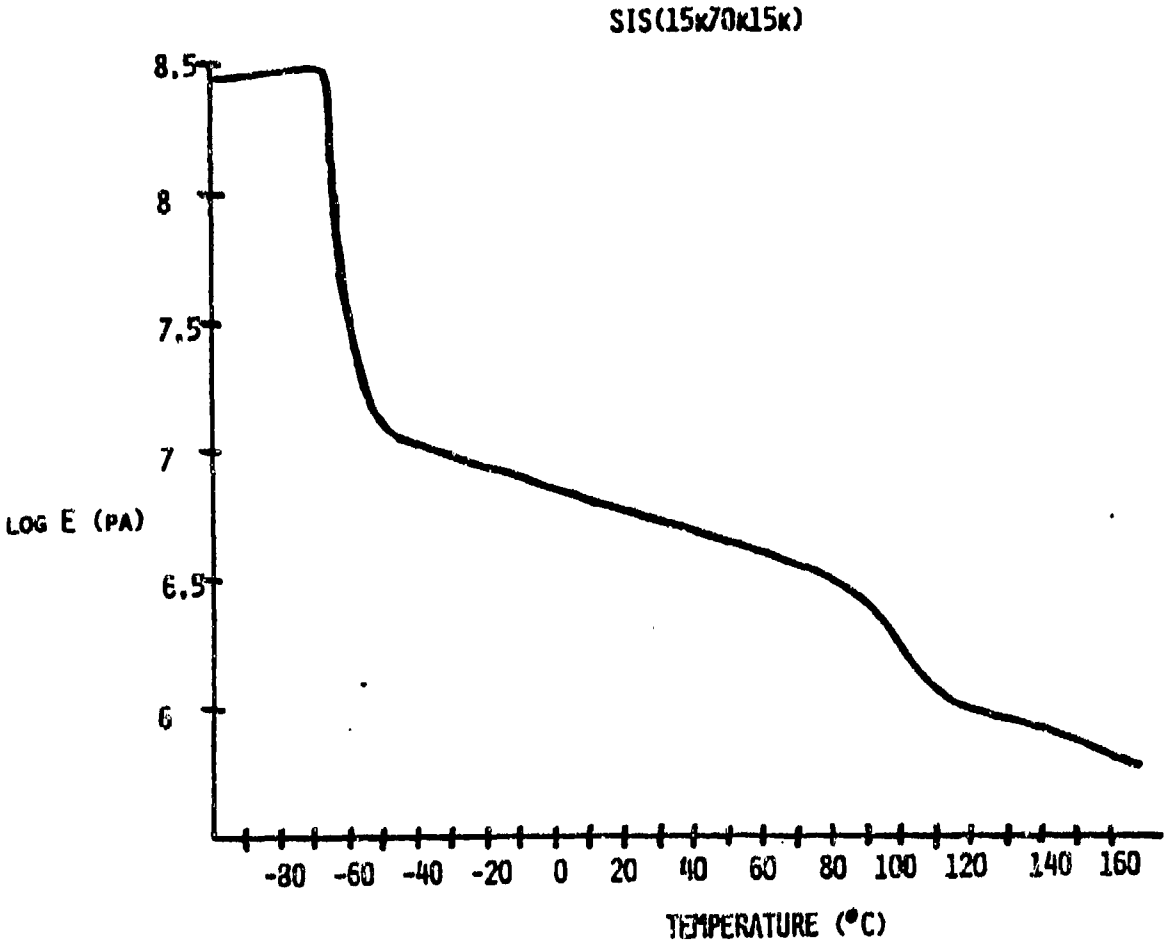


Figure 5.3-12. Dynamic Mechanical Behavior of an S-I-S Triblock Copolymer

5.3.4. References.


1. M. Szwarc, M. Levy, and R. M. Milkovich, J. Am. Chem. Soc., 78, 2656(1956).

2. M. Szwarc, "Carbanions, Living Polymers, and Electron-Transfer Processes", Wiley-Interscience, New York, 1968.

3. M. Morton, "Anionic Polymerization, Principles and Practice", Academic Press, New York, 1983.

4. M. Morton and L. J. Fetters, Macromolecules, 2, 453(1969).

5. M. Szwarc, Adv. in Poly. Sci., 49, 1(1983).

6. R. N. Young, R. Quirk and L. J. Fetters, Adv. Poly. Sci., 56, 1984.

7. J. E. McGrath, Editor, "Anionic Polymerization: Kinetic, Mechanisms and Synthesis, ACS Symposium Series No. 166, 1981.

8. A. Noshay and J. E. McGrath, "Block Copolymers: Overview and Critical Survey" Academic (1977).

9. G. Reiss, G. Hurtrez, and P. Bahadur, Encyclo. Poly. Sci. and Eng., 2nd Edition, Vol. 2, John Wiley & Sons, New York, 1985.

10. L. H. Tung, G. Y. S. Lo, and D. E. Beyer, Macromolecules, 11, 616(1978).

11. L. H. Tung, G. Y. S. Lo, U.S. Patents 4,182,818(1980); 4,196,153 (to Dow Chemical) (1980).

12. L. H. Tung, G. Y. S. Lo, J. W. Rakshys, and D. E. Beyer, U.S. Patents, 4,200,718(1979); 4,201,729(1980); 4,205,016 (to Dow Chemical) (1980).

13. R. C. Morrison and C. W. Kamineski, U.S. Patent (to Lithium Corp.) 3,725,368 (1973).

14. P. Lutz, E. Franta, and P. Rempp, C. R. Seances Acad. Sci., Ser. C., 283, 123(1970).

15. G. Popov and G. Schwarchula, Plast. U. Kautch., 26, 263(1979).

16. P. Guyot, J. C. Favier, H. Uytterhoeven, M. Fontanille, and P. Sigwalt, Polymer, 22, 1724(1981).

17. P. Guyot, J. C. Favier, M. Fontanille, and P. Sigwalt, Polymer, 23, 73(1982).

18. R. P. Foss, H. W. Jacobson, and W. H. Sharkey, Macromolecules, 10, 287(1977).

19. G. G. Cameron, G. M. Buchan, Polymer, 20, 1129(1979).

20. P. Lutz, E. Franta, and P. Rempp, Polymer, 23, 1953(1982).

21. H. Hocker and G. Latterman, Makromol. Chem., 158, 191(1972).

22. H. Hocker and G. Latterman, J. Polym. Sci., Polym. Symp., 54, 361(1976).

23. H. Hocker and G. Latterman, Angew Chem. Int. Ed. Eng., 19, 219(1980).

24. M. Morton and L. J. Fetters, Rubber Rev., 48, 359(1975).

25. J. M. Hoover and J. E. McGrath, Polymer Preprints 27(2), 150, 1986; J. Poly. Sci., in press, 1986.

26. A. D. Broske, T. L. Huang, J. M. Hoover, R. D. Allen, and J. E. McGrath, Polymer Preprint 25(2), 85(1984).

27. A. D. Broske and J. E. McGrath, Polym. Preprint 26(1), 241(1985).

28. J. E. McGrath, R. D. Allen, J. M. Hoover, T. E. Long, A. D. Broske, S. D. Smith, and D. K. Mohanty, Polymer Preprints 27(1), 183(1986).

29. A. D. Broske and J. E. McGrath, J. Poly. Sci., in preparation; A. D. Broske, Ph.D. Thesis, Virginia Polytechnic Institute and State University, 1987.

30. P. Bres, M. Viguier, J. Sledz, F. Schue, P. E. Black, D. J. Worsfold, and S. Bywater, Macromolecules, 19, 1325 (1986).

## 5.4. Ion-containing Block and Random Copolymers

5.4.1. Introduction. Ion-containing polymers (ionomers) are receiving ever increasing attention due to the dramatic effects that small amounts of ionic groups exert on polymer properties (1-4). Increases in tensile strength, modulus, melt and solution viscosity, glass transition temperature, and a broadening of the rubbery plateau are some of the major changes that occur when ionic groups are incorporated into polymers. The extent of property modification depends generally on the type, amount, and distribution of ionic groups in the polymer. Although utilization of a wide variety of ionic groups is possible, carboxylates and sulfonates have thus far received considerable attention. Polymer backbones modified most widely include polyethylene, polystyrene, polyacrylates, polypentenamers, ethylene-propylene-diene terpolymers and polysulfones (4-9). However, the major difficulty in this field is the lack of available synthetic methods that would lead to the preparation of well-defined ionomeric structures.

Ion-containing polymers are prepared via two fundamentally different approaches. The first method involves a postpolymerization reaction in which the ionic group is "grafted" onto a preformed polymer (4,10,11), whereas in the second method a vinyl monomer is directly copolymerized with an unsaturated acid or salt derivative. Another possibility, which in fact is a combination of the above two approaches, is to copolymerize two covalent monomers and then derivatize one by, for example, ester hydrolysis (12). Carboxylated ionomers are generally synthesized by the direct copolymerization of acrylic or methacrylic acid with vinyl monomers. The copolymers produced are then either partially or completely neutralized with bases to incorporate the various counterions (e.g., $Na^+$, $K^+$, $Zn^{++}$, etc.) into the system. Sulfonate groups are most often introduced into the polymer backbone via postpolymerization reactions using sulfonating agents such as acetyl sulfate or $SO_3$/triethylphosphate complex in a suitable solvent (4,10,11). The sulfonic acid groups introduced into the polymer backbone are then neutralized. This method of sulfonation is difficult and is limited to only backbones which provide suitable sites for sulfonation. Therefore, although sulfonated ionomers reportedly exhibit association properties far superior to carboxylated systems (4), relatively limited work appears in the literature on the direct synthesis of sulfonated ionomers from the respective monomers (13,14).

The synthesis routes discussed above usually result in random placement of ionic groups along the polymer backbone, thus making characterization and interpretation of structure-property studies quite difficult. Previous work on the synthesis of well-defined block and graft ionomers based on polystyrene and poly(2- or 4-vinylpyridine) have been done by Selb and Gallot (15,16). They have synthesized these copolymers via anionic polymerization at -70°C using diphenylmethylsodium as the initiator in THF. They have also investigated the solution behavior of the resulting ionomers after quaternization (17). More recently Gauthier and Eisenberg (30) have demonstrated the synthesis of styrene-vinylpyridinium ABA block ionomers and studies their thermal and mechanical properties. Recent work with so-called telechelic ionomers, where the ionic groups are located only at the chain ends, may also simplify this characterization problem (18-21).

We are currently exploring new routes to the synthesis of ionomers with controlled architecture, i.e., with control over the amount and location of ionic groups in the polymer backbone. One of our main interests is the synthesis of ion containing block copolymers. The applicability of anionic polymerization in the synthesis of block copolymers and other well-defined model systems is well documented (22-24). Not as well appreciated, however, is the blocky nature that certain emulsion copolymerizations may provide. Thus, we have utilized both anionic and free radical emulsion polymerization in the preparation of model ionomers of controlled architecture. In this section, the synthesis and characteristics of sulfonated and carboxylated block ionomers by both free radical emulsion and anionic polymerization followed by hydrolysis will be discussed.

5.4.2. Experimental.

5.4.2.1. Emulsion copolymerization. Sodium-p-styrene sulfonate (SST) was supplied by Exxon Research and Engineering Co. and used without further purification. n-Butyl acrylate was a product of Polysciences, Inc. and was passed through a column of neutral alumina, twice, before use to remove the inhibitor. Potassium persulfate and sodium bisulfate were recrystallized from distilled water and dried under vacuum. Nonionic emulsifier (ATLOX 8916 TF) was a product of ICI Americas Inc. 1-Dodecanethiol (Aldrich) was used as the chain transfer agent. Double-distilled and deoxygenated water was used throughout the emulsion reactions.

Copolymerizations were carried out in a 4-necked, 250 ml round bottom flask fitted with a mechanical stirrer, condenser, thermometer, and gas ($N_2$) inlet. Temperature was controlled in the 60-70°C range and the reaction times were varied between 5 and 24 hours. The emulsion recipe used is given in Table 5.4-1.

At the end of the reactions the stable latex obtained was poured into teflon-coated aluminum pans and dried in an air oven. The products were then dissolved in THF and coagulated in a methanol/water mixture several times, before final drying.

5.4.2.2. Anionic copolymerization. Anionic techniques were used to synthesize the block polymers which function as precursors to ion-containing block polymers. Monomers were carefully dried by repeated vacuum distillation from $CaH_2$. Distillation from dibutyl magnesium was also utilized for the final purification of the hydrocarbon monomers, styrene and diphenyl ethylene. The methacrylate monomers may also be finally purified via the trialkyl aluminum approach (25), although this was not necessary as the Rohm & Haas iso-butyl methacrylate (IBMA) used in this study proved to be exceedingly pure. THF was dried by double distillation from sodium/benzophenone complex.

Block polymerizations were conducted in THF at -78°C under an inert atmosphere. The polymerization route employed is shown in Scheme 5.4-1. Typically, the styrene monomer was charged into the polymerization reactor with THF, followed by rapid addition of sec-butyl lithium. The polystyryl

Table 5.4-1. Typical Emulsion Copolymerization Recipe

| | |
|---|---|
| Water | 80 mL |
| Vinyl Monomer | 20 g |
| Sulfonated Styrene | 0-2 g |
| Emulsifier | 0.8 g |
| $K_2S_2O_8/NaHSO_3$ | 0.08/0.04 g |
| 1-Dodecanethiol | 0-0.1 g |

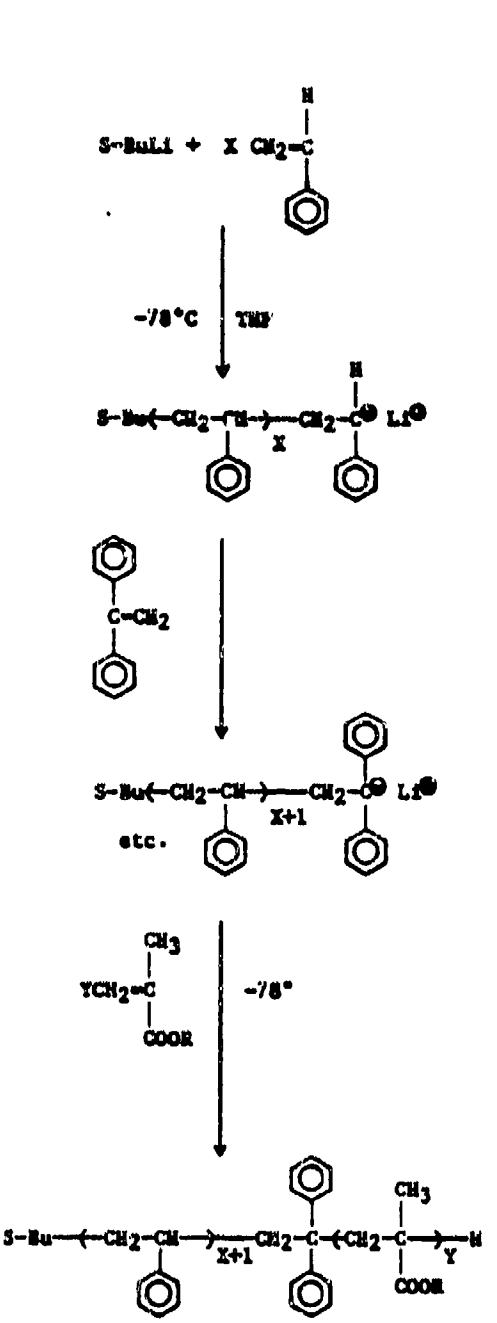

Scheme 5.4-1. Anionic Synthesis of Styrene/IBMA Block Copolymer

lithium was then "capped" with 1,1-diphenyl ethylene to form less basic, more hindered anions so as to avoid deleterious side reactions to the methacrylate carbonyl. Just before the addition of methacrylate monomer (IBMA), a small amount of capped polystyryl lithium was removed for GPC analysis. Termination was performed several minutes after the addition of the methacrylate monomer, using a methanol/acetic acid mixture. The polymers were generally isolated by precipitation in methanol. During the synthesis reactions molecular weights ($\bar{M}n$) of the polystyrene and poly(isobutyl) methacrylate) blocks kept constant at 40,000 and 10,000 g/mole respectively.

After drying this block polymer precursor, partial hydrolysis of the methacrylate block lead to the ion-containing block copolymer. The hydrolysis route is shown in Scheme 5.4-2. The hydrolysis method employed utilized potassium superoxide as a general route to ester cleavage to generate in a direct fashion potassium carboxylate unit.

Typically, the copolymer is dissolved in a mixed solvent system such as THF/Dimethyl sulfoxide or Toluene/DMSO. A three-fold excess of powdered $KO_2$ (Alfa) is then added. Reaction time and temperature depend on degree of cleavage desired as well as the type and nature of the ester alkyl group. The reaction is quenched with water. The ion-containing block copolymer is then reprecipitated and dried.

5.4.2.3. Characterization of products. Intrinsic viscosities were determined in THF at 25°C using Ubbelohde viscometers. Molecular weights were also analyzed using a Waters 150C GPC with microstyragel columns, although Bondagel columns were used in some experiments. Thermal characterization of the products was performed on a Perkin Elmer Thermal Analysis System 2. Tg's were determined by DSC with a heating rate of 10°C/minute. TMA penetration curves were obtained with a constant load of 10g and heating rate of 10°C/minute. Stress-strain tests were carried out using an Instron Model 2211 Tester. Dog-bone-shaped samples were punched out of compression molded polymer films using standard dies. Tests were performed at room temperature with a crosshead speed of 10 mm/minute. Infrared spectra were obtained on a Nicolet MX-1 FT-IR Spectrometer.

5.4.3. Results and Discussion.

5.4.3.1. Emulsion copolymerization of n-butyl acrylate and sulfonated styrene. We have investigated the direct copolymerization of sulfonated styrene (SST) with n-butyl acrylate to produce ionomers. It was demonstrated that emulsion polymerization is a useful and potentially important technique in the synthesis of sulfonate ion-containing polymers by direct reaction between the ionogenic and covalent monomers, provided that a "water soluble initiator system" is used. Some workers have already reported the used of an organic-soluble peroxide and a water-soluble reducing agent during similar reactions in order to generate effective copolymerization at the micelle interfaces (13,14).

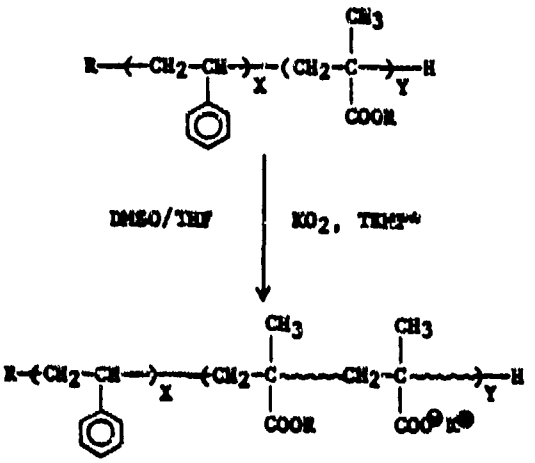


*R=Me, T=25°C
R=i-Butyl, T=85°C

Scheme 5.4-2. Synthesis of Ion-Containing Block Copolymers via Superoxide Hydrolysis

During our studies we used both sodium and potassium salts of SST and they behaved similarly as expected. The emulsifier was a nonionic "alkylphenoxy-ethylene oxide"-type surfactant with a Hydroplilic-Lyophylic Balance value of 15.4. The amount of SST charged was varied between 0 and 10 percent by mole. The latex obtained after the reaction was fairly stable in each case. Table 5.4-2 provides the data on the synthesis of n-butyl acrylate and sulfonated styrene ionomers. As expected in emulsion polymerizations we were able to obtain fairly high yields. In the first four reactions no chain transfer agent (CTA) was used and except sample 1, which is the control poly(n-butyl acrylate), we were not able to dissolve any others (samples 2, 3 or 4) in any single solvent or solvent combinations. This is attributed to the combined effects of very high molecular weights of the polymers produced and strong ionic interactions between the pendant sulfonate groups on the polymers chains and possibly the residual end groups derived from the initiator. Although these materials were not soluble, they were easily compression moldable at temperatures around 200°C and all yielded clear, transparent films. However, when a small amount of an organic soluble chain transfer agent (1-dodecanethiol) was used, it was possible to obtain ionomers which were soluble in solvents such as tetrahydrofuran, chloroform and toluene/methanol.

As can be seen from the last column of Table 5.4-2, DSC studies did not indicate any change in the glass transition temperature of the polyacrylates due to the presence and/or concentration of the ionogenic monomer (SST) incorporated. We have observed the same behavior in styrene, methyl acrylate and other systems (26). Other workers have also reported similar results in ionomers synthesized by the direct reactions of various acrylic acid salts and covalent vinyl monomers (27). This indicates either the simultaneous homopolymerization of both monomers or a "block" copolymerization. We were, however, unable to detect any high temperature transitions in DSC due to the very small amounts of SST incorporated and the sensitivity of DSC method. In methyl acrylate/SST system at 8 mole percent SST level we were able to detect a second Tg at 330°C for the ionic block (28). However, when we studied the thermomechanical behavior of these materials via TMA in the penetration mode, we were able to see the dramatic effects of ion incorporation even at very containing polymers compared to the control poly(n-butyl acrylate). This is illustrated in Figure 5.4-1. Attempts to physically blend two homopolymers showed that they were highly incompatible as expected and there was no enhancement in the thermal or mechanical properties of resulting materials. The films obtained by blending were very cloudy showing the dispersion of poly(sulfonated styrene) in polyacrylate. On the other hand, compression molded films of the copolymers synthesized appeared macroscopically "homogeneous" and transparent, all of which indicates the formation of blocky structures. Our kinetic studies on the copolymerization of SST and methyl acrylate in emulsion also show the formation of "blocky" ionomers (28).

Stress-strain behavior of n-butyl acrylate-SST ionomers are given in Figure 5.4-2. It is clear that the incorporation of sulfonate groups has a

Table 5.4-2. Synthesis of n-Butyl Acrylate Sulfonated Styrene Copolymers

| No | nBuA (g) | SST (g) | SST (%mol) | Reaction T,°C | Reaction t,hr | CTA (g) | Yield (%) | Tg °C |
|---|---|---|---|---|---|---|---|---|
| 1 | 10.0 | -- | -- | 60 | 19 | -- | 85 | -55 |
| 2 | 10.0 | 0.52 | 2.8 | 65 | 9 | -- | 95 | -55 |
| 3 | 10.0 | 1.01 | 5.5 | 65 | 9 | -- | 93 | -55 |
| 4 | 10.0 | 1.90 | 9.8 | 60 | 5.5 | -- | 93 | -55 |
| 5 | 11.0 | 0.99 | 5.5 | 67 | 24 | 0.13 | 82 | -55 |
| 6 | 25.0 | 0.40 | 1.0 | 62 | 5 | 0.09 | 91 | -55 |
| 7 | 24.2 | 0.80 | 2.0 | 68 | 5 | 0.09 | 72 | -- |
| 8 | 23.3 | 1.12 | 2.9 | 68 | 5.5 | 0.05 | 65 | -- |
| 9 | 23.3 | 1.50 | 3.8 | 68 | 5.5 | 0.05 | 68 | -55 |

#2-5, $K^+$ salt, #6-9, $Na^+$ salt

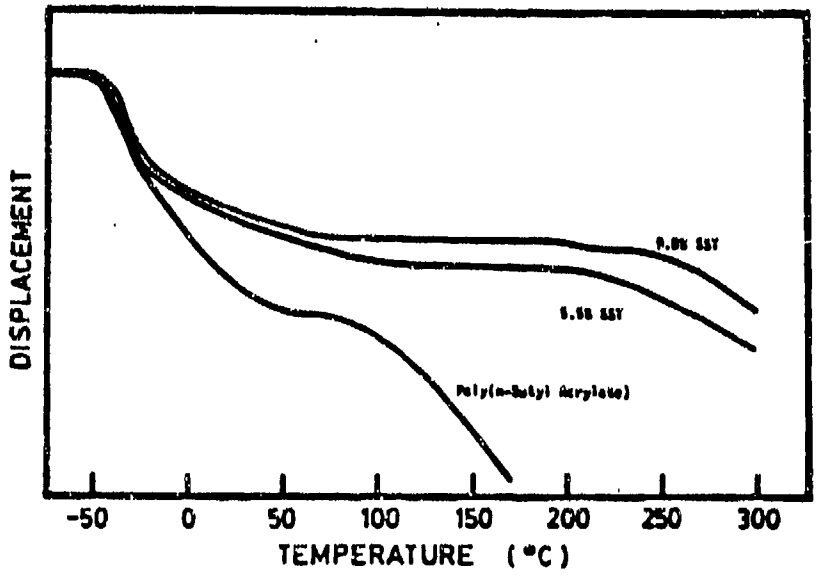


Figure 5.4-1. TMA Penetration Curves for n-Butyl Acrylate/sulfonated Styrene Ion-Containing Copolymers

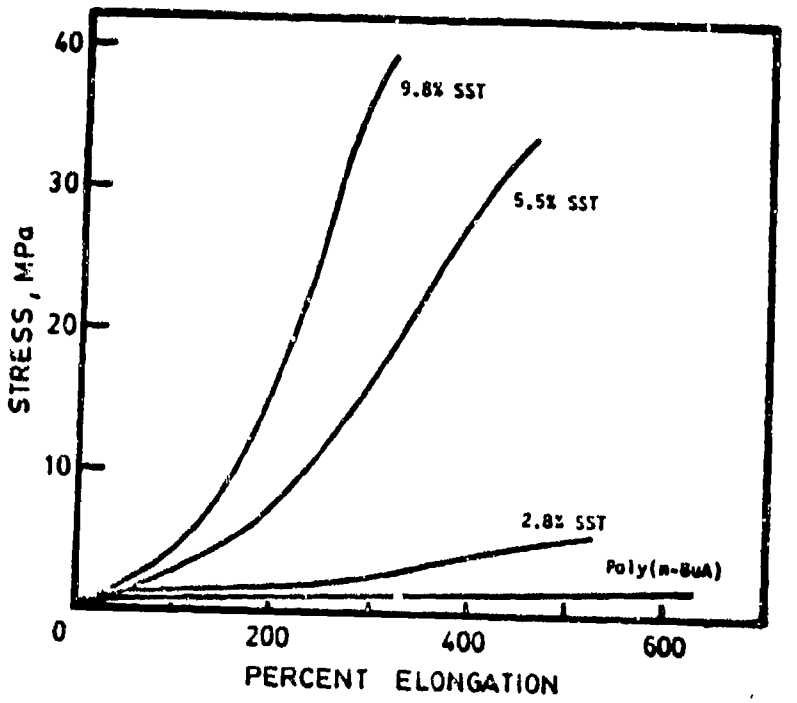


Figure 5.4-2. Stress-strain Behavior of n-Butyl Acrylate/sulfonated Styrene Ion-containing Copolymers

remarkable effect on the behavior of resulting materials. Compared with n-butyl acrylate homopolymer, introduction of approximately 5 mole percent of SST into the copolymer increases the tensile strength more than 40-fold. The increase in the overall strength is proportional to the level of ion content. Modulus values of the resulting ionomers increase and elongation at break slightly decrease with increasing ion content. TMA and stress-strain results may indicate that in this system optimum properties can be obtained at a SST level of about 5 mole percent.

5.4.3.2. Block ionomers through anionic polymerization and hydrolysis. The novel reaction scheme which we had proposed for "blocky" ionomers through emulsion polymerization prompted us to prepare very well-defined ion-containing block copolymers through anionic polymerization. The initial system chosen for synthesis, modification and characterization was the polystyrene-poly(isobutyl methacrylate) diblock (PS-PIBM DB) copolymer. This particular system was chosen for the following reasons:

- The availability, ease of purification, and well established polymerization characteristics of styrene
- The large body of literature available on polystyrene based ionomers.
- Isobutyl methacrylate (Rohm and Haas) is a methacrylate monomer of high purity.
- The methacrylate ester group may be converted, via hydrolysis, to a carboxylate ion.

These polystyrene-methacrylate copolymers with block molecular weights of 40,000 and 10,000 g/mole respectively, are thus precursors to carboxylate ion-containing block copolymers.

As evident from the GPC chromatograms in Figure 5.4-3, both the diphenyl ethylene-capped polystyrene and the PS-PIBM diblock copolymers have narrow molecular weight distributions. More importantly, no detectable homopolymer contamination is present in the very pure diblock. This high structural integrity was achieved by taking the following precautions.

- Capping of the PB "Front Block" with 1,1-DPE to afford a highly hindered, less basic macromolecular initiator for methyacrylate polymerization.
- Slow addition at -78°C of IBMA to avoid thermal termination.
- Utilization of high purity methacrylate monomers.

Hydrolysis of this well-defined diblock material proved to be quite difficult. A variety of acidic and basic hydrolysis attempts were made, with little or no success. We then found evidence in the literature (29) for a facile new hydrolysis method which had achieved very fast hydrolysis of methyl laurate by using solid potassium superoxide ($KO_2$). We have used

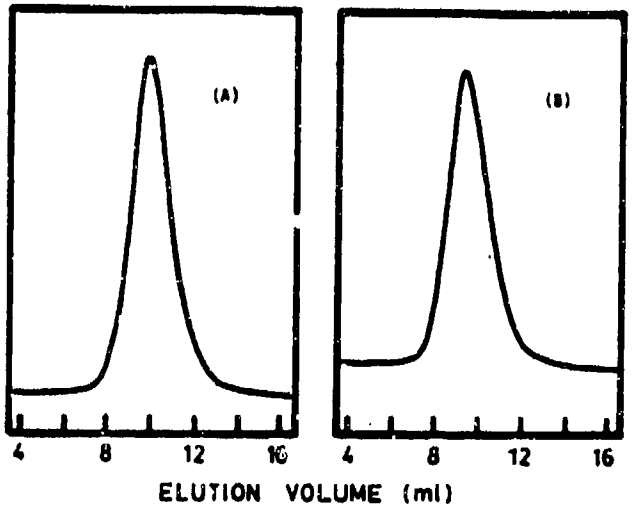


Figure 5.4-3. Size Exclusion Chromatograms of (A) Polystyrene Front Block ($\bar{M}n$) 40,000 g/mole) and (B) Polystyrene/poly(isobutyl methacrylate) Diblock Copolymer ($\bar{M}n$ 50,000 g/mole)

this new method successfully in the hydrolysis of polymethyl methacrylate (PMMA). Elvacite 2041 (DuPont PMMA) was rendered water soluble by simply stirring over $KO_2$ at room temperature overnight. Scheme II shows the hydrolysis route employed. As is indicated in the scheme, although PMMA is hydrolyzed at room temperature, the bulkier iso-butyl ester group is much more resistant to this hydrolysis reaction, and indeed, even at 80°C the hydrolysis is slow as judged by FT-IR. Figure 5.4-4 shows a typical FT-IR spectrum of the partially hydrolyzed diblock in the acid form. The extent of hydrolysis versus reaction time is shown in Table 5.4-3 where the absorbance ratio of acid to ester is given. As can be seen, there appears to be an induction period in this hydrolysis reaction. This may be due to the heterogeneous nature of $KO_2$ in THF/DMSO. We have also carried out these reactions in toluene/DMSO solvent mixture which quite surprisingly gives a much more homogeneous reaction mixture. These $KO_2$ reactions performed in toluene/DMSO solvent systems show no induction period, thus leading to much shorter reactions times. It should also be noted that no degradation of the polymer resulted from these reaction conditions as noted from GPC analysis on acidified "ionomers," using bondagel columns and THF solvent at room temperature.

Characterization of the thermal and mechanical properties of these systems show several marked similarities with the poly(butyl acrylate sulfonated styrene) emulsion polymers discussed earlier. Transparent films were produced by compression molding under high pressures at 250°C. These ion-containing block copolymers were insoluble in all solvents tried, but dissolved quickly when several drops of HCl are added to convert the carboxylate ions to carboxylic acid groups. As seen in Figure 5.4-5, the block ionomer having 10 mole percent ionic content shows a very highly extended rubbery plateau in the TMA experiment compared to the diblock precursor. At the same time, dynamic mechanical analysis (DMTA) shows no change in the glass transition behavior of the polystyrene matrix with ion content, as well as highly extended rubbery plateau behavior with a very differently synthesized butylacrylate-sulfonated styrene ionomers via emulsion copolymerization.

5.4.4. Conclusions.

Both emulsion copolymerization of butyl acrylate/sulfonated styrene with a water-soluble initiation system, and anionically synthesized diblock ionomers based on the ester hydrolysis of methacrylate blocks show no effect of ion content on the Tg of the matrix however provide a highly extended rubbery plateau to the resulting ionomers.

Our work on the synthesis of model ionomer systems by anionic polymerization is continuing. The architectural effects of these ionomers having controlled structures are being compared with their random counterparts.

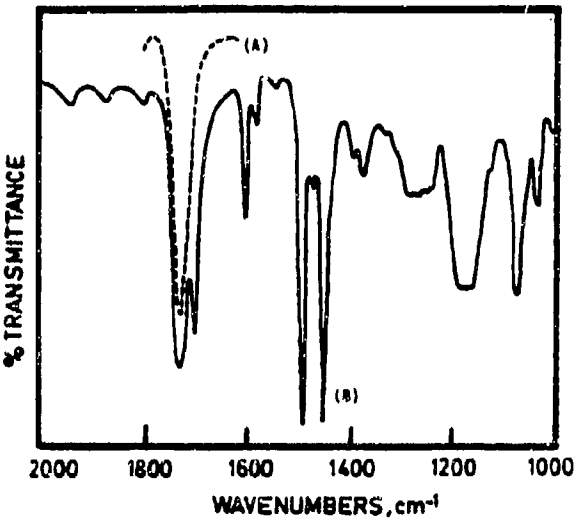


Figure 5.4-4. FT-IR Spectra of (A) Polystyrene/poly(isobutyl methacrylate) Diblock Copolymer and (B) Carboxylated Block Ionomer Obtained After Hydrolysis with $KO_2$

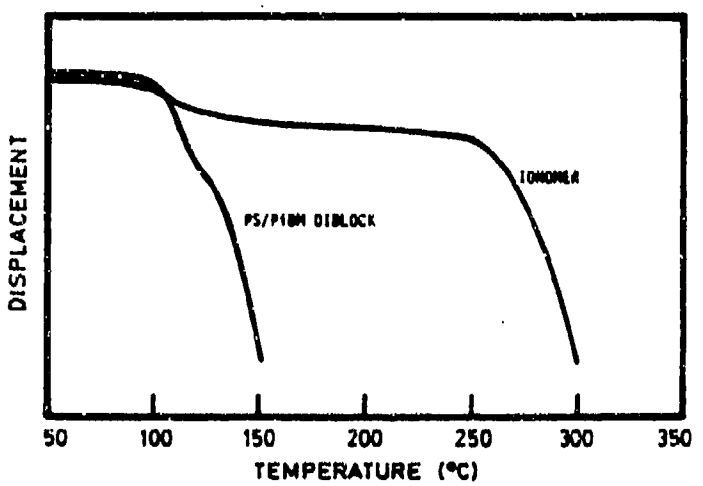


Figure 5.4-5. TMA Penetration Behavior of PS/PIBM Diblock Copolymer and Carboxylated Ionomer (5 mole percent-$COO^- K^+$) Obtained after Hydrolysis

Table 5.4-3. Studies on Superoxide Hydrolysis and Characterization of the Products

| Sample No. | Rxn. Time (Hr.) | El. Vol. (GPC) | $A_A/A_E$ (FT-IR) |
|---|---|---|---|
| I | 0 | 28.8 | 0 |
| II | 1 | 28.7 | 0 |
| III | 2 | 28.8 | 0 |
| IV | 6 | 28.8 | 0.44 |
| V | 13 | 28.8 | 0.64 |
| VI | 17 | 29.3 | 1.15 |

## 5.4.5. References


1. L. Holliday, Ed., "Ionic Polymers", Applied Science Publishers, London 1975.

2. A. Eisenberg and M. King, "Ion-Containing Polymers", Academic Press, New York, 1977.

3. W. J. MacKnight and T. R. Earnest, Jr., Macromol. Revs., 16, 41 (1981).

4. R. D. Lundberg and H. S. Makowski, "Ions in Polymers", Ed. A. Eisenberg, Adv. Chem. Ser., No. 187, ACS, Washington, D.C., 1980, Chapter 2.

5. M. F. Hoover and G. B. Butler, J. Polym. Sci., Polym. Symp., 45, 1 (1974).

6. K. Sanui, R. W. Lenz and W. J. MacKnight, J. Polym. Sci., Polym. Chem., 12, 1965 (1974).

7. C. Azuma and W. J. MacKnight, J. Polym. Sci., Polym. Chem., 15, 547 (1977).

8. H. S. Makowski, R. D. Lundberg, L. Westerman and J. Bock, "Ions in Polymers", Ed. A. Eisenberg, Adv. Chem. Ser., No. 187, ACS Washington, D.C., 1980, Chapter 1.

9. B. C. Johnson, I. Yilgor, C. Tran, M. Iqbal, J. P. Wightman, D. R. Lloyd and J. E. McGrath, J. Polym. Sci., Polym. Chem., 22(3), 721 (1984).

10. J. P. Quentin, Sulfonated Polyarylether Sulfones, U.S. Pat., 3,709,841, Rhone-Poulenc, January 9, 1973.

11. A. Noshay and L. M. Robeson, J. Appl. Polym. Sci., 20, 1885 (1976).

12. R. D. Allen, T. L. Huang, D. K. Mohanty, S. S. Huang, H. D. Qin and J. E. McGrath, Polym. Prepr., 24(2), 41 (1983).

13. R. A. Weiss, R. D. Lundberg and A. Werner, J. Polym. Sci., Polym. Chem., 18, 3427 (1980).

14. B. Siadat, B. Oster and R. W. Lenz, J. Appl. Polym. Sci., 26, 1027 (1981).

15. J. Selb and Y. Gallot, Polymer, 20, 1259 (1979).

16. J. Selb and Y. Gallot, Polymer, 20, 1273 (1979).

17. J. Selb and Y. Gallot, Makromol. Chem., 181, 809 (1980).

18. G. Broze, R. Jerome and Ph. Teyssie, Macromolecules, 14, 224 (1981).

19. G. Broze, R. Jerome and Ph. Teyssie, Macromolecules, 15, 920 (1982).

20. G. Broze, R. Jerome, Ph. Teyssie and C. Marco, J. Polym. Sci., Polym. Phys., 21, 2205 (1983).

21. S. Bagrodia, Y. Mohajer, G. L. Wilkes, R. F. Storey and J. P. Kennedy, Polym. Bull, 9, 174 (1983).

22. A. Noshay and J. E. McGrath, "Block Copolymers: Overview and Critical Survey", Academic Press, New York, 1977.

23. J. E. McGrath, Ed., "Anionic Polymerization: Kinetics, Mechanisms and Synthesis", ACS Symp. Ser., No. 166, Washington D.C., 1981.

24. M. Morton, "Anionic Polymerization: Principles and Practice", Academic Press, New York, 1983.

25. R. D. Allen and J. E. McGrath, Polym. Prepr., 25(2), 9 (1984).

26. I. Yilgor and J. E. McGrath, to be published.

27. Z. Wojtzack and K. Suchocka-Galas, IUPAC Int. Symp. Macromol., Strassbourg, France (1981). Proc. p. 311.

28. I. Yilgor, K. A. Packard, J. Eberle, R. D. Lundberg and J. E. McGrath, IUPAC Int. Symp. on Macromol., Bucharest, Romania (1983) Proc., I-10, p. 27.

29. N. Kornblum and S. Singaram, J. Org. Chem., 44, 4727 (1979).

30. S. Gauthier and A. Eisenberg, Polym. Prepr., 25(2), 113 (1984).

## 5.5. Morphology and Properties of Poly(Urea-Urethane) Elastomers

5.5.1. Introduction. In the past decade numerous detailed studies have been carried out for investigating the structure-property relationships in various segmented polyurethanes. A wide variety of aromatic and aliphatic diisocyanates and low molecular weight diol or amine chain extenders have been employed. The chain extenders commonly used for the hard segment have about 2 to 12 carbon atoms. The soft segments have been typically 1,000 to 3,000 molecular weight polyester, polyether or polybutadiene polyols. Many of these studies have established that in segmented polyurethanes, phase separation of the urethane hard segment into microdomains can take place even when the segmental length is relatively short. The primary driving force for domain formation is the strong intermolecular interaction between the urethane units which often have aromatic character and are capable of forming interurethane hydrogen bonds. Several workers have also observed the presence of hydrogen bonding between the urethane NH groups and oxygen of the macroglycol ether or ester linkage (1,2). This observation is consistent with the postulate that some hard segments are dissolved in the soft-segment matrix phase or vice versa. Polyurethanes are not high-temperature polymers and cannot be used for continuous application at temperatures in excess of 100°C. At high temperatures, polyurethanes begin to degrade thermally in an oxidative environment and/or may lose their two phase texture due to phase mixing (3).

The incorporation of urea linkages in polyurethane hard segments has a profound effect on the phase separation and domain structure of polyester or polyether-based polyurethane-ureas (PEUU). This is due to the high polarity differences between the hard and soft segments and the likely development of a three dimensional urea hydrogen bonding network (4-6). These urea linkages can be introduced by allowing an isocyanate group to react with an amine group. As a result of their improved hydrogen bonding capability, good elastomeric behavior has been observed in other urea-linked segmented copolymers which contained as low as 6 percent hard segment by weight (7,8).

From the literature it is obvious that a variety of polyurethane-urea copolymers have been prepared and studied. Sung et al. (5,9,10) have described the properties of segmented PEUU's based on tolylene-2,4-diisocyanate (TDI), ethylenediamine (ED) and poly(tetramethylene oxide) (PTMO), a polyether glycol also referred to as polytetramethylene glycol. The morphological investigation by small angle x-ray scattering (SAXS) has been carried out by Abouzahr et al. (11) on these materials. In contrast, Khransovskii (12) studied the PEUU composed of PTMO, TDI and 4,4'-diaminodiphenyl methane (DAM). The hard segments formed in both these polyurethane-ureas are capable of only limited crystallization because of the unsymmetric structure of TDI units. Ishihara et al. (13-15) have reported on the synthesis and behavior of more crystallizable polyurethane-ureas based on PTMO, methylene bis(4-phenyliso-cyanate) (MDI), and DAM. A symmetric MDI/DAM hard segment would have better packing efficiency than a non-symmetric TDI/DAM hard segment. As a result, much stronger hard

segment domains would be obtained with the former and the copolymer would be expected to display a stronger mechanical response. As compared to MDI/polybutadiene diol (BD) based polyurethanes, the thermal properties would no doubt be enhanced because of the complete aromatic nature of the hard segments.

Unfortunately, the large thermodynamic incompatibility between the two types of segments and hydrogen-bonding capability of the hard segments also make the synthesis and processing of these segmented polyurethane-ureas very difficult. The problem also arises because the reaction between amine and isocyanate groups proceeds at a much faster rate than the reaction of isocyanate and hydroxyl groups. In a one-step bulk polymerization, the high reactivity of $-NH_2$ and -NCO groups could result primarily in the formation of polyurea which can prematurely precipitate out of the reaction mixture. Some success is achieved when a strong polar group is attached to the diamine component to retard the isocyanate-amine reaction, e.g., MDI and 3,3'-dichloro-4,4'-diaminodiphenyl methane (MOCA). Use of the latter diamine has been discontinued because of carcinogenic hazards. Solution polymerization of PEUU's is sometimes possible when the reaction mixture is maintained at low temperatures to control the $-NH_2$/-NCO reaction. However, the solution polymerization approach suffers from the difficulty of obtaining a good common solvent for all the reaction components. In brief, the choice of solvent clearly affects the degree of polymerization and a mechanically weak polymer would be obtained if the overall molecular weight of the segmented copolymer is low.

Attempts have been made to synthesize the MDI/DAM-based segmented polyurethane-urea by addition of stoichiometric amounts of water to the mixture of PTMO and MDI. Adding controlled amounts of water would convert the excess MDI into DAM by the reaction scheme as illustrated below.

$$RNCO + H_2O \longrightarrow [RNHCOOH] \longrightarrow RNH_2 + CO_2\uparrow$$

The water molecule causes the formation of the unstable carbamic acid which decomposes further to yield DAM and $CO_2$ and is given off in the process. This approach, although promising, is difficult to use effectively because of water immiscibility with the reaction system. As a consequence, addition of water results in the formation of water droplets and a copolymer with heterogenous properties may thus be obtained.

Historically, in 1948, Saunders and Slocombe (16) reported that tertiary alcohols dehydrate at reasonably high temperatures in the presence of isocyanate groups. Although no mechanism was proposed, it was postulated that a tertiary alcohol would produce water in the presence of a weak acidic environment. Therefore, it may be possible to synthesize segmented polyurethane-ureas by taking advantage of such a proposed dehydration reaction. Specifically, a mixture of isocyanate-capped polyether, diisocyanate and a tertiary alcohol, when heated under inert conditions, could result in the formation of a PEUU. This could result from the fact that the tertiary alcohol would dehydrate and the water generated would cause the formation of an amine group by the reaction with isocyanate.

Next, this amine-terminated prepolymer unit would react with MDI to serve as the chain extender for the MDI-based hard segments. Thus, this scheme provides a novel approach to the synthesis of segmented PEUU's as high molecular weight copolymers can be obtained by a homogeneous, in situ chain-extension step involving essentially two terminal isocyanate groups. Since the water is introduced only at molecular levels, it should be consumed immediately in the formation of amine. Quantities of water in the form of droplets are thus avoided and the resulting copolymers might be expected to be compositionally more uniform.

Using the above procedure, novel segmented polyurethane-ureas have been successfully prepared and some synthesis details have already been reported (17). These copolymers are obtained by reacting PTMO and excess MDI (or TDI) at high temperatures. Either tertiary cumyl or dicumyl alcohol (CA or DCA) was added for the purpose of providing the in situ conversion of isocyanate groups. Two series of PEUU were prepared using both tertiary alcohols. The molecular weight (Mn) of the polyether macroglycol ranged from 650 to 2000. Each series of samples contained three levels of hard segment content chosen to maintain a comparable hard segment fraction.

We are currently (18) attempting to establish the reaction mechanism by which the isocyanate group is converted into an amine group. Dehydration of the alcohol may not be necessary. An intermediate carbamate can also explain the polymerization phenomenum. The current paper reports on our investigation of structure-property relationships in these novel segmented polyurethane-ureas. For this purpose, it was desirable to determine how the mechanical and thermal properties were affected with hard-segment content, crystallization and length of the soft and hard segment. The chemical composition was thus used to control the size, shape and the degree of order in these segmented copolymers. Finally, these PEUU's with symmetric and aromatic hard segments were compared with conventional PTMO/MDI/BD polyurethane and other polyurethane-ureas reported in the literature.

5.5.2. Experimental. Segmented polyurethane-urea copolymers were synthesized by a step-growth (condensation) reaction involving the prepolymer and amine-terminated groups as chain extender. The prepolymers were prepared by reacting poly (tetramethylene oxide) glycol [DuPont's Teracol$^{(R)}$] with excess 4,4'-diisocyanatodiphenyl methylene (MDI) or a 80/20 mixture of 2,4- and 2,6- toluenediisocyanate (TDI) [Mobay Chemical Co.]. Macroglycol of molecular weights 650, 1,000, 2,000 was employed as the soft segments in these elastomers. The polyols were dried at 60°C in a vacuum oven for 48 hours prior to use. The diisocyanates were vacuum distilled and middle cuts were stored at 0°C before use.

Tertiary alcohols, dicumyl alcohol (The Goodyear Tire & Rubber Company) and cumyl alcohol (Aldrich) were used to carry out the necessary conversion of excess isocyanate groups to amine groups as mentioned earlier. Thus, these tertiary alcohols are not directly involved in the chain extension step. The amount of excess MDI and tertiary alcohols determines the hard segment content in the polyurethane-urea samples. The composition of the various

copolymers synthesized is listed in Table 5.5-1. To carry out the reaction, MDI was charged into a $N_2$-filled resin kettle equipped with a high torque mechanical stirrer at room temperature. PTMO was then slowly delivered by means of a syringe into the reactor at 110°C over a period of 20 minutes. The mixture was then continuously stirred at 110°C for 1 hour. The specified tertiary alcohol was then added to the mixture of prepolymer and excess MDI. The molar ratio of alcohol to isocyanate was about 1:2. The reaction was then allowed to continue for another 3 hours at 150°C under inert conditions. At temperatures below 110°C no significant change in the bulk viscosity was observed, indicating that the uncatalyzed chain extension step cannot be carried out at these low temperatures. However, at 150°C an immediate increase in the viscosity was observed. By changing the molar ratio of MDI and PTMO, a series of samples with systematically varied hard segment content and relative block length were synthesized. The resulting copolymer was extracted with THF for 24 hours to remove low molecular weight impurities, if any. The final product was dried in a vacuum oven for 36 hours at 70°C. A clear polymer solution resulted when this polymer was dissolved in N,N dimethyl formamide (DMF) at 100°C suggesting that an essentially linear polymer was obtained.

Films of the segmented PEUU copolymer and a control polyurethane (Estane(R), BF Goodrich) were prepared by compression molding the dry material at 200 to 240°C and 10,000 pounds per square inch. The temperature was slightly higher when the hard segment content was increased to 41 weight percent MDI. The material was first heated in the press for 2 to 3 minutes and the pressure was then raised slowly. The film was kept in the press for about 5 minutes prior to its removal. After removal from the press, all samples were immediately quenched to room temperature and placed under vacuum in a dessicator until further testing. No obvious degradation of the materials at these high temperatures was observed as all the films were transparent or translucent (for materials based on 2,000 MW PTMO and MDI) after removal. The segmented polyurethane-urea copolymer obtained with 2000 molecular weight PTMO, MDI and CA is referred to as PTMO-2,000-MDI-31-CA, where 31 represents the weight percent of the hard segment. A similar nomenclature is employed for all other samples.

Structural characterization of the polymers was obtained by FT-IR and NMR spectroscopy using a Nicolet MX-1 and Varian EM-390 spectrometer. The IR spectra for the oligomers and the copolymers were obtained from solution cast films on KBr discs. Dog-bone specimens were cut from the films for mechanical testing of the segmented copolymers. Mechanical measurements included stress-strain, stress relaxation, tensile hysteresis and permanent set behavior. All these tests were performed on an Instron Model 1122 at room temperature. All stress-strain and hysteresis measurements were carried out at a strain rate of 200 percent per minute based on the initial sample length.

Dynamic mechanical spectra were obtained with a Rheovibron Model DDV II-C at 110 Hz and the Dynamic Mechanical Thermal Analyzer (DMTA) manufactured by Polymer Laboratories, England at 1Hz. The approximate heating rate for the sample was maintained near 3°C per minute in the Rheovibron and 5°C per minute for the DMTA.

Table 5.5-1. Characteristics of Various Polyurethane-Ureas Synthesized

| Sample | Mole Ratio MDI/PTMO/CA or DCA | % Urea Content |
|---|---|---|
| PTMO-2000-MDI-23.3-CA | 2.5/1/1.5 | 40 |
| PTMO-2000-MDI-31-CA | 3.7/1/2.7 | 57 |
| PTMO-2000-MDI-41-CA | 5.6/1/4.6 | 70 |
| PTMO-2000-MDI-31-DCA | 3.7/1/1.35 | 57 |
| PTMO-1000-MDI-31-DCA | 1.8/1/0.4 | 29 |
| PTMO- 650-MDI-31-DCA | 1.2/1/0.1 | 9 |
| PTMO-2000-TDI-31-CA | 5.3/1/2.2 | 69 |
| PTMO-2000-MDI-31-BD | CONTROL | 0 |

$$\% \text{ Urea Content} = \frac{\text{No. of all possible urea linkages}}{\text{Total urea and urethane linkages}}$$

Thermal analysis (DSC, TGA, TMA) of the block copolymers was performed on a Perkin-Elmer System 2 and System 4. Experiments were carried out under a helium or nitrogen atmosphere using a heating rate of 10°C per minute. The DSC and TMA scans were started at -140°C, whereas thermal degradation studies (TG) began at 50°C. During TMA measurements, a constant load of 10 g was employed.

The formation of domain structure (microphase separation) was also verified by using small angle x-ray analysis (SAXS). An automated Kratky small angle x-ray camera was utilized for the SAXS experiments. The x-ray source was a Siemens AG Cu 40/2 tube, operated at 40 kilovolts and 20 milliamps by a GE XRD-6 generator. A Cu Kα-radiation of wavelength .154 nanometers was obtained by Ni-foil filtering. A Philips table-top X-ray generator PW 1720 was utilized in conjunction with a standard vacuum-sealed Statton (Warhus) camera to obtain wide-angle x-ray diffraction (WAXD) patterns for the copolymers. The samples were approximately 0.5 mm thick and an exposure time ranging from 10 to 24 hours was used depending on the system.

5.5.3. Results and Discussion. In order to characterize the reaction mechanism and to confirm the formation of urea linkages, infrared spectra were obtained from the polymer films cast on KBr disks. The FT-IR spectra for sample PTMO-2000-MDI-31-CA confirmed the incorporation of urea linkages by the presence of an absorption peak at 1640 $cm^{-1}$ which is attributed to the hydrogen-bonded urea carbonyl. No absorption peak, corresponding to this wavenumber was observed for the PTMO-2000-MDI-31-BD polyurethane (ESTANE(R)) control material where urea groups are absent. The IR spectra obtained on the polymerization byproduct, collected from the sides of the reaction kettle, indicated the presence of an olefin absorption in the spectra. The absorption peaks appearing at 1640 $cm^{-1}$ and 850 $cm^{-1}$ correspond to the C=C stretch and $=CH_2$ wag, respectively, and compare well with an authentic IR spectra for α-methylstyrene. This was to be expected when cumyl alcohol was utilized. These absorption peaks in the polymerization condensate imply that there can be two possible reaction schemes by which the t-alcohols interact with isocyanate groups. These two schemes are illustrated in Figure 5.5-1. The first scheme indicates the formation of unstable carbamate which ionically dissociates to produce $CO_2$ from the unstable anion and an amine-terminated moiety. The second scheme would require dehydration of t-alcohols initially, which is then followed by formation of amine terminated groups through the more widely considered carbamic acid route. A recent detailed study (18) carried out on model reactions seems to indicate that the former mechanism is more likely to take place. However, a dual-reaction mechanism where both mechanisms compete may also be possible.

5.5.3.1. Mechanical analysis. The engineering stress-strain curves for segmented MDI-based polyurethane-ureas are shown in Figure 5.5-2 through Figure 5.5-4. All curves are shown up to the fracture stress of the sample. The Young's modulus, ultimate tensile strength, and ultimate elongation were determined from these measurements and are listed in Table 5.5-2 for each sample. It is well accepted that the tensile behavior for a thermoplastic elastomer generally depends upon the size, shape and

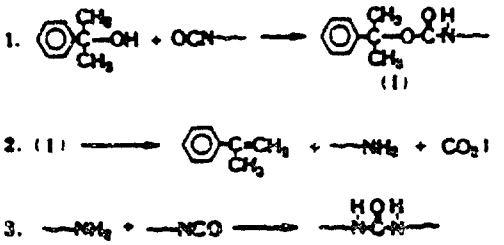

Scheme 1

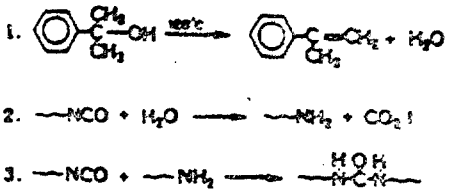

Scheme 2

Figure 5.5-1. Scheme 1 - Possible Urea Formation Mechanism Via Carbamate Rearrangement and Scheme 2 - Possible Urea Formation Mechanism Via Tertiary Diol Dehydration

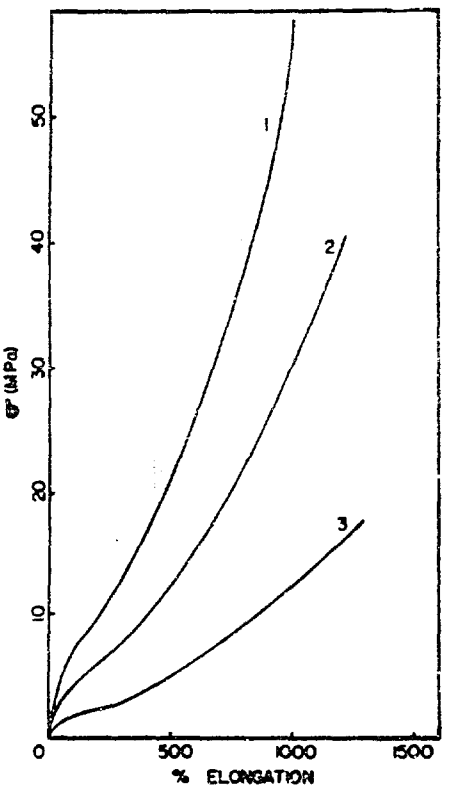


Figure 5.5-2. Stress-strain Curves For Various Segmented Poly-urethane-urea Copolymers Indicating the Dependence of Tensile Behavior on the Soft Segment Molecular Weight. (1) PTMO-2000-MDI-31-DCA, (2) PTMO-1000-MDI-31-DCA, and (3)PTMO-650-MDI-31-DCA

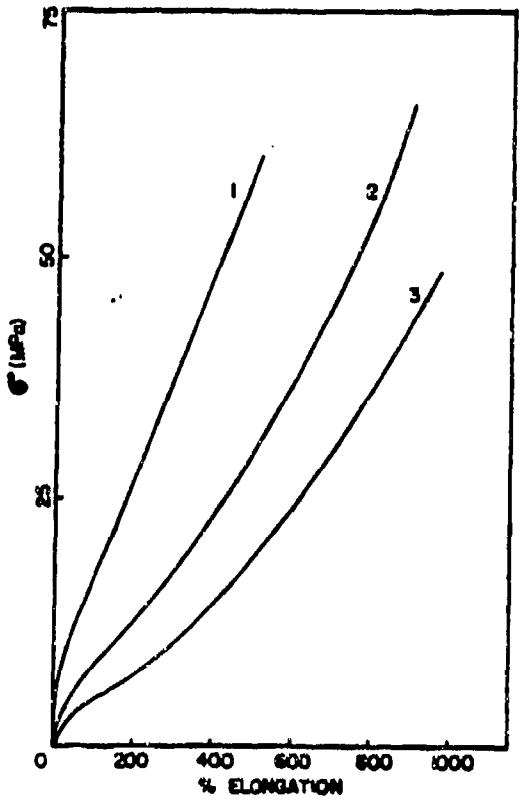


Figure 5.5-3. Stress-strain Curves Showing the Effect of Hard Segment Content on the Tensile Behavior of Various Segmented Polyurethane-urea Copolymers. (1) PTMO-2000-MDI-41-CA, (2) PTMO-2000-MDI-31-CA,and (3) PTMO-2000-MDI-23.3-CA

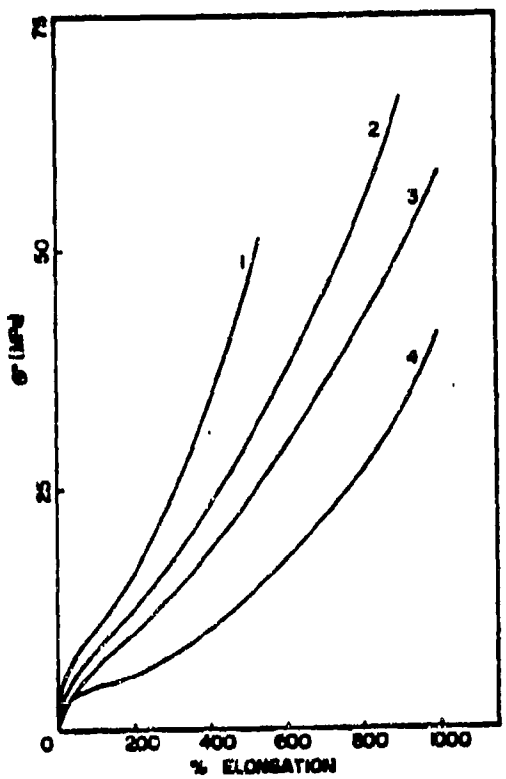


Figure 5.5-4. Stress-strain Behavior for Various Segmented Polyurethane-urea Copolymers. (1) PTMO-2000-TDI-31-CA, (2) PTMO-2000-MDI-31-CA, (3) PTMO-2000-MDI-31-DCA, and (4) PTMO-2000-MDI-31-BD

concentration of the hard segments; intermolecular bonding within the hard domains; and the molecular weight of the soft segments (19,20). The tensile behavior of these segmented copolymers establishes the expected correlation with these parameters.

In Figure 5.5-2, the stress-strain behavior for materials with different soft segment molecular weights but the same hard segment content are shown. The results indicate that the Young's modulus and the tensile strength in these samples increase as the hard-segment length is increased. This can be explained on the basis of the increase in the hard-segment length necessary to maintain the same hard-segment content with increasing molecular weight of the soft segments. Increasing the block length not only increases the aspect ratio of the dispersed hard domains but also leads to a higher degree of order in the hard domain since this results in more urea linkages per hard-segment unit. Although the sample PTMO-650-MDI-31-DCA has a higher density of the hard-segment units, the pseudo-multifunctional cross-links formed by the hard domains are shorter and likely weaker. As a consequence of these poorly defined hard domains, the sample PTMO-650-MDI-31-DCA exhibits lower mechanical strength.

The stress-strain behavior for polyurethane-urea elastomers based on 2,000 molecular weight PTMO is shown in Figure 5.5-3 as a function of increasing hard-segment content. It is indicated that the mechanical response of these materials is strongly affected when hard-segment content is raised from 23.3 percent to 41 percent by weight. The observed behavior can be explained on the basis of the introduction of a higher volume fraction of hard segments as well as a higher degree of order in the hard domains. The higher modulus and tensile strength with increasing hard segment content in these samples is also consistent with their greater urea content which results in more cohesive hard domains.

The results in Figure 5.5-4 are presented to bring out the effect of varying intermolecular binding forces; hard segment symmetry or shape; and finally the use of two different tertiary alcohols (namely CA and DCA). All four samples indicated in this figure have 31 percent hard segment by weight. A comparison among these curves indicates that the lowest ultimate tensile strength is displayed by sample PTMO-2000-MDI-31-BD (ESTANE(R)). This sample differs from the rest in the sense that it does not contain any urea linkages. Clearly, the weaker interdomain secondary binding forces result in less cohesive hard domains and may limit the development of a three- dimensional hydrogen bonding network. Phase separation is, no doubt, also affected and a possible larger interfacial region and/or higher segmental mixing present in ESTANE(R) could be responsible for higher initial tensile modulus. The lack of symmetry in the ESTANE(R) hard domains (MDI/BD vs. MDI/DAM) may also influence the tensile behavior as the packing of the hard segments would not be efficient either.

When cumyl alcohol is used instead of dicumyl alcohol to carry out in situ chain extension, some dissimilarity between the mechanical behavior of the corresponding copolymers is observed. This disparity presumably is a consequence of the differences in the chain extension step caused by the

Table 5.5-2. Mechanical Properties of Segmented Polyurethane-Ureas

| Sample | Ultimate Tensile Strength (MPa) | Young's Modulus (MPa) | %Elongation at Break |
|---|---|---|---|
| PTMO-2000-MDI-23.3-CA | 49.0 | 15.1 | 1000 |
| PTMO-2000-MDI-31-CA | 67.5 | 17.6 | 900 |
| PTMO-2000-MDI-41-CA | 59.0 | 104.5 | 600 |
| PTMO-2000-MDI-31-DCA | 59.0 | 11.4 | 1000 |
| PTMO-1000-MDI-31-DCA | 40.5 | 9.3 | 1100 |
| PTMO-650-MDI-31-DCA | 17.5 | 6.8 | 1300 |
| PTMO-2000-TDI-31-CA | 50.5 | 35.6 | 550 |
| PTMO-2000-MDI-31-BD | 41.0 | 13.2 | 1000 |

nature of the two tertiary alcohols involved. This difference may affect the distribution of hard-segment lengths and would be narrower in the copolymer where CA is employed. In either case, it appears that the copolymer prepared with DCA apparently has less order in the hard domains and possibly a larger interfacial region between the two phases due to a larger distribution in the hard-segment length. The SAXS results (discussed later) have also indicated that at the same hard-segment content, the thickness of the interfacial zone is larger in the copolymers when DCA is used for the chain extension step. The differences in the mechanical properties, observed for the copolymers obtained via these two alcohols, is therefore an indication of the differences in the chain extension step caused by these two reactants. When the degree of chain extension is small (23.3 percent hard segment by weight), the difference between the tensile properties of the segmented copolymer prepared by the two tertiary alcohols is also small.

The difference in the TDI and MDI based polyurethane-ureas, however, is observed because of two reasons. First, for constant hard segment content by weight, TDI based copolymers have a higher concentration of urea linkages since the molecular weight of one TDI unit is less than that of a MDI unit. Hence a stronger mechanical response is obtained owing to a higher degree of cohesiveness. The second reason is interrelated with the dissimilarities observed in the orientation behavior of the soft-segment chains upon deformation for the two representative copolymers. As will be discussed shortly, it was found by WAXS analysis that strain-induced crystallization of the PTMO chains occurs at lower elongations for TDI based system as compared to samples with equal weight percent of MDI-based hard segments. An earlier onset of the crystallization in the TDI system is also likely to increase the stress level in the sample. The reasons for this observed difference in the crystallization behavior will be discussed in more detail when the dynamic mechanical and WAXS results are presented.

5.5.3.2. Dynamic mechanical analysis. To investigate the compositional dependence of the local scale motion as well as cooperative segmental motion which may exist in these segmented polyurethane-urea copolymers, dynamic mechanical spectra were obtained. It was also of interest to determine the mechanical and thermal properties in light of the role played by the variety of hydrogen bonding possibilities in these materials. Figures 5.5-5 and 5.5-6 show the overall dynamic behavior in terms of storage ($E'$) and loss ($E''$) modulus as a function of temperature.

The dynamic mechanical results in Figure 5.5-5 demonstrate the effect of hard-segment content for a fixed molecular weight of the polyether soft segment. A rubbery plateau, from the $E'$ curves, is observed to be composition-dependent and extends to 200°C for 23.3 percent hard-segment content material and near 300°C for the sample with 41 percent hard-segment content. The plateau modulus also increases significantly upon increasing the hard-segment content in the sample. An increase in the order of hard domains arising from hard-segment content results in the formation of a stiffer material which is reflected in the $E'$ behavior. Interestingly, the plateau modulus in these polyurethane-ureas is nearly one order of

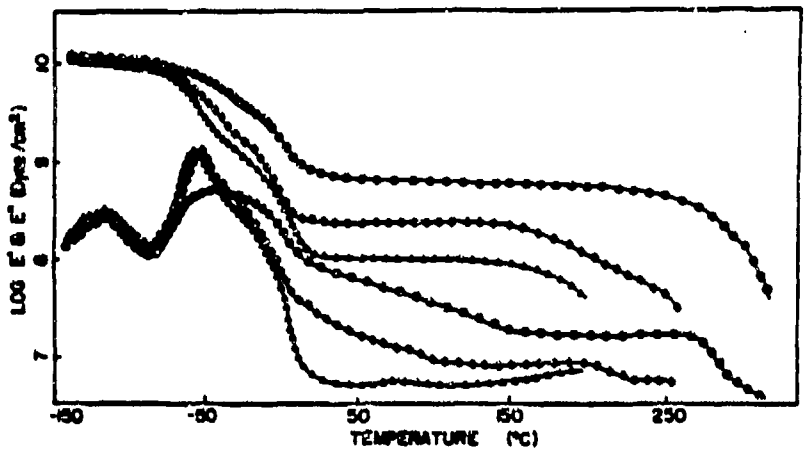


Figure 5.5-5. Dynamic Mechanical Spectra for Segmented Polyurethane-urea Copolymers. (●) PTMO-2000-MDI-41-CA, (▲) PTMO-2000-MDI-31-CA and (▲) PTMO-2000-MDI-23.3-CA Determined on the Rheovibron. 100 Hz frequency. Curves 1-3 are for Storage Moduli Data and Curve 4-6 are for Loss Modulus Data.

magnitude higher than that reported for a MDI/ED-based PEUU with a similar hard-segment content (21). The loss modulus curves appear to be complex as a number of damping peaks (or shoulders) are observed. The various relaxations, responsible for the origin of these peaks, are now discussed.

The secondary loss peak near -120°C is designated as the $\gamma$ relaxation. The value for this peak has been reported to lie between -130 and -100°C at 110 Hz by several workers (21-26). This peak has been ascribed to the motion of methylene sequences. The magnitude and location of the $\gamma$ peak is found to be nearly independent of the hard-segment content. The $\gamma$ relaxation temperature observed in these copolymers is in excellent agreement with the reported value (-120°C) for polyolefin systems. This indirectly suggests that the degree of phase separation achieved in these copolymers may be very high. This is expected because of the highly polar nature of the aromatic urea linkages that form the hard segments in these copolymers.

The primary relaxation observed near -55°C in the dynamic mechanical spectra at 110 Hz for these copolymers is designated as the $\alpha_a$ relaxation and has been attributed to the glass transition temperature of the soft segments (21-23). The intensity and location of the $\alpha_a$ peak is strongly dependent on the chemical composition of the samples. An increase in the hard segment content at constant prepolymer molecular weight broadens the $\alpha_a$ relaxation and decreases its intensity. This is accompanied by a shift of the peak temperature to a higher temperature. It appears that the $\alpha_a$ relaxation process involves motion within the amorphous portion of the flexible prepolymer chains. Thus it may be inferred that increasing the aromatic urea content will tend to restrict the motion of the prepolymer phase and thus shift the $\alpha_a$ transition to a higher temperature.

On the high temperature side of the $\alpha_a$ peak, a mechanical dispersion is indicated as a shoulder near 0°C. This transition is designated as $\alpha_c$ and is related to the melting of crystallites of the soft segments. The melting point of PTMO homopolymer has been reported to lie near 35°C (27). An even higher value (nearly 49°C) of $T_m$ has been reported by Dreyfus (38) for extremly high molecular weight PTMO. The lower $T_m$ of the soft segment observed here is believed to be due to the lower molecular weight of the PTMO segments in these copolymers or to the formation of small and/or imperfect crystallites.

The existence of $\delta$ relaxations in dynamic mechanical behavior has been observed for conventional MDI/BD based polyurethanes and shown to be associated with the hard segments of the copolymer (22, 23). The first $\delta$ relaxation near 80°C was ascribed to the annealing effects associated with the poor ordering in the hard domains. The high temperature $\delta'$ relaxation near 200°C in the dynamic mechanical spectra has been attributed to the melting of the hard segment crystallites (23). For these polyurethane-ureas copolymers the $\delta$ relaxation is barely visible in the loss modulus curve. This indicates that any further ordering of the hard segments does not take place in 2,000 molecular weight PTMO-based copolymers. This is not surprising as the hard domains are more cohesive in these copolymers due to the presence of urea linkages and the large thermodynamic

incompatibility between the two segment types. One other relaxation is observed over 200°C and is dependent on the hard-segment content. This relaxation is assumed to be associated with the melting of the hard segment microcrystallites with urea linkages and this dispersion is designated as δ'. An endotherm at these temperatures was also observed by DSC. The melting point of the MDI/DAM "hard segment" control has been reported to be 370°C (15). The same Tm value has also been observed in this laboratory, although we are not certain that this represents the value associated with very high molecular weight components.

Figure 5.5-6 shows the dynamic mechanical behavior of segmented polyurethane-ureas as a function of the molecular weight of the prepolymer. The results indicate that the $\alpha_a$ transition shifts to a lower temperature as the molecular weight of the soft segments is increased. This shift can be explained on the basis of longer, more ordered and well-defined domain structure which results when the molecular weight of the macroglycol is increased at constant hard-segment content. The intensity of the $\alpha_a$ peak is also composition dependent and decreases with increasing segment molecular weight. This occurs because of the onset of crystallinity in the soft segments as the molecular weight of PTMO is increased. For the 650 and 1,000 molecular weight polyether glycol prepolymer, the $\alpha_c$ relaxation was not observed. This is consistent with other observations that the soft segment blocks crystallize only when their molecular weight is in excess of 1,000, (23) although higher hard/soft segment mixing present in these systems may also prevent the crystallization of the soft segments. The δ and δ' relaxation peaks are indicated for these materials by a slight deflection in the dynamic mechanical spectra. The γ relaxation peaks appear to be molecular weight dependent as they shift to low temperatures for high molecular weight prepolymer based materials of the same hard segment content. This may indicate a higher degree of segmental mixing as the molecular weight of the soft segment is lowered for the same hard segment content.

The length and extent of the rubbery plateau is also shown to depend on the molecular weight of the macroglycol employed. The plateau modulus is higher for samples where 2,000 molecular weight soft segments are utilized as compared to samples where the soft-segment molecular weight is lower. This behavior is attributed to the existence of less well defined domain structure when low molecular weight macroglycols are used. For copolymers prepared from higher molecular weight polyether glycols, high prepolymer molecular weight based copolymers, better phase separation is obtained and enhanced physical crosslinking and/or filler effects (arising from the presence of hard segment domains) dominate the properties. As a consequence, the effective degree of domain formation is improved in the high segment molecular weight materials. Additionally, for samples with the same hard-segment content, the concentration of urea groups is higher for samples with higher molecular weight prepolymer whose hydrogen bonding network improves intradomain cohesion.

5.5.3.3. Thermal analysis. The thermomechanical analysis (TMA) spectrum was obtained for these polyurethane-ureas to observe the transitions

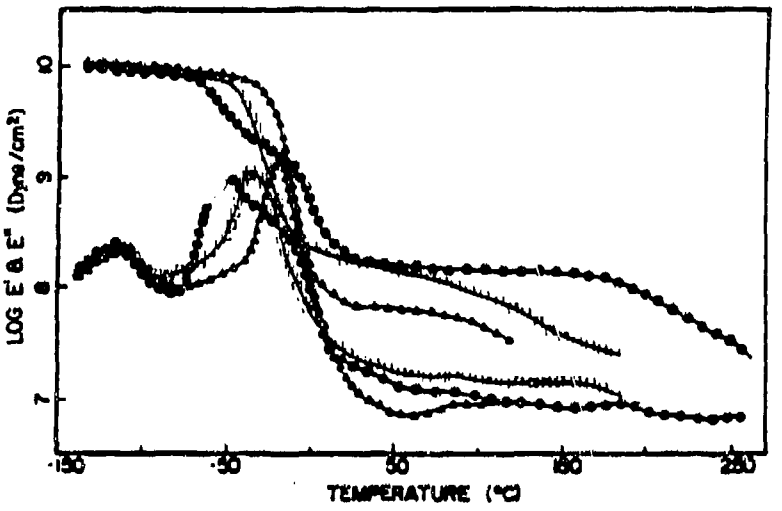


Figure 5.5-6. Dynamic Mechanical Spectra for (●) PTMO-2000-MDI-31-DCA, (□) PTMO-1000-MDI-31-DCA and (▲) PTMO-650-MDI-31-DCA. Frequency 110 Hz

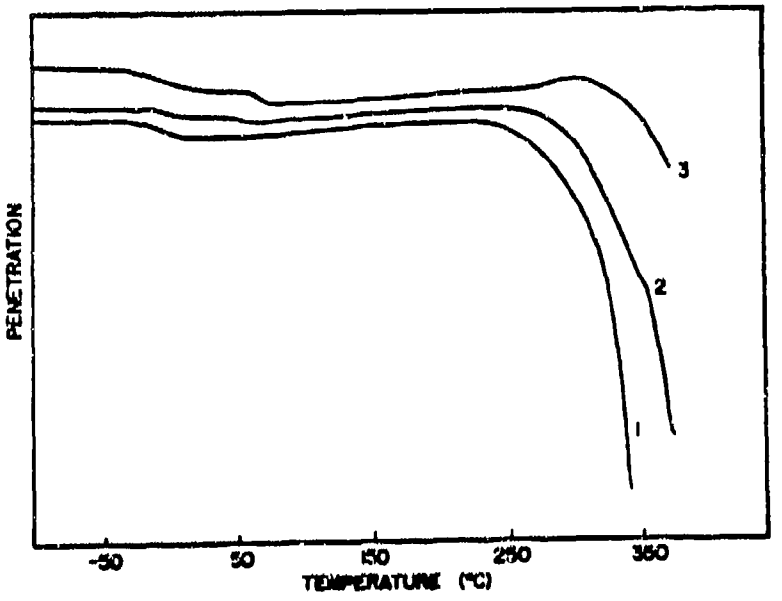


Figure 5.5-7. Thermomechanical Penetration Curves for Various Samples with Different Hard Segment Content. (1) PTMO-2000-MDI-41-CA, (2) PTMO-2000-MDI-31-CA, and (3) PTMO-2000-MDI-23.3-CA

associated with the hard and soft segments. Figure 5.5-7 compares the TMA measurements of three representative copolymers with different hard-segment contents. The primary transition near -50°C is ascribed to the soft segment glass transition. The hard-segment transition is indicated to be composition dependent and varies from 240 to 300°C as the hard-segment content is increased from 23.3 to 41 percent by weight. The nature and length of the rubbery plateau depends on the hard-segment content and is higher for segmented copolymers with higher hard-segment content. The TMA response is also affected when the molecular weight of the soft segment is varied at a constant hard-segment content (see Figure 5.5-8). These results are consistent with the fact that the sequence length also increases as a function of hard-segment content. In Figure 5.5-8, these MDI-based polyurethane-ureas are compared with Estane, a conventional diol-extended polyurethane. One significant feature observed in the ESTANE(R) is its relatively low softening temperature (120°C). In contrast, the strength and service temperature have been dramatically improved with the incorporation of 29 and 59 weight percent aromatic urea groups in polyurethane-ureas. In general, the results obtained from TMA penetration curves are in agreement with the dynamic mechanical behavior discussed earlier.

Thermogravimetric analysis on these materials provide strong evidence of the somewhat improved thermal stability due likely to the existence of a three-dimensional urea hydrogen bonding network as well as the complete aromatic nature of the hard segments. The thermogravimetric analysis behavior was observed to be nearly independent of the composition and hence only one curve is indicated for MDI-based copolymers. These materials exhibit little weight loss up to 300°C, but lose 50 percent of their weight by about 400°C.

As discussed in the preceding section, a number of different transitions were observed with dynamic mechanical measurements. In order to verify these transitions or relaxations, differential scanning calorimetry (DSC) thermograms were obtained for these polyurethane-urea copolymers. This study also allowed the determination of composition dependence of various transitions associated with hard and soft segments. Table 5.5-3 presents a summary of the low temperature DSC results for the segmented copolymers. Data on various thermal events occurring in the component prepolymers are also indicated in this table. The transitions observed by DSC are in good agreement with the $\alpha_a$, $\alpha_c$, $\delta$, and $\delta'$ relaxations obtained by dynamic mechanical spectroscopy. No signs of the $\gamma$ relaxation were indicated by the DSC thermograms but a transition associated with the melting of the crystallites was observed in the thermal scans.

Annealing studies were also carried out to investigate the morphological changes in segmented elastomers induced by annealing and quenching as a function of both time and temperature. For unannealed samples, the low-temperature thermograms contain the transitions associated with the soft segments and are presented in Figures 5.5-9 and 5.5-10. The thermograms in Figure 5.5-9 show the low-temperature transitions for various copolymers prepared with different molecular weight polyether glycol but the same hard

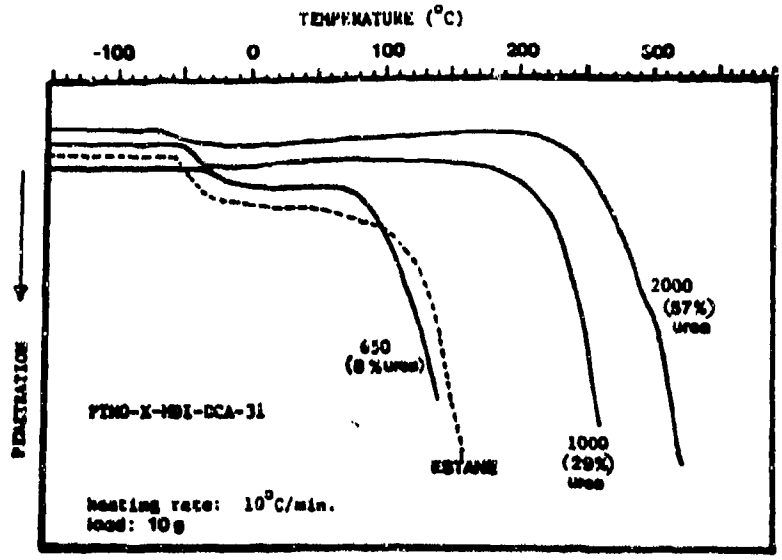


Figure 5.5-8. TMA Penetration Curves of the PEUU's with Different Soft Segment Lengths

Table 5.5-3. Results From Low Temperature DSC Scans (°C) For Segmented Polyurethane-Urea Copolymers

| Sample | Tg | | | Tc | Tm |
|---|---|---|---|---|---|
| | From | To | Midpoint | | |
| PTMO-2000-MDI-23.3-CA | -83 | -61 | -75.2 | -43.1 | 2.5 |
| PTMO-2000-MDI-31-CA | -86 | -62 | -74.7 | -34.1 | 3.5 |
| PTMO-2000-MDI-41-CA | -84 | -54 | -72.0 | -35.1 | 11.7 |
| PTMO-2000-MDI-31-DCA | -89 | -57 | -73.7 | -35.7 | 8.8 |
| PTMO-1000-MDI-31-DCA | -59 | -29 | -47.9 | ND | ND |
| PTMO- 650-MDI-31-DCA | -58 | -19 | -38.3 | ND | ND |
| PTMO-2000-MDI-31-CA | -84 | -62 | -76.3 | ND | ND |
| PTMO-2000-MDI-31-BD | -64 | -29 | -49.0 | ND | ND |
| PTMO-2000 | -- | -- | -78.0 | -- | 24,27 |
| PTMO-1000 | -- | -- | -82.0 | -- | 28,37 |
| PTMO-650 | -- | -- | -84.0 | -- | 23,36 |

a: all temperatures in °C; ND: not determined

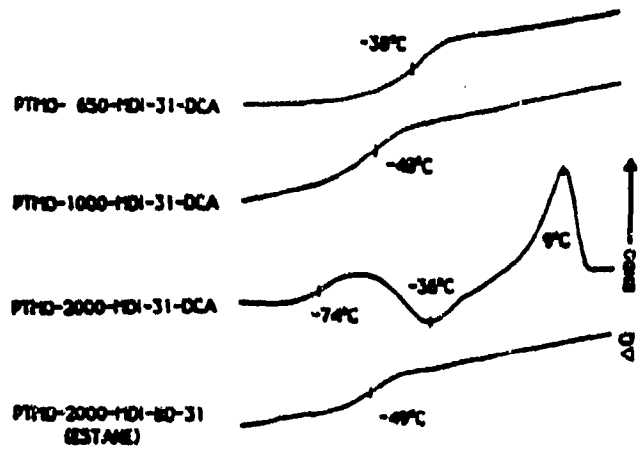


Figure 5.5-9. Low-temperature DSC Curves of the PEUU's with Different Soft Segment Lengths

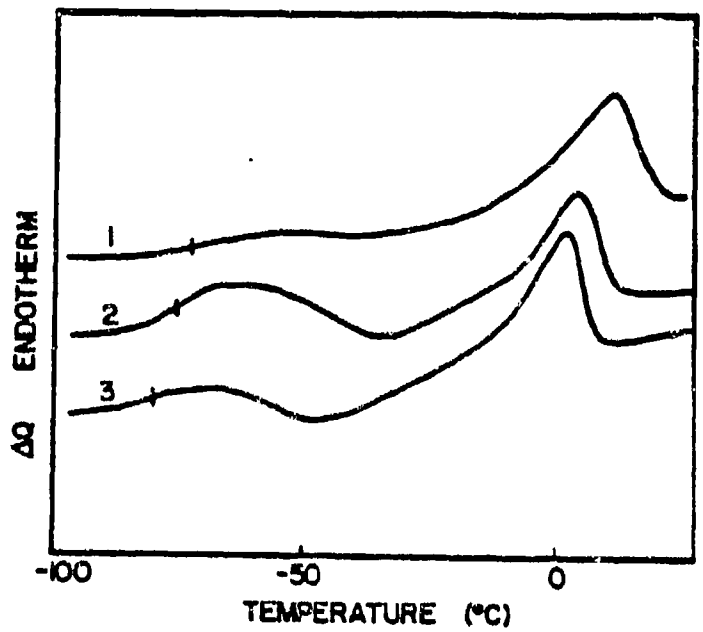


Figure 5.5-10. DSC Thermograms for Various Samples with Different Hard Segment Content. (1) PTMO-2000-MDI-41-CA, (2) PTMO-2000-MDI-31-CA and (3) PTMO-2000-MDI-23.3-CA

segment content. For PEUU based on the polyether glycol 2,000 molecular weight, the soft-segment glass transition occurs at -75°C and is followed by an in situ crystallization exotherm near -40°C and melting endotherm at about 10°C. Crystallization and melting transitions were not observed for copolymers derived from the lower molecular weight polyether glycols.

For polyurethane-urea samples prepared with 650 or 1,000 molecular weight PTMO, the glass transition temperatures were observed at -38 and -48°C, respectively. These Tg's are substantially higher than the glass transition temperature reported in Table 5.5-3 for pure PTMO (-84 and - 82°C, respectively). This indicates either a significant amount of interfacial mixing or an existence of mixed hard segments in the soft matrix of these materials, the extent of which is likely determined by the amount and length of both segments. In addition, the anchoring of soft segments at the phase boundaries of a domain structure would also raise the Tg due to the restrictions imposed by the coupling at the interface. The width of the glass transition zone is also longer for lower molecular weight polyether glycol-based copolymer, suggesting a higher degree of segment mixing. The partial mixed segment morphology indicated for samples with 650 or 1,000 molecular weight PTMO can be described by two models (6). The first would consider the presence of polyether segments in the hard domains and/or hard segments dispersed in the polyether matrix. The second model acknowledges the existence of a broad interfacial region between the relatively pure hard- and soft-segment domains. The DSC and SAXS analyses (discussed later) on these materials seem to suggest a model which combines the basic aspects of both models. However, Cooper's (21) IR results on polyurethane-ureas have indicated that urea carbonyls are completely hydrogen bonded. If one accepts this point of view, then only a few individual hard segments should be dissolved in the soft-segment matrix, although small hard domains (a few small coupled hard segments) could no doubt still be miscible.

All low-temperature DSC thermograms on copolymers with 2,000 molecular weight PTMO (see Figure 5.5-10) indicate the presence of crystallization and melting transitions, above the glass transition. The presence of a melting endotherm is observed, as expected, by virtue of the greater molecular weight of soft segments involved. The crystallization exotherm is thus due to the soft segment. At room temperature, these segments are just above their melting temperatures so that rapid cooling below room temperature is effectively a melt quench to an amorphous glassy state below Tg. When reheated, the soft segments crystallize above their glass transition temperature.

From Table 5.5-3 and Figure 5.5-10, it is to be noted that for constant soft-segment molecular weight, the Tg of the soft segment increases with hard-segment content. This may suggest that an increase in the aromatic urea content tends to restrict the motion of the soft segments thus shifting the Tg to higher temperatures. However, the presence of a larger interfacial region in the high hard-segment content material may also raise the Tg. The SAXS results (discussed later) on these materials tend to favor the second postulate.

Interestingly, the DSC results in Figure 5.5-10 also reveal that a lower glass transition also promotes a lower soft-segment crystallization temperature (Tc). The melting endotherms in these copolymers are observed to be shifted to lower temperatures as the hard-segment content is decreased. This implies that the proportion of hard segments present in the soft-segment matrix decreases as the hard-segment content is increased. As more hard segments are present in the soft matrix, the melting point would be depressed because of a dilution effect. On comparing the areas under the crystallization and melting peaks, it is found that the difference is largest for the sample with the highest hard-segment content. These results indicate that the soft segments in the sample with highest hard-segment content crystallize faster and can be explained by two separate phenomena. The first one has to do with the larger crystallization window (Tg-Tm) available for the fast crystallization of soft segments. Faster crystallization could also occur due to the presence of less hard-segment impurities in the soft segment matrix. When significant amounts of hard-segment impurities are present in the matrix, as may be the case for samples with lower hard-segment content, then they could interfere with the crystallization of the soft segments. As a result, when the sample is quickly quenched, only a small proportion of the soft segments would crystallize. Therefore it is hypothesized that the difference between the areas under the crystallization and melting peaks may be correlated to the purity of the soft phase.

The Tg exhibited by the 2,000 molecular weight PTMO-based copolymer is much lower (near -75°C) as compared to those of copolymers with lower soft segment molecular weight. This indicates that the mixing of the hard and soft segments is minimal when higher molecular weight polyethers are employed and that the Tg value can also be used as an indication of the relative purity of the soft-segment regions.

From these DSC results it also appears that the Tg for polyurethane-urea copolymers also depends on the type of tertiary alcohol used to promote the chain extension step. When DCA is used, the Tg is higher as compared with those of the copolymers where CA was utilized. These results are consistent with the differences observed in the mechanical behavior. In DCA-based PEUU's, a less well-ordered domain structure is obtained, probably because of a larger hard-segment length distribution as discussed earlier. DSC curves also suggest that hard segment/soft segment mixing is affected by the hard-segment type and the affinity of one segment for the other. For MDI/BD based polyurethanes, a relatively high value of Tg is indicated implying the existence of large scale mixing of hard and soft segments. This mixing in conventional MDI/BD based polyurethanes may also be caused by higher compatibility between the two types of segment compared to MDI/DAM based PEUU's.

While the sample PTMO-2000-MDI-31-CA displays the existence of both crystalline and melting temperature transitions, no such activity is observed in PTMO-2000-TDI-31-CA. The Tg of the soft segments in TDI-based materials is lower than that of MDI-based materials, suggesting better phase separation in the latter. It appears that the unsymmetric

configurations of TDI units cause the the formation of random hard-segment structures which inhibit, but not necessarily eliminate, the crystallization of soft segments under identical thermal histories.

The DSC scans were also obtained for two polyurea systems which form the hard segments in the MDI-based copolymers. These polyureas were obtained by reacting MDI with DAM at low temperatures for 2 hours or MDI with CA at high temperatures (150°C) for 15 hours. For both materials a Tm is observed at about 370°C. The same melting temperature has also been reported for MDI/DAM polyureas by Ishihara et al. (15). A heat of fusion of 110 calories/gram was determined for the MDI/DAM-based polyureas assuming no degradation of the sample. For MDI/CA-based polyureas, a lower heat of fusion is observed because a completely crystalline structure is not obtained. This hypothesis is confirmed by the existence of glass and crystallization transitions in the thermograms. Partially amorphous polyureas are obtained because the material likely undergoes some branching, but short of a three-dimensional network formation, during synthesis at high temperatures. A diffuse amorphous halo was also observed in the powder diffraction patterns obtained for the MDI/CA polyurea. The high Tm and $\Delta H_m$ are, no doubt, responsible for the well-defined crystalline structure which is formed mainly through hydrogen bonding and the stacking interactions of aromatic rings. The presence of strong and high-temperature-melting hard domains in these polyurethane-ureas is also likely to be responsible for the their superior mechanical properties and high tempera-ture performance in comparison to diol extended conventional polyurethanes.

5.5.3.4. Wide-angle x-ray diffraction. The differences in the onset of strain-induced crystallization behavior of MDI- and TDI-based polyurethane-ureas copolymers was investigated with the aid of wide-angle x-ray diffraction (WAXD). Flat plate diffraction patterns were obtained from two representative copolymers at various elongations (Figure 5.5-11). In the undeformed state, both samples show an isotropic arrangement of the amorphous segments and only a broad diffuse halo is observed. At higher elongations the anisotropy in the sample is indicated by the azmuthal dependence of the diffraction patterns. When strain-induced crystallization of the soft segments occurs, the reflections corresponding to the oriented crystallites may be observed as sharp reflections along the equator. For MDI-based PEUU's these spots are observed when the sample elongation is more than 300 percent. The TDI-based system, however, develops these spots at only 110 percent elongation. This indicates that for MDI-based copolymers, the phenomenon of strain-induced crystallization takes place at a much higher elongation than the TDI-based materials. The reason for this unusual behavior may lie in the nonsymmetric configuration of the TDI hard segments, but this is only a speculation. It may appear that the WAXD results are in direct conflict with the DSC and dynamic mechanical results discussed earlier. Those results had suggested that although the soft phase in TDI based copolymers was more pure as compared to the MDI-based materials, the random hard segment structures developed by the nonsymmetric TDI units may have been responsible for the absence of cold crystallization behavior. If more hard-segment impurities are present

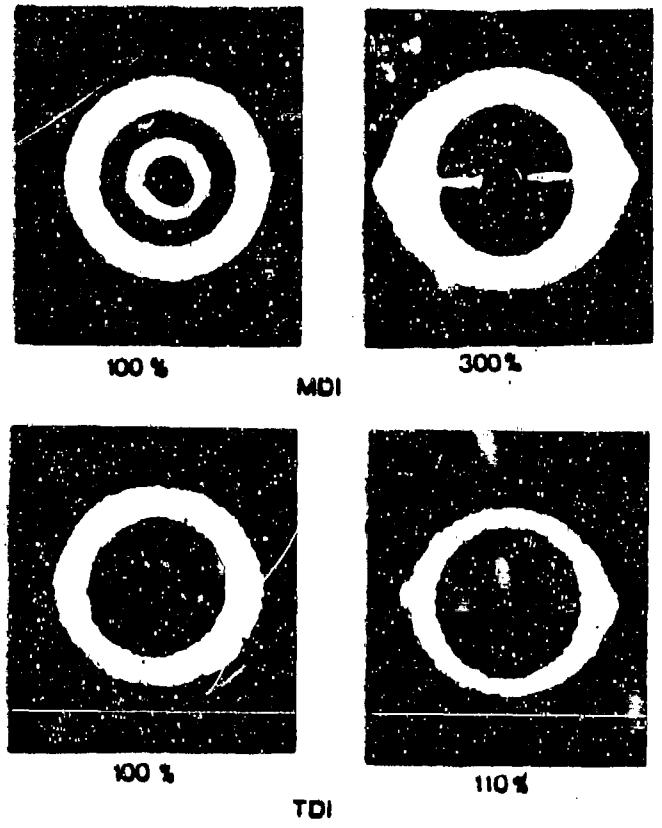


Figure 5.5-11. Wide-angle Diffraction Patterns for PTMO-2000-MDI-31-CA and PTMO-2000-TDI-31-CA at Different Elongations

in the soft matrix for MDI-based materials, then on deformation the soft-segment chains should experience less orientation effects as compared to the TDI-based materials. If this is true, then MDI-based PEUU's might show strain-induced crystallization at a much higher overall elongation in contrast to the TDI-based systems. The authors again point out that these latter statements are only speculations at this time.

5.5.3.5. Small-angle x-ray analysis. In order to more directly determine the differences in the structural arrangement as a function of sample composition, the morphology in these segmented polyurethane-urea copolymers was investigated via SAXS. To accomplish this, the interdomain spacing, interfacial boundary thickness and extent of segmental mixing were determined as a function of composition variables. The analysis of SAXS data is relatively straightforward and detailed information on the determination of various morphological parameters has been discussed elsewhere (28-35).

The slit smeared x-ray data was obtained on a Kratky small-angle camera and subsequently corrected for parasitic and background (thermal) scattering. The resulting x-ray scattering profiles for three polyurethane-urea copolymers at constant hard-segment content are shown in Figure 5.5-12. All curves show the presence of a shoulder or maximum followed by a gradual fall off in the intensity. The location of the maximum (or shoulder) depends on the composition and appears at higher angles when either hard-segment content (at constant soft-segment molecular weight) or soft-segment length (at the same hard-segment content) are reduced. A more defined peak occurs in place of a shoulder when the hard-segment content for a high molecular weight polyether glycol is increased. The breadth of the scattered intensity profile is also larger for lower segment molecular weight materials suggesting a larger distribution of domain sizes and/or interdomain spacings. For PTMO-2000-MDI-41-CA the scattering profile is rather sharp indicating a narrow distribution of interdomain spacings. The same trends are seen in Figure 5.5-13 for the collimation-corrected intensity profiles as well. For sample PTMO-650-MDI-31-CA, the lack of a distinct phase-separated structure causes the scattered intensity to be lower and the position of the shoulder is also not well defined. The mixing of the two different segments apparently leads to the lowering of the mean square electron density fluctuation in the system and the scattered intensity is lower as a result of lower electron density contrast. This causes a large statistical error in the intensity profile and presents problems during data analysis.

The interdomain spacing or d-spacings were determined from the location of the peak in the collimation corrected intensity profiles using Bragg's law and are listed in Table 5.5-4. Values of the interdomain spacings were also determined by 1-D correlation function analysis. The values of the interdomain spacing obtained by the two approaches are in reasonable agreement with each other. The results indicate that the interdomain spacing is affected by changes in the composition as would be expected. For example, sample PTMO-2000-MDI-23.3-CA displays a spacing of 12 nm while a value of 11 nm is observed for PTMO-2000-MDI-31-CA. At constant

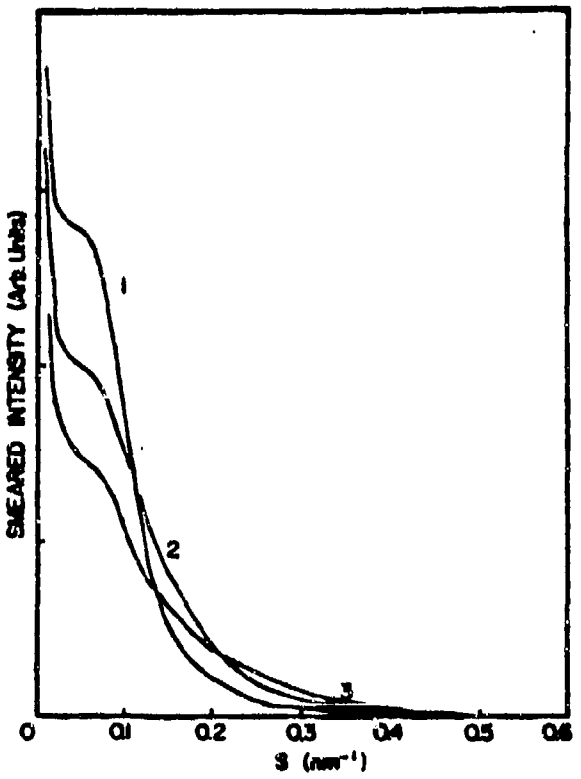


Figure 5.5-12. Smeared SAXS Scattered Intensity Profiles for (1) PTMO-2000-MDI-31-DCA, (2) PTMO-1000-MDI-31-DCA and (3) PTMO-650-MDI-31-DCA

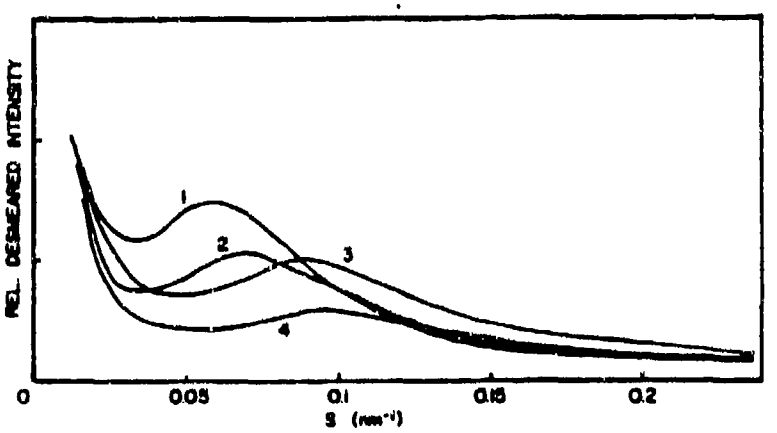


Figure 5.5-13. Desmeared SAXS Scattered Intensity Profiles for (1) PTMO-2000-MDI-31-CA, (2) PTMO-2000-MDI-23.3-CA, (3) PTMO-2000-MDI-31-BD and (4) PTMO-1000-MDI-31-DCA

Table 5.5-4. Interdomain or D-Spacing in nm for Segmented Polyurethane-Urea Copolymers

| Sample | by Bragg's law (nm) | From 1-D Correlation Function (nm) |
|---|---|---|
| PTMO-2000-MDI-23.3-CA | 17.5 | 12.0 |
| PTMO-2000-MDI-31-CA | 16.5 | 11.0 |
| PTMO-2000-MDI-31-DCA | 15.5 | 10.5 |
| PTMO-1000-MDI-31-DCA | 12.4 | 9.3 |
| PTMO- 650-MDI-31-DCA | 10.5 | -- |
| PTMO-2000-MDI-31-BD | 11.8 | 9.2 |

hard- segment content of 31 percent by weight, the interdomain spacing increases from 9.3 to 11 nm as the molecular weight of the soft segment is increased from 1,000 to 2,000, respectively. As the molecular weight of the soft segment is increased, the hard-segment length also increases at constant hard-segment content and as a result, not only the order in hard-segment domains is increased, but the interdomain spacing increases as well. The d-spacing increases as well when the higher molecular weight polyethers are employed. These results along with the morphological insight obtained from other techniques, indicate that hard-segment ordering is reflected in the values of the interdomain spacing.

It has been suggested by Porod that for an ideal two phase system, the desmeared scattered intensity at high angles varies with the reciprocal of fourth power of the scattering vector. A reciprocal third power dependence is observed when slit smeared data is used. This implies that the product $I.s^4$ or $I.s^3$ reaches a constant value at large angles for collimation corrected and slit smeared scattered intensities respectively. The variable s is called the scattering vector and is related to the angle of observation of the scattered intensity from the center of the beam. A negative slope in a plot of $I.s^3$ vs $s^2$ indicates the existence of diffuse phase boundaries. All but one sample indicated the presence of a diffuse two phase structure in the materials. The TDI-based copolymers, however, display a near zero slope which is indicative of sharp phase boundaries. This observation is consistent with the DSC results where the same copolymer showed the lowest Tg for the soft segments. However, these results only indicate that the thickness of the interfacial zone present in the material may be small and does not rule out the solubilization of one component in other. An estimate of the thickness of the diffuse interfacial boundaries, as indicated by the negative slopes, can be determined by various graphical methods (35).

A detailed investigation of the diffuse boundary thickness was carried out using the slit smeared scattered intensities. The interfacial thickness parameter, $\sigma$, was estimated by several graphical procedures and the results are reported in Table 5.5-5. The value of $\sigma$ is related to the interfacial boundary thickness assuming a sigmoidal gradient of electron density across the interface. The results for interfacial thickness parameters are comparable with previously reported values of $\sigma$ for segmented polyether polyurethanes (28,29). Interestingly, the diffuse boundary zone is found to be larger for samples containing the higher hard-segment content. A comparison of the interfacial boundary thicknesses for copolymers prepared with CA and DCA shows that the thickness is greater in copolymers prepared with the latter. This result is consistent with the earlier rationalization and differences in thermal and mechanical properties observed for the two copolymers. However, at constant hard-segment content, the interfacial thickness determined for low molecular weight PTMO is smaller in comparison to materials based on higher soft-segment molecular weight. This result would appear to be in conflict with most observations which indicate better phase separation for cases where longer segments are employed. First it must be clarified that a larger thickness of the interfacial regions <u>does not</u> necessarily point to a poor phase separation or a higher degree of segmental mixing in the material.

Table 5.5-5. Interfacial Thickness Parameter (in nm) by Various Methods

| Sample | Koberstein | Ruland[1] | Bonart | Exponential | Ruland[2] |
|---|---|---|---|---|---|
| PTMO-2000-MDI-23.3-CA | 0.205 | 0.196 | 0.263 | 0.186 | 0.182 |
| PTMO-2000-MDI-31-CA | 0.335 | 0.283 | 0.426 | 0.301 | 0.280 |
| PTMO-2000-MDI-31-DCA | 0.264 | 0.234 | 0.339 | 0.240 | 0.224 |
| PTMO-1000-MDI-31-DCA | 0.109 | 0.100 | 0.160 | 0.113 | 0.110 |
| PTMO-2000-MDI-31-BD | 0.130 | 0.145 | 0.179 | 0.127 | 0.126 |

1. Using a plotting routine of $sI(s)$ vs. $1/s^2$.
2. Using a plotting routine of $s^3I(s)$ vs. $s^2$.

The parameter indicating the degree of phase separation, σ, is also dictated by the relative lengths of the hard and the soft segments. For example, for a hypothetical sample A where the interfacial thickness is small, the fraction of the interfacial region could be large as compared to another sample B which may have higher interfacial thickness but the fraction of the interfacial region is small. Sample B, in such a case, would show a better overall degree of phase separation as compared to sample A. The reason for this unexpected observation may also lie in the molecular arrangement of the copolymer chains obtained with low molecular weight prepolymer. It has been shown that the presence of this type of intrasegmental mixing would cause a positive deviation in the Porod's plot (35). If this occurs then the obtained value of σ is an artifact representing the net result of two opposing phenomena. Based on these arguments, it can also be explained why polyurethane elastomers show lower interfacial thickness by x-ray analysis as compared to these PEUU elastomers despite repeated observations by other techniques that polyether polyurethanes are not as well phase-separated in comparison. Hence, the values of σ do not give any direct indication of the degree of phase separation but only an estimate of the interfacial thickness. A better indication of the degree of phase separation is obtained by the determination of the electron density variance.

Electron density variance was estimated from the scattering intensity profiles corrected for background scattering as discussed elsewhere (31,35). These variances or mean square electron density fluctuations, $\overline{\Delta\rho}^{2}$, and $\overline{\Delta\rho}^{2}_{c}$, can provide valuable insight into the state and degree of phase separation as shown by Bonart (36,37). The term $\overline{\Delta\rho}^{2}$ is determined through the calculation of the invariant while the term $\overline{\Delta\rho}^{2}_{c}$ is calculated assuming complete phase separation. The ratio $\overline{\Delta\rho}^{2}/\overline{\Delta\rho}^{2}_{c}$ on a semi-quantitative basis, reflects the overall degree of phase separation. A value of unity obtained for the ratio indicates a completely phase-separated material while a lower value would indicate a reduced amount of segmental mixing. The term $\overline{\Delta\rho}^{2}_{c}$ is the electron density variance for an ideal two-phase system. This ideal variance in electron density can be calculated from the knowledge of the chemical composition and mass density of the component phase by assuming complete phase separation with sharp phase boundaries. The results of the electron density variance obtained for different copolymers, are presented in Table 5.5-6. In all cases, the $\overline{\Delta\rho}^{2}$ is smaller than the ideal variance $\overline{\Delta\rho}^{2}_{c}$. This indicates that some phase mixing is present in all samples. The ratios of the two variances were also calculated and are reported in the last column of Table 5.5-6. The degree of phase separation, as indicated by this ratio, is found to be higher for copolymers with higher hard-segment content.

When presented in this fashion, even the sample PTMO-1000-MDI-31-DCA indicates a less phase-separated structure in comparison to PTMO-2000-MDI-31-DCA. Polyether polyurethane based on MDI/BD (ESTANE (R)), which had indicated a smaller interfacial thickness, shows a considerable amount of mixing between the two types of segments. In general, a good correlation can be found between the degree of phase separation as determined by x-ray analysis and mechanical and thermal characteristics observed earlier.

Table 5.5-6. Degree of Phase Separation as Determined by Electron Density Variance

| Sample | $\overline{\Delta\rho}^{2}, \times 10^{4}$ (mol. elec/cc)$^2$ | $\overline{\Delta\rho}^{2} \times 10^{3}$ (mol. elec/cc)$^2$ | $\overline{\Delta\rho}^{2}, / \overline{\Delta\rho}^{2}_{c}$ |
|---|---|---|---|
| PTMO-2000-MDI-23.3-CA | 7.654 | 1.664 | 0.46 |
| PTMO-2000-MDI-31-CA | 10.175 | 2.098 | 0.56 |
| PTMO-2000-MDI-31-DCA | 7.978 | 1.664 | 0.48 |
| PTMO-1000-MDI-31-DCA | 8.373 | 2.032 | 0.43 |
| PTMO- 650-MDI-31-DCA | 6.873 | 1.964 | 0.35 |
| PTMO-2000-MDI-31-BD | 5.324 | 1.331 | 0.40 |
| PTMO-2000-TDI-31-CA | 8.412 | 2.103 | 0.41 |

## 5.5.4. Conclusions.

It has been shown that it is possible to synthesize novel polyurethane-ureas by utilizing either the rearrangement characteristics of branched carbamates and/or the dehydration characteristics of tertiary alcohols at a sufficiently high temperature. Mechanical, thermal, dynamic mechanical and x-ray experiments were carried out to characterize the morphology and properties of polyether polyurethane-urea copolymers of systematically varying hard-segment type, hard-segment content, soft-segment molecular weight, and block length. The results obtained for these materials were compared with those from conventional polyurethanes to investigate the effect of intermolecular hydrogen bonding on molecular arrangement.

The tensile behavior was observed to depend primarily on the degree of order in the hard domains. It was shown that this order can be improved by increasing either the hard-segment content at constant molecular weight of the soft segment or soft-segment molecular weight at the same hard-segment content. Both approaches increase the concentration of urea linkages in the material and hence the tensile properties. In addition to the differences in the orientation behavior, the TDI-based materials were stiffer than those based on MDI because of higher urea content at the same weight percent, hard-segment content. This suggests that the cohesion in hard-segment domains is improved through the formation of three-dimensional urea hydrogen bonding in the polyurethane-urea copolymers. The filler effects of the hard domains are enhanced as well because of higher hard-segment content. At comparable hard-segment content, all materials indicated enhanced mechanical strength over polyether polyurethanes chain extended with butanediol.

From dynamic mechanical measurements on these copolymers, the extent and nature of the rubbery plateau was shown to be composition dependent. The results also indicated a higher degree of phase separation in the samples when order in the hard segment domains was increased by altering the composition. As many as five different types of relaxation mechanisms were observed over a wide temperature range. The α relaxation associated with annealing effects was not observed when the concentration of urea linkages was increased. TMA and TGA results also supported the earlier conclusions drawn from the mechanical and dynamic mechanical studies. Introduction of polar urea segments were shown to somewhat enhance the thermal stability of these materials.

Good agreement with dynamic mechanical measurements was observed for DSC results as well. The glass transition temperature was determined to be lower when either the molecular weight of the soft segment was increased or hard-segment content was decreased. The location of the soft segment Tg was shown to be correlated with the crystallization and melting temperatures as well. DSC behavior also provided the correlation between the degree of phase separation and higher mechanical strength.

Differences in strain induced crystallization behavior were observed for MDI- versus TDI-based hard segments in the copolymers by wide angle x-ray

diffraction. The small-angle x-ray results provided valuable insight to the morphological architecture of the materials. Values of interdomain spacing were shown to reflect the extent of hard-segment ordering in the sample. Except for the TDI-based system, negative deviations from Porod's law were observed and the thickness of the interfacial zone was estimated based on these deviations. Calculation of the SAXS invariant was used to examine the overall degree of phase separation in the sample and was found to be consistent with earlier observations.

5.5.5. References


1. G. A. Senich and W. J. MacKnight, Macromolecules, 13, 106 (1980).

2. V. W. Srichatrapimuk and S. L. Cooper, J. Macromol. Sci. Phys., B15, 267 (1978).

3. G. L. Wilkes, S. Bagrodia, W. Humphries and R. Wildnauer, J. Polym. Sci., Polymer Letters Ed., 13, 321 (1975).

4. R. Bonart, L. Morbitzer and E. H. Muller, J. Macromol. Sci. Phys., B9, 447 (1974).

5. C. S. Paik Sung, T. W. Smith and N. H. Sung, Macromolecules, 13, 117 (1980).

6. K. Knutson and D. J. Lyman, Adv. in Chem., American Chemical Society, 199, (1982).

7. D. Tyagi, I. Yilgor, J. E. McGrath and G. L. Wilkes, Polymer, 25, 1807 (1984).

8. D. Tyagi, I. Yilgor, J. E. McGrath and G. L. Wilkes, Polym. Bull., 8, 543 (1982).

9. C. S. Paik Sung, C. B. Hu and C. S. Wu, Macromolecules, 13, 111 (1980).

10. C. S. Paik Sung and C. B. Hu, Macromolecules, 14, 212 (1981).

11. G. L. Wilkes and S. Abouzahr, Macromolecules, 14 , 456 (1981).

12. ". A. Khransovskii, Doklady Akademii Nauk SSSR, 244(2), 408 (1979).

13. I. Kimura, H. Ishihara, H. Ono, N. Yoshihara, S. Nomura and H. Kawai, Macromolecules, 7, 355 (1974).

14. H. Ishihara, I. Kimura, K. Saito and H. Ono, J. Macromol. Sci., Phys., B10, 591 (1974).

15. H. Ishihara, I. Kimura, K. Saito and H. Ono, J. Macromol. Sci. Phys., B22, 713 (1983).

16. J. H. Saunders and R. J. Slocombe, Chem. Rev., 43 , 203 (1948).

17. B. Lee, D. Tyagi, G. L. Wilkes and J. E. McGrath, Paper presented at the Annual ACS Meeting at Philadelphia, August 1984; Rubber Division Meeting, Los Angeles, April 1985; Sagamore Conference on Elastomers, July 1985.

18. B. Lee, J. E. McGrath, D. Tyagi and G. L. Wilkes, Polym. Prepr., American Chemical Society, Div. Polym. Chem., 27(1), 100 (1986).

19. L. E. Nielsen, Rheo. Acta, 13, 86 (1974).

20. L. R. G. Treloar, The Physics of Rubber Elasticity, 3rd Ed., Clarendon, Oxford, 1975.

21. C. B. Wang and S. L. Cooper, Macromolecules, 16, 775 (1983).

22. H. N. Ng, A. E. Allegrezza, R. W. Seymour and S. L. Cooper, Polymer, 14, 255 (1973).

23. D. S. Huh and S. L. Cooper, Polym. Eng. Sci., 11(5), 369 (1971).

24. T. Kajiyama and W. J. MacKnight, Macromolecules, 2, 254 (1969).

25. T. F. Schatzky, J. Polym. Sci., 57, 496 (1962).

26. A. H. Willbourn, J. Polym. Sci., 34, 569 (1959).

27. N. G. McCrum, B. E. Read and G. Williams, in Anelastic and Dielectric Effect in Polymeric Solid, John Wiley, New York (1967).

28. Z. Ophir and G. L. Wilkes, J. Polym. Sci. Polym. Phys. Ed., 18, 1469 (1980).

29. J. T. Koberstein and R. S. Stein, J. Polym. Sci. Polym. Phys. Ed., 21, 1439 (1983).

30. J. T. Koberstein and R. S. Stein, J. Polym. Sci. Polym. Phys. Ed., 21, 2181 (1983).

31. J. W. C. Van Bogart, Ph D Thesis, department of Chemical Engineering, University of Wisconsin, 1981. (University Microfilms 81-7545).

32. A. Guinier and G. Fournet in Small Angle Scattering of X-rays, J. Wiley & Sons, London, 1955.

33. L. E. Alexender in X-ray Diffraction Methods in Polymer Science, Wiley, New York, 1969.

34. O. Glatter and O. Kratky in Small Angle X-ray Scattering, Academic Press, New York, 1982.

35. D. Tyagi, Ph.D. Dissertation, Department of Chemical Engineering , Virginia Polytechnic Institute and State University, 1985.

36. R. Bonart and E. H. Muller, J. Macromol. Sci. Phys., B10, 177 (1974).

37. R. Bonart and E. H. Muller, J. Macromol. Sci., Phys. B10, 345 (1974).

38. P. Dreyfus, Polytetrahydrofuran, Gordon & Breach, New York, 1982.

## DISTRIBUTION LIST

(1) Commander
Defense Technical Information Center
Bldg. 5, Cameron Station
ATTN: DDAC
Alexandria, Virginia 22314

(2) Manager
Defense Logistics Studies
Information Exchange
ATTN: AMXMC-D
Fort Lee, Virginia 23801-6044

(3) Commander
U. S. Army Tank-Automotive Command
ATTN: AMSTA-DDL (Technical Library)
Warren, Michigan 48397-5000

(4) Commander
U. S. Army Tank-Automotive
Command
ATTN: AMSTA-CF (Orlicki)
Warren, Michigan 48397-5000

## GLOSSARY OF TERMS

GPC--gel permeation chromatography

M-P--megapaschals

EPDM--ethylene-propylene diene rubbers

TPE's--thermoplastic elastomers

RIM--reaction injection molding

LPG--low pressure gas

psig--pounds per square inch gas

ml--milliliter

UV--ultraviolet

O.D.--outer diameter (coil)

I.D.--inner diameter (coil)

rpm--revolutions per minute

MWD--molecular weight distribution

BR--butyl rubber

PI--polyisoprene

NR--natural rubber

IR--isoprene rubber

PB--polybutadiene

TBS--tertiary-butyl styrene

mol--mole

g--gram

mmol--millimole

1.37 M--1.37 molar

ABS--absorbance

nm--nanometer

THF--tetrahydrofuran

GC--gas chromatography

SEC--size exclusion chromatography

Tg's--glass transition temperatures

DMSO--dimethylsulfoxide

TMA--thermomechanical analysis

1.4 n--1.4 normal

HPLC--high performance (pressure) liquid chromatography

FTIR--Fourier transform infrared spectroscopy

GLC--gas liquid chromatography

FT ($^{1}$H)--Fourier transform (proton) NMR

DDPE--1,3 bis(phenyl ethenyl) benzene

NMR--nuclear magnetic resonance

mol. wt.--molecular weight

<Mn>--number average molecular weight

Me--methyl

MPa--megapaschals

HLB (value)--hydrophobic-lyophobic balance

IBMA--isobutyl methacrylate

PMMA--polymethyl methacrylate

psi--pounds per square inch

kV--kilovolt

mA--milliampere

TGA--thermogravimetric analysis

DSC--differential scanning calorimetry

cal/gm--calories per gram

°C--degrees celsius

s.s.--stainless steel

ca.--circa

DPE--diphenyl ethylene

PD--polydispersities

PMS--paramethyl styrene

S-I-S--styrene-isoprene-styrene copolymer

S-B-S--styrene-butadiene-styrene copolymer

B-I-B--butadiene-isoprene-butadiene

B-I--butadiene-isoprene

I-B-I--isoprene-butadiene-isoprene

PIP--polyisoprene

$N_2$--nitrogen gas

DVB--divinyl benzene

DMTA--dynamical mechanical thermal analysis

Hz--Hertz

Ni-nickel

π/c--osmotic pressure/concentration

$A_2$--second virial coefficient

E'--modulus

Pa--paschals

% E--percent elongation

% H--percent hydrogenation

DIB--m-diisopropenyl benzene

M--molar (moles/l)

TEA--triethyl amine

Di-PIP--1,2, dipiperidinoethane

ABS--acrylonitrile-butadiene-styrene copolymer

UV/vis--UV/visible spectroscopy

$E_a$--energy of activation

IBMA--isobutylmethacrylate

DMSO--dimethylsulfoxide

SST--sulfonated styrene

CTA--chain transfer agent

PS-PIBM DB--polystyrene-isobutyl methacrylate diblock

PMMA--poly methyl methacrylate

HCl--hydrochloric acid

PEUU--polyether-based polyurethane-ureas

TDI--toluene-2,4-diisocyanate

ED--ethylene diamine

PTMO--poly(tetramethyleneoxide)

SAXS--small angle x-ray scattering

MDI--methylene bis(4-phenylisocyanate)

DAM--diamino diphenyl methane

BD--polybutadiene diole

CA or DCA--dicumyl alcohol

DMF--dimethyl formamide

WAXD--wide angle x-ray diffraction